OPTIMAL SIZING AND OPERATION OF PUMPING SYSTEMS TO ACHIEVE ENERGY EFFICIENCY AND LOAD SHIFTING

by

He Zhang

Submitted in partial fulfilment of the requirements for the degree

Master of Engineering (Electrical)

in the

Faculty of Engineering, Built Environment and Information Technology

Department of Electrical, Electronic and Computer Engineering

UNIVERSITY OF PRETORIA

April 2011

SUMMARY

OPTIMAL SIZING AND OPERATION OF PUMPING SYSTEMS TO ACHIEVE ENERGY EFFICIENCY AND LOAD SHIFTING

by

He Zhang

Promotor: **Prof. J.F. Zhang**

Co-promotor: **Prof. X. Xia**

Department: **Electrical, Electronic and Computer Engineering**

University: **University of Pretoria**

Degree: **Master of Engineering (Electrical)**

Keywords: Pump, energy efficiency, load shifting, operational cost, POET, optimal capacity selection, optimal control, MPC, variable speed drive, mixed integer PSO.

This dissertation presents a pumping system operation efficiency improvement solution that includes optimal selection and control of the water pump. This solution is formulated based on the performance, operation, equipment and technology (POET) framework. The focus is on the minimization of the operational energy cost. This efficiency improvement solution is divided into three stages in accordance with the operation category of the POET framework. The first stage is to select the optimal pump capacity by considering both energy efficiency and load shifting requirements. The second stage is to develop a flexible pump controlling strategy that combines and balances the contributions from energy efficiency and load shifting. The last stage is to improve the robustness of the control system using the closed-loop model predictive control approach.

An optimal pump capacity selection model is formulated. In this model, additional capacity requirements for load shifting are considered along with the traditional energy

efficiency requirements. By balancing the contributions from load shifting and energy efficiency, the operational energy cost can be reduced by up to 37%.

An optimal pump control is formulated. The objective of this control model is to balance the energy efficiency and load shifting contributions during the operation and minimize the operational energy cost. This control model is tested under different operational conditions and it is compared to other existing control strategies. The simulation and comparison results show that the proposed control strategy achieves the lowest operational energy cost in comparison to other strategies.

This optimal pump control model is further modified into the closed-loop model predictive control format to increase the robustness of the control system under operation uncertainties.

A mixed integer particle swarm optimization algorithms is employed to solve the optimization problems in this research.

OPSOMMING

OPTIMALE ONTWERP, SELEKSIE EN BEHEER VAN POMPSTELSELS MET DIE DOEL OM ENERGIE DOELTREFFENDHEID EN LAS VERSKUIWING OPTIMAAL TE BENUT

deur

He Zhang

Studieleier: **Prof. J.F. Zhang**

Mede-studieleier: **Prof. X. Xia**

Department: **Elektriese, Elektroniese en Rekenaar Ingenieurswese**

Universiteit: **Universiteit van Pretoria**

Graad: **Magister in Ingenieurswese (Elektiese Ingenieurswese)**

Sleutelwoorde: Pomp, energiedoeltreffendheid, lasverskuiwing, bedryfskoste, POET, optimale kapasiteit, optimale beheer, MPC, Veranderlike spoed motor, gemengde heelgetal PSO.

Hierdie verhandeling bied 'n verbeterde oplossing vir die operasionele doeltreffendheid van pompstelsels wat die optimale keuse en beheer van die waterpomp insluit. Hierdie oplossing is geformuleer op 'n raamwerk wat werkverrigting, bedryf, toerusting en tegnologie in ag neem. Die oplossing fokus op die vermindering van bedryfsenergie koste. Hierdie oplossing is onderverdeel in drie fases soos bepaal deur die bedryfskategorie gegrond op die bogenoemde raamwerk: Die eerste fase is die keuse van die optimale pompkapasiteit deur beide energiedoeltreffendheid en lasverskuiwing in ag te neem. Die tweede fase is om 'n buigbare pompbeheer strategie te ontwikkel wat 'n goeie balans handhaaf tussen die onderskeie bydraes van energiedoeltreffendheid en lasverskuiwing.

Die derde fase is om die stabiliteit van die beheerstelsel te verbeter deur gebruik te maak van 'n geslote-lus beheermodel met voorspellende beheer (Predictive Control).

'n Model vir die keuse van optimale pompkapasiteit is geformuleer. In hierdie model word vereistes vir addisionele pompkapasiteit vir lasverskuiwing sowel as vereistes in terme tradisionele energiedoeltreffendheid in ag geneem. Deur die regte verhouding tussen die onderskeie bydraes van energiedoeltreffendheid en lasverskuiwing te vind kan 'n besparing van tot 37% op die energiekoste verkry word.

Optimale pompbeheer is geformuleer. Die doel van die beheermodel is om die bydraes van energiedoeltreffendheid en lasverskuiwing te balanseer en om die bedryfsenergie koste te minimiseer. Hierdie beheermodel is getoets onder verskillende bedryfstoestande en dit is vergelyk met ander bestaande beheerstrategiee. Die simulasie en vergelyking van resultate toon dat die voorgestelde beheerstrategie die laagste bedryfsenergie koste behaal in vergelyking met ander strategiee.

Hierdie optimale pomp beheermodel is verder aangepas in 'n geslote beheermodel met voorspellende beheerformaat om die stabiliteit van die beheerstelsel te verbeter onder onsekere bedryfstoestande.

'n Gemende heelgetal partikel swerm optimisasie (Mixed interger particle swarm optimization) algoritme is gebruik om die optimiseringsprobleme op te los tydens hierdie navorsingsoefening.

LIST OF ABBREVIATIONS

DSM	Demand side management
EE	Energy efficiency
LM	Load management
LS	Load shifting
POET	Performance, operation, equipment and technology
MPC	Model predictive control
VSD	Variable speed drive
PSO	Particle swarm optimization
MD	Maximum demand
TOU	Time of use
NMD	Notified maximum demand
R	Rand, South African currency, one rand is equivalent to about 0.143 US dollar.

Contents

CHAPTER 1. INTRODUCTION

This dissertation defines a pumping system operational efficiency improvement scheme, which covers the optimal design and optimal operational control. The focuses of the optimal design and operational control are to combine and balance the contributions of energy efficiency (EE) and load shifting (LS) in order to minimize the operational energy cost.

1.1 OUTLINE OF THE DISSERTATION

This chapter introduces the background of the research problems and briefly describes the research approach. Chapter 2 covers the literature survey, which includes a detailed description of the research problems, the research approach and the contributions of this research. Chapter 3 describes the formulation of a mixed integer particle swarm optimization (PSO) algorithm, which is the platform of all the simulations. In Chapter 4, an optimal pump capacity selection algorithm is defined and tested. In Chapter 5, a flexible optimal pump operation control strategy is defined and tested. In Chapter 6, the optimal control strategy defined in Chapter 5 is modified into a closed-loop model predictive control (MPC) format and evaluated. Chapter 6 includes the conclusion for this research and recommendations for further research.

1.2 BACKGROUND

The demand for electricity is increasing throughout the world, which results in higher energy cost and additional greenhouse gas emissions. This is of particular concern in South Africa, where large-scale load shedding was recently required to reduce the electricity demand [1], [2].

To assist to solve this problem, demand side management (DSM) initiatives are pursued. DSM initiatives are less expensive, cleaner, faster and have lower risks than building new power plants [3]. According to [4], DSM can be divided into two categories, EE and load

management (LM). Some articles prefer to exclude EE from DSM and form a separate EE category, such as [5]. Despite the different definitions of DSM, the definitions of EE and LM are fairly consistent. EE aims to reduce the net amount of energy consumed, whilst LM aims to reduce the load in the peak demand period. The most common form of the LM method is load shifting (LS). For LS, the operations are shifted, as much as possible, from periods of high energy demand to lower energy demand periods [4].

1.3 APPROACH

According to the operation category of the performance, operation, equipment and technology framework [6] [7], operational efficiency can be sub-divided into physical, time and human coordinations.

The research objective is to define a pump operational efficiency improvement scheme based on the POET framework. The operational efficiency improvements for this research are measured in monetary terms, hence the aim of this research is to minimize the operation energy cost.

The first part of this research is to define an optimal pump capacity selection model. The second part is to define a variable speed drive (VSD) based optimal pumping control strategy. Both the optimal selection and control models are formulated based on the principle of combining and balancing EE and LS saving contributions to achieve minimal operational energy cost.

The third part focuses on increasing the system robustness against human and system induced errors. The optimal pumping control strategy defined in the second part is converted into a closed-loop optimal control model using the MPC approach. This closed-loop optimal control model is tested through simulations to evaluate its robustness and operational performance.

These models are tested under different operational conditions to evaluate their performance and characteristics. The simulated results are compared with the existing selection and operational strategies to illustrate whether the approach of combining EE and LS is more beneficial.

The simulations require solving binary and continuous variables simultaneously, hence a mixed integer PSO platform is developed to match the requirements of this research.

CHAPTER 2. LITERATURE REVIEW

This chapter covers the literature survey. It includes a detailed description of the research problems, the research approaches and the contributions of this research.

2.1 DEMAND SIDE MANAGEMENT

According to [8] South Africa is currently suffering from a severe electricity shortage as a result of recent rapid economic growth. The local energy supplier, Eskom, does not have sufficient power-generating facilities to keep up with this increasing demand. Load shedding has been introduced to prevent a collapse of the national electricity supply system. This severely affects the country's economy and its inhabitants' daily life. Experts predict that the risk of load shedding will remain high until at least 2013, unless Eskom takes immediate action to ameliorate the situation.

To correct the situation, Eskom has embarked on capital expansion and DSM programs [2]. The aim of the capital expansion program is to refurbish old mothballed power stations and to build new peak and base load power stations. The aim of the DSM program is to affect the timing or the amount of electricity used by customers [2] [9]. The DSM program is very important, because DSM initiatives are less expensive, cleaner, faster and have lower risks than building new power stations [3].

DSM was introduced during the 1970s energy crisis with the aim to influence customer appliance selection and energy use patterns to achieve the desired impact or load shape [11].

Over the years of development, DSM has gone through three stages of transformation, namely the command and control without incentives stage, command and control with incentives stage and the recent customer-driven and customer-finance stage [10].

The unit price of electricity has been increased tremendously in comparison to the 1970s, along with the introduction of many additional charges such as time of use (TOU) and maximum demand (MD). Many companies have started to realize that DSM not only

helps to stabilize the electricity grid, but that it also makes very good financial sense.

About 20% of all industrial electricity is consumed worldwide by pumping systems alone [8]. The dominant type of pump by far is the centrifugal pump, hence it is one of the biggest energy consumers in modern industry. It is a common practice for companies, even nations, to set a power consumption reduction target for their pumping systems. For these reasons, the centrifugal pumping system is an ideal and meaningful subject for DSM. In this research, the centrifugal pump is the only type of pump considered and the word "pump" refers to the centrifugal pump.

2.2 ENERGY EFFICIENCY AND LOAD MANAGEMENT OF DSM

According to [4] DSM can be divided into two categories, EE and LM. Some articles prefer to exclude EE from DSM and form a separate EE category such as [5]. Despite the different definitions of DSM, the definitions of EE and LM are fairly consistent.

EE aims to reduce the net amount of energy consumed. EE improvement techniques can be applied to a wide range of applications, for example, efficient lighting [12], variable speed drives [13], solar water heating systems [14] and energy-efficient motors [15]. EE helps to lower the electricity demand and also reduces greenhouse gas emissions.

For LM, unlike EE, the load is simply moved, but the net amount of consumed energy is not changed. Various techniques are used for LS, for example direct load control [16], real-time pricing [17] and TOU pricing [18]. This dissertation focuses on the TOU pricing technique of LM. With this technique, the utilities do not actively manage the load, but customers are encouraged to reschedule loads to reduce electricity costs. This technique is referred to as LS.

2.3 TARIFF STRUCTURES

In addition to the traditional flat tariff structure where the electricity cost per kilowatt hour is fixed, TOU and MD tariffs are introduced to encourage user-side load management.

The TOU charge is based on a higher kWh rate during high-demand periods, whilst MD charges are based on fixed fees per maximum kVA or kW for a month [19]. MD is measured as the highest average demand in kVA or kW during any integrating period. The integrating period is generally 30 minutes, and it coincides with the TOU periods [19].

Table 2.1: Summary of the Tshwane 11kV TOU tariff tariff [19].

Period	**Cost**
Off-peak (0:00 to 6:00 and 22:00 to 24:00)	
High-demand (winter)	0.1187 R/kWh
Low-demand (summer)	0.1049 R/kWh
Standard (6:00 to 7:00 and 10:00 to 18:00)	
High-demand (winter)	0.1411 R/kWh
Low-demand (summer)	0.1383 R/kWh
Peak (7:00 to 10:00 and 18:00 to 22:00)	
High-demand (winter)	0.8205 R/kWh
Low-demand (summer)	0.2628 R/kWh
Maximum demand charge	66.50 R/kVA

The MD is different from the notified maximum demand (NMD) [19] [20]. The NMD is the agreed limit on the monthly MD. In other words, a customer agrees that his MD will not exceed his NMD. A customer that exceeds the NMD is typically charged a penalty fee. This dissertation focuses on the MD only, because by optimizing the MD the NMD is automatically adhered to.

In this dissertation, the 2008 Tshwane municipality's 11kV TOU tariff [19] is used. The detailed cost of the high and low-demand TOU and MD tariff are summarized in Table 2.1. The optimization models in this dissertation are all formulated and simulated based on these tariffs.

2.4 PUMP-RELATED DEFINITIONS

The key terms used in this dissertation are defined in this section prior to the relative chapters.

The term "pumping system" refers to the pumps and the environment in which the pump operates. The term "system" by itself refers to the elements that have an influence on the operation and performance of the pump. The system characteristics can be summarized using a system curve.

The term "flow rate" is used to represent the actual output flow rate of the pump in m^3/hour. The flow rate of a pump can be adjusted using devices such as a valve or VSD. The term "capacity" refers to the maximum pump operational output flow rate.

Capacity is different from the manufacturer-specified maximum pump output flow rate, since the performance of a pump varies significantly with different system characteristics.

The term “head” is used to measure pump-related pressure values in meters. The pump head is the pressure of the water leaving the pump, and the system head is the pressure required to achieve a specific flow rate in a given system.

2.5 POET FRAMEWORK

According to the study on the classification of energy efficiency, [6] summarizes different energy efficiency components into four categories, namely performance, operation, equipment and technology. Performance efficiency of an energy system is determined by external but deterministic system indicators such as production, cost, energy sources, environmental impact, technical indicators and others. Operational efficiency is evaluated by the proper physical, time and human coordination of different system components. Equipment efficiency is a measurement of the energy output of isolated individual energy equipment with respect to the given technology design specifications. Technology efficiency is decided by the efficiency of energy conversion, processing, transmission and usage. Technology efficiency is often evaluated by feasibility, life-cycle cost and return on investment [7]. The relations of the four POET efficiencies can be best illustrated in Figure 2.1.

The pumping system efficiency improvement falls under the operation category. This is shown by the encircled area in Figure 2.1. Operational efficiency is a system-wide measure, which is evaluated by considering the proper coordination of different system components. This coordination of system components consists of the physical, time and human coordinations [7]. In a pumping system, physical coordination is the matching and sizing of the physical system, time coordination is the timing and control of the operation and human coordination is the human influences.

2.5.1 Physical coordination

The physical coordination is the matching of equipment to operational requirements. The selection of appropriate equipment is a complex and important task. The degree of equipment matching directly influences operational efficiency and cost. The optimal selection of equipment is highly regarded in operational efficiency improvement. Examples of optimal equipment selections are shown in [21], [22] and [23].

Article [22] illustrates that simulation with different operational conditions is one of

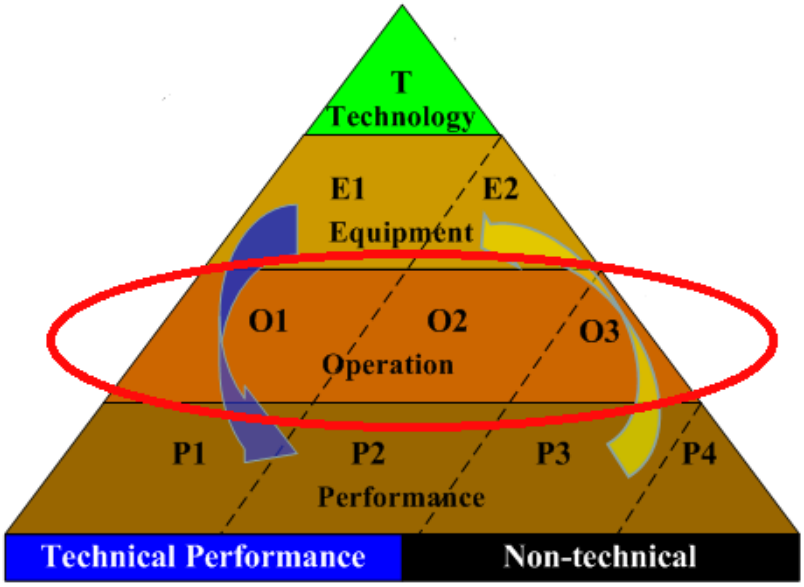

Figure 2.1: Graphical illustration of the POET framework. Taken from [7], with permission.

the best ways to assist decision-makers in the selection of the most economic mixture of equipment. This hypothesis is consolidated with a case study on a dual-purpose plant. Another important aspect of an optimal design pointed out in [22] is that despite the efforts being put into effective planning and analysis of trends, statistics show that deviations from projections are still frequent. Such deviations would normally invalidate optimal selection of the major equipment, which relies largely on correct forecasting of the requirements.

As pointed out in [24] and [25], operational energy cost is by far the biggest contributor to pump life cycle cost. It is shown in [25] that up to 90% of the pump life cycle cost comes from energy consumption, and pump energy consumption can generally be reduced up to 20% through proper pump selection. For a pump to operate efficiently without wasting energy, its performance characteristics must be suitable for the intended service.

Reference [26] points out that the correct selection of a pump is the first step in guaranteeing efficient and appropriate performance, as well as reliable operation. This article summarizes a large volume of existing literature and derives steps to select the most suitable pump. This article points out that currently, from both engineering and economic standpoints, the efficiency of the pump-motor set is of the upmost importance; the selection of the pump and motor should ensure high efficiency values, aiming for the lowest possible energy consumption per volume of pumped fluid.

In [25], [26], [27] and [28], the fundamentals of EE based pump selections are illustrated. Case studies of pump selection in industrial environments are illustrated in [31], [29] and [30]. Many versions of software are also developed to assist the optimal selection of pump capacities, as described in [32], [33] and [24]. In [34], [35] and [36], optimization algorithms are developed to select the ideal pump or combination of pumps optimally.

Reference [27] demonstrates in detail the ways to select water pumps based on the pump and system characteristics. The pumping efficiency varies for different operating points of the pump. The pump operating point is determined by the pump characteristics and system characteristics. The pump and system characteristics can be represented by the pump characteristic and system curves. The operating point of a pump can be determined by the intersection of the two curves [37]. In the case where the pump and the system are perfectly matched, the operating point is at the point of maximum efficiency.

In [34], an optimal pump selection algorithm is illustrated. The algorithm is based on solving a non-linear programming problem. The algorithm optimally selects the pump type, capacity, and number of units, which will achieve the minimum operating energy consumption for a given water demand curve. The characteristics of a range of pumps are approximated into quadratic equations and the optimization algorithm selects the best combination of pumps that operate with the minimum energy consumption while satisfying the operational requirements. This method is validated through a case study on an inland intensive fish farm where high levels of energy consumption reduction is achieved. The mathematical pump and system characteristics approximation method used in this article simplifies the computation of the operating point, efficiency and input power of a pumping system and enables them to be utilized in optimization algorithms.

Similar approximation methods are also used in [35]. However, in [35] an algorithm is derived to compute the ideal pump characteristics based on the system characteristics, which will result in minimal operational energy consumption.

2.5.2 Time coordination

The time coordination section of the operation category focuses on the optimal control of the pump operation. In the early days of pump utilization, valves were used to control the output rate of the pump. Valve control is still widely used today, because it has the advantages of being cheap and simple to implement. However, pumps controlled by valves have very poor EE [38]. Other common pump controls include: on/off control, VSD control and optimal control.

References [39] to [50] are EE oriented pump operation controls. The focus of these articles is on ensuring that energy consumption is kept to a minimum during operation. These include modifying impellers [39]; minimizing the power consumption for a given demand by operating with the optimal combinations of different sized pumps, [40] to [43]; using VSD, [40] to [49]; and generating power by using a pump as a turbine during peak hours [50].

In Reference [41] a pump scheduling problem based on a genetic algorithm is proposed. The objective is to maximize the efficiency of pump operation and at the same time balance the total water flow rate of the system. The efficiency of a pumping station is defined in this article as the ratio between input power and the useful output power of the pumping system. The useful output power is computed by multiplying the total flow rate with the generated head. The input power is derived by using mathematically approximated pump and system characteristics similar to [34] and [35]. The algorithm maximizes efficiency by selecting, from a pool of pumps under control, the optimal combination of pumps to be activated. This optimal combination of pumps will satisfy the water demand with minimal energy consumption. Other water supply efficiency improvement strategies, such as [40], [42] and [43], follow a similar approach where different combinations of pumps are scheduled to minimal energy consumption. In these articles, the efficiency and the input power of the fixed speed pumps are estimated using the hydraulic equation, the pump characteristics or both.

In recent years, VSD has been used to replace valve control to improve the pump EE with great success. As reference [44] points out, the installation of VSD represents perhaps the most tangible measures to save electrical energy. The principle behind the VSD energy savings is also shown in [44]. The power drawn by the pump is dependent on the motor rotational speed and the input power increases at a cubic rate with respect to the increase in the motor rotational speed. The motor rotational speed is proportional to the output rate, hence a slight reduction in the output rate and the motor rotational speed results in a significant input power reduction. Pumps are often oversized because of the added safety margin. This causes additional unnecessary energy consumption. As shown in [44], only with VSD can one escape the danger of over sizing. VSD reduces the output rate by reducing the rotational speed of the motor, which lowers the power consumption. In [45] and [46], VSDs are applied to different pump-related applications and significant power consumption reductions are achieved. Other benefits of VSD are illustrated in [44]; these include power factor correction and reduction in the start-up current and dynamic stress of the pumps.

The method of computing the VSD energy savings is illustrated in [47]. In this article a comprehensive step-by-step derivation of the pump energy consumption for different motor rotational speeds is illustrated along with the common errors that people make when

carrying out such computations. The pump characteristics and system characteristics are also approximated using quadratic equations. The effect of the motor speed changes on the pump characteristics is mathematically described using affinity laws [48]. The operating point for a given motor rotation speed is computed using the combination of the affinity laws, pump performance and system characteristics. The actual input power is computed based on the pump operating point. In comparison to other VSD saving computation efforts, [47] is one of the most accurate and complete articles.

References [48] and [49] are examples of the use of optimal control in VSD operations. In [48], an optimal control model is established with the aim of achieving the lowest energy consumption for a cooling system pump operation in a high-speed wire factory. The model computes an optimal VSD speed setting for each of the connected pumps. The aims of this system are to balance the pressure of each pump and ensure that the pumps are all operating at the highest possible efficiency while satisfying the water demand. The pump characteristics and the affinity laws are utilized to derive the efficiency and input power of the pumps at different operating points. In reference [49] a mathematical model for the optimum parameters of centrifugal pumps is established, and the minimum total electric power consumption of the fixed-speed pumps and variable speed pumps is taken as the objective function. Reference [49] is similar to [48] in terms of the objective and method of pump control. However, in [49], the pump consumption is derived using the hydraulic equation whereas in [48] the pump input power is derived based on the manufacturer-specified pump input power curve.

References [52] to [61] are pump LS problems. These articles cover most LS scenarios, such as single pump operation [52] and [53]; multiple pumps operation, [54] and [55]; operating under TOU tariff and MD tariff, [56] and [57]; multi-objectives optimal pump control, [58] to [60]; and actual case studies [61]. In all of the above cases an optimization model is used to compute a set of operation schedules based on the physical constraints and the different tariff structures; all the pumps are controlled with an on-off controller and a reservoir is in place as a buffer to allow schedule changeability.

In [52], a simple and effective LS strategy is illustrated. In this article an ultrasonic water level accurately detector allows the user to monitor and control of the reservoir water level. A pumping system is used to maintain the water level in the reservoir automatically at a preset level by pumping water into the reservoir. Prior to the high electricity price periods, the reservoir is allowed to be filled to a higher level by increasing the reservoir level setting. During high electricity cost periods, this reservoir level setting is significantly lower to minimize the operation of the pumps and the electricity cost. This article illustrates that the principle of the LS is the same regardless of the complexity, and the principle is to shift the load as much as possible from the high electricity price period to the lower ones.

In [56] an open-loop optimal control model is developed and simulated for a hypothetical water supply system. The main idea in [56] is to consider the future water demand in the optimization of the MD charge. The daily water demand is modeled as a Markov process, which is then used in a dynamic programming algorithm to determine daily operation MD limits for a month. The daily MD limit is then used as a constraint in the daily optimization schedule.

Reference [53] defines and evaluates an MPC strategy with binary integer programming optimization for LS in a water pumping scheme. Both TOU and MD charges are considered in the control model. The control model yields a near optimal on/off switching sequence, which reduces TOU and MD based electricity costs. This article improves on [56] by implementing a closed-loop control, which improves the robustness of the control model under operational uncertainties. In this article, the MD is reduced by operating the pump at shorter time intervals. This is a unique approach; however the pumps have to be switched on and off frequently, which increases wear and tear on the pump and reduces the life span of the pump as well as increasing pump maintenance cost.

Reference [59] solves multiple conflictive objectives in terms of Pareto optimality. Its approach links a well-known multi-objective optimizer, SPEA2, with a hydraulic simulator, EPANET, in order to provide a Pareto set of explicit schedules. In this pump scheduling problem, the operation of a number of pumps is scheduled over a period. The main goal is to minimize the cost of supplying water. This cost consists of the TOU energy consumption charge, MD charge and maintenance cost.

In [62], an hourly discretized optimization model for the determination of operational planning in a pump-hydro system is presented. This pumping system is designed to supply water, as well as to regularize the irrigation flows and produce electric energy. In this system there are both pumping and hydropower generating stations. This system is a reversible type of system, which, enables pumping in one station and power production in a parallel station. The intention is to obtain the pump and turbine operation time for each hour, so that maximum benefit from hydropower production and minimum costs from the pumping station energy consumption are attained. The principle is to pump as much water as possible to a high level storage tank during off-peak hours, and during peak-hours, the pump operation is minimized and the stored water is used to supply the needs and generate electricity by running the water through a turbine. This article presents a pump optimal operation strategy that has elements of both EE and LS.

Reference [61] is a measurement and verification study on a completed pumping LS project in South Africa. In this study, it is shown that this LS project manages to shift 15.1 MW of energy demand out of the peak periods. It is also shown that the EE of the

operation is improved by approximately 3%. This EE improvement was unintentional and was achieved by chance.

In [63], an optimal switching control and a VSD based optimal control are proposed to improve the EE of a belt conveyor system at the operational level, where TOU tariff, ramp rate of belt speed and other system constraints are considered. An energy calculation model of the belt conveyors is proposed. Based on this energy model, a VSD based optimal control model is formulated. In this control model LS and EE are performed simultaneously. LS improves the operational energy cost by coordinating the VSD operation rate with respect to the TOU tariff. The improvement of EE is achieved through coordinating the belt speeds and feed rates and consequently the energy consumption is reduced. This article demonstrates the flexibility and financial benefits of a VSD based conveyer belt control strategy through a case study on a coal conveyer system.

2.6 RATIONALE FOR THIS STUDY

The POET framework is a generalized classification of the EE components, and it is designed to be applied to practical DSM problems. However it has only been proposed recently, and there are little practical validation and few applicability studies on this framework.

The existing studies on pumping system operation cost optimization are predominantly isolated either in the field of optimal design or optimal operation. There is little evidence of a pumping system operation cost reduction scheme that encompasses both optimal selection and operational control.

The references mentioned in Section 2.5.1 focus only on EE improvement. If EE is the only factor considered during the selection of the pumps, the selected pumping capacity tends to be minimal, since additional capacity will cause energy wastage. In cases where a sufficiently sized reservoir is available as a buffer, the designer will typically select the pump capacity in accordance with the average water demand. However, in a case where the facility is charged under a TOU tariff, it is ideal to implement LS to reduce the energy cost. In order to do so, additional pumping capacity is required to shift the load out of the peak hours and still satisfy the water demand.

As pointed out in [22], an issue associated with optimal design is the rigidness of the design. When the operational parameters change, such as a tariff and demand change, the chance is that the current optimal design will lose its optimality. Designers often have to compensate for the risks of parameter variation by designing for the worst

case scenario, which will significantly reduce operational efficiency. Ideally, a flexible pump control mechanism can be used to compensate for the rigidness of the optimal design. This flexible controller should be able to adapt to any changes occurring in the operational parameters to ensure that the operation is adjusted to be once again optimal in terms of operational efficiency.

Section 2.5.2 addresses some of the articles on the existing method of pump operation control. From the collected articles, the DSM related pump operation control improvement can be seen to be divided into two separate approaches, namely the EE and LS improvements. The only studies found to implement both EE and LS in one pumping project are [62] and [61]. However, [62] is not a true EE improvement since the overall efficiency is boosted by using the pump as a turbine to generate electricity when it is profitable to do so. Reference [61] was initially an LS project but after implementation it was found that the overall efficiency was improved by chance.

Reference [63] successfully implemented both EE and LS in a single belt conveyor system utilizing VSD. This article has demonstrated that it is possible and at the same time very profitable to combine EE and LS. In addition, it has also demonstrated the flexibility of the VSD based controller, which is ideal for compensation of the design rigidness mentioned earlier. Since both belt conveyor and pump are motor-driven devices with similar properties, VSD should also be used to formulate an EE and LS combined pump control for a pumping system.

Most of the optimal control strategy studies, such as [36], [41] and [42], are in the form of open-loop control. Open-loop control is sufficient for simulation purposes but it is difficult to implement it in real life owing to simplification errors and operational uncertainties. Without feedback from the actual operation the controller is isolated from the plant and is unable to correct any unforeseen changes and errors in the system.

An MPC approach is implemented in [53] and [63]. These articles demonstrate the ability of the MPC strategy to increase the robustness of the control system under uncertainties. The biggest advantage of the MPC is its ability to predict future output values based on current and past measurements, and make appropriate changes to the control variables to achieve the desired target [64]. This characteristic enables the MPC to correct any form of system errors.

The proposed strategy resembles [53] and [63] in the fact that the control model and the operational information are all based on estimations, and there is a high level of operational uncertainty. Therefore it is necessary to implement a closed-loop control strategy.

2.7 APPROACH OF THIS STUDY

2.7.1 Hypothesis

The first hypothesis is that a complete pump efficiency improvement scheme can be developed following the operational section of the POET framework.

The second hypothesis is that EE and LS can be combined and balanced in the selection and operational control of water pumps, such that the operational cost can be minimized.

2.7.2 Realization stages

This dissertation focuses on the equipment-related physical and time coordinations of the operation category. Human coordination is not covered in this dissertation. Nevertheless, human coordination is still a vital part of overall system operation, since humans are involved in every stage of the operation. Proper human coordination is essential for a pump system to operate at its optimal efficiency.

The main content of this dissertation is divided in accordance with physical and time coordinations categories. Because of the complexity of the time coordination stage, it is further divided into two stages. Hence the formulation of the pumping system operation efficiency improvement strategy consists of three stages.

The first stage is to develop an optimal pump capacity selection model. This model selects the optimal pump capacities for a pumping system with the objective of minimizing the operational energy cost by balancing the EE and LS contributions.

The second stage is the formulation and testing of a flexible open-loop pump control strategy that minimizes the operational energy cost by maximizing the net savings from EE and LS contributions using a VSD based controller. This proposed pump control strategy, with its flexibility, should be able to adapt to any known system changes and adjust itself to ensure the operational cost minimum.

The third stage is the formulation and testing of a closed-loop MPC strategy, based on the open-loop control strategy from the previous stage. This closed-loop MPC strategy should be able to improve the system's robustness and automatically compensate for any unknown system variations.

2.7.3 Pump power consumption prediction functions

In order to minimize the pump operation energy consumption, the pump operation power consumption under different scenarios must be accurately predicted. Hence relationships between the optimization variables and the pump power consumption need to be formulated.

Two types of pump power consumption functions are needed for this research. The first type is a relationship between the pump capacity and the pump power consumption. This relationship is referred to as the capacity-power function. The capacity-power function is used in the optimal pump capacity selection model, and it estimates the pump power consumption for different choices of pump capacity. The second type is a relationship between the pump flow rate and the pump power consumption. This relationship is referred to as the flow-power function. The flow-power function is used in the optimal control strategy, and it computes the pump power consumptions for different flow rate settings of a VSD controlled pump.

As pointed out in [65], such input power prediction functions used for optimization should not be too complex, like the one in [66], otherwise the optimization algorithms might become unsolvable.

References [34] and [35] illustrate that the pump characteristics and system characteristics can be accurately estimated by quadratic equations. It is possible to transform the existing graphical information into mathematical equations, which is essential for the derivation of the capacity-power and flow-power functions.

Pump power consumption prediction functions for fixed speed pumps are used in [40] to [43]. Since the operating points of these pumps are fixed, these functions are derived from the hydraulic equation. This type of fixed speed pump input power function can be used to formulate the capacity-power function.

More complex pump input power prediction function formulations involving VSD controls are attempted in [48], [49], [65] and [67]. References [48] and [49] do not consider the system characteristic curve but rather use affinity laws to predict the operating points for different speeds. The affinity laws are only applicable to free running pumps, which are not connected to any system and are not constrained from the system losses such as the friction of the pipes [47]. When a pump is installed into a system, the changes in the operating point associated with changes in motor rotational speed follows the non-linear system curve, not affinity laws. Hence, the accuracy of [48] and [49] are poor. Reference [67] assumes a linear system loss curve which deviates significantly from real life. Reference [65] formulates a flow-power function by measuring the changes in power

with respect to change in rotational speed.

A more simple and accurate method of computing the power consumption of a VSD controlled pump for different flow rates is illustrated in [47]. The pump power consumption is computed analytically based on the design parameters and VSD settings. This method is used as the foundation to formulate the flow-power function.

2.7.4 VSD implementation complication

There is a complication in using VSD for LS in pump optimal control. A centrifugal pump can only operate above a given minimum motor rotation speed, otherwise the water will just swirl within the tubes and nothing will be pumped out [37]. Unlike in the case of a conveyor belt [63], the speed of the VSD can be adjusted from 0 to maximum without any problem. Operating a pump below its minimum motor rotation speed will not only waste energy, but also cause the pump to overheat. The VSD therefore only has a small range of speed adjustment, typically between 25% and 50% of the maximum motor rotation speed. This limited range of adjustment significantly restricts the level of LS and the associated savings for VSD controlled pumps.

To solve this problem, the controller must switch off the pump completely when the operation is below the minimum motor rotation speed. Hence an on/off controller is used together with the VSD controller. Normally the on/off controller is on and the VSD is responsible for all the flow rate adjustments. When the ideal motor operating speed is below the minimum speed, the on/off controller will take over, switch the pump off and achieve the necessary LS.

2.7.5 Particle swarm optimization

Continuous and binary variables have to be solved simultaneously in optimal control models in this research, hence mixed integer programming is required. The standard optimization tools, such as those found in MATLAB, are not suitable for such operations. Other forms of optimization algorithms have to be used.

Particle swarm optimization (PSO) is a population based search algorithm based on the simulation of the social behavior of birds within a flock. In PSO, individuals, referred to as particles, are “flown” through hyper-dimension search space in the process of searching for the optimal solution. Changes to the position of the particle within the search space are based on the social-psychological tendency of individuals to emulate the success of other individuals. The changes to a particle within the swarm are therefore

influenced by the experience or knowledge of its neighbors [68].

PSO is a simple-to-implement algorithm that is effective in optimizing a wide range of objective functions. Conceptually, it seems to lie somewhere between genetic algorithms and evolutionary programming. It is highly dependent on stochastic processes, like evolutionary programming. The adjustment toward best solution of the population by the particle swarm optimizer is conceptually similar to the crossover operation used by genetic algorithms. It uses the concept of fitness, as do all evolutionary computation paradigms [68].

Unique to the concept of particle swarm optimization is flying potential solutions through hyperspace, accelerating toward "better" solutions. Other evolutionary computation schemes operate directly on potential solutions, which are represented as locations in hyperspace. Much of the success of particle swarms seems to lie in the agents' tendency to hurtle past their target [68]. The stochastic factors allow thorough search of spaces between regions that have been found to be relatively good, and the momentum effect caused by modifying the extant velocities rather than replacing them results in overshooting, or exploration of unknown regions of the problem domain.

PSO has been widely used to solve industrial optimization problems, such as in [53], [69] and [70]. Reference [53] is a pumping schedule optimization problem. In this article, PSO is compared with genetic algorithm. It is found that the PSO algorithm excels by its flexibility and adaptability in accommodating either discrete or continuous types of optimization variables. Its simplicity allows for straightforward implementation, with relatively high execution speeds compared to other evolutionary algorithms, alongside a high convergence rate towards acceptable solutions [53].

Despite the advantages of the PSO algorithm, it was originally designed to solve continuous variable problems. Modifications to the standard algorithm are necessary in order to solve mixed integer optimization problems.

Many researchers have managed to derive novel methods to solve discrete variables using PSO. References [71], [72] and [73] are binary PSO strategies. Since binary optimization is a specialized form of integer optimization, integer PSO approach references are also applicable to this research. References [74], [75] and [76] are integer PSO strategies. Among these articles, only [76] describes a constrained problem formulation. The optimization models of this research are all constrained ones, hence [76] is used as the binary PSO formulation foundation in this research. The algorithm proposed in [76] is analyzed and tested to determine whether it is suitable for the application of this research. If the test does not yield the promised results, a binary PSO suitable for this research will be developed.

2.8 RESEARCH PROCESS AND MODELING

The research comprises the following sequential activities:

1. The existing mixed integer PSO algorithms are evaluated. Since PSO was originally designed for continuous variable optimization and its continuous variable optimization performance has been approved in many articles, the focus of the evaluation is on binary variable optimization.

2. The evaluation results are not satisfactory, and hence a binary PSO optimization algorithm is developed for the purpose of this research. Tests are performed to ensure that the developed algorithm is indeed more suitable than the existing ones.

3. An optimal pump capacity selection model is defined. The objective of this optimization model is to select the optimal pump capacities such that the operational energy cost is minimized with respect to the tariff structure, demand and system constraints. The pump capacities and the optimal operation LS schedule are optimized simultaneously to ensure the maximization of the combined EE and LS savings.

4. Simulations on the optimal pump capacity selection model are conducted under different tariff structures and system limitations. The results are evaluated.

5. Through the simulations, the rigidness of the optimal design becomes apparent. This leads to the development of a flexible pump operation control strategy, the VSD on/off controller.

6. The open-loop optimal control model for the VSD on/off controller is defined. The objective of the model is to compute a set of VSD flow rate settings and a corresponding set of on/off schedules, which ensures that the pump satisfies its operational requirement with minimal energy cost.

7. The methods of formulating a pump flow-power function that predicts the required input power for a different flow rate or motor rotation speed of a pump are derived. Two derivation approaches are illustrated, namely the measurement approach and the theoretical approach.

8. Tests are conducted to evaluate the performance of the VSD on/off controller. Simulations are conducted based on a case study under different tariff structures. The tariff structures considered are flat tariff, MD tariff, high-demand TOU tariff, low-demand TOU tariff, high-demand TOU with MD tariff, and low-demand TOU with MD tariff.

9. Four of the most common pump control strategies are simulated under the same case study with different tariff structures. The four pump controls are valve control, level based on/off control, VSD control and optimal on/off control. The simulated operational energy costs of each of the four controls under different tariff structures are compared with the corresponding VSD on/off energy costs.

10. The open-loop VSD on/off optimal control model is converted into a closed-loop optimal control model using the MPC approach.

11. The closed-loop MPC optimal control model is simulated based on the case study parameters for a control duration of one week. The results are compared and evaluated against the open-loop results.

12. Further simulation is conducted to test the robustness of the closed-loop MPC approach. An error is introduced into the system and the process of error detection and correction is documented and appraised. The open-loop control model is also simulated under the same operational conditions with the same error. The open-loop results are compared with the MPC results.

2.9 MULTI-LEVEL PUMPING SYSTEM

In this research, the optimal pump selection and control models are formulated for multi-level pumping system. An example of a multi-level pumping system is shown in Figure 2.2. The classification of the different levels is based on the pump arrangement. At each level there is one cluster of pumps. This cluster of pump can consists of one or more interconnected pumps that shares the same input and output pipes. However, it is possible to have multiple reservoirs at each level.

2.10 HOW THIS APPROACH ADDRESSES CURRENT DEFICIENCIES

The selected approach addresses the deficiencies described in Section 2.6 as follows:

1. This research uses the POET framework to define a pumping system efficiency improvement strategy.

2. An optimal pumping capacity selection model is formulated based on not only EE criteria, but also LS requirements.

3. EE and LS improvements are combined in a pump operational energy cost minimization optimal control model.

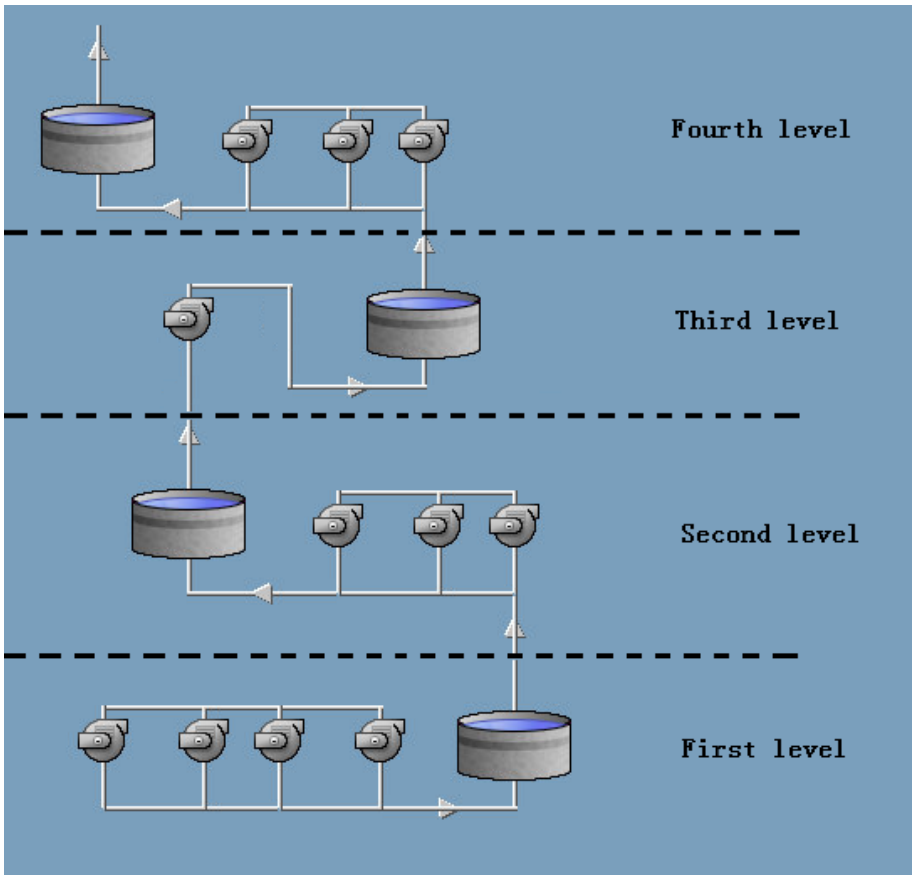

Figure 2.2: Example of a multi-level pumping system, Figure modified based on [61].

4. In this research, methods of pump input power prediction function derivations are formulated. The derived input power prediction functions provide a reasonably accurate estimation of the actual input power and can easily be used in an optimization algorithm.

5. This research further consolidates the importance of the closed-loop approach in real-life optimal control scenarios.

6. A binary variable PSO algorithm is developed to suit the needs of the optimization requirements of this research.

2.11 CHALLENGES AND LIMITATIONS OF THE SELECTED APPROACH

The challenges and limitations of this approach are:

1. The maintenance cost of the pump operation is not considered in this research.

2. The pump input power prediction functions are derived from estimation and are simplified, hence their accuracy is not 100%.

3. The current pump input power prediction functions apply to only a fresh water pumping system. Modifications are needed for other pumping applications, such as oil pumping and slurry pumping systems.

4. The effects of pump aging are not included in the pump input power prediction functions.

5. The formulations of the optimization models and the binary PSO algorithm are challenging.

2.12 CONTRIBUTIONS OF THIS STUDY

The contributions of this study can be summarized as follows:

1. This research affirms the practical applicability of the POET framework [6] by developing a water pumping efficiency improvement strategy based on the operation category of the POET framework.

2. This research illustrates that it is insufficient to maximize only the EE in the selection of pumps during the design stage, such as in [21] to [35]. It also illustrates

that when a facility is charged under TOU tariffs it is more profitable to also take optimal LS requirements into account, and the operational energy cost is significantly reduced when selecting the pumps considering both EE and LS.

3. This research illustrates that EE and LS can also be combined into an optimal control strategy for the pump operation, similar to [63].

4. This combination of EE and LS is proven, through simulations and comparison with other leading pump control strategies, to be flexible and effectively reduce the operational energy cost under all operational scenarios considered.

5. Static input power and flow rate models for fixed and variable speed pumps are formulated, based on [40] to [43] and [47], and then implemented in the optimization algorithms.

6. This research validates the convergence of the electricity cost savings of the closed-loop MPC approach to the open-loop controller [53].

7. This research validates the robustness of the MPC approach [53].

8. In this research a binary variable PSO algorithm is developed based on continuous PSO [68]. This algorithm can be used alongside the continuous variable PSO algorithms to solve mixed integer optimization problems. The developed mixed integer PSO algorithm is proven to be more effective and efficient to solve the optimization problems in this research than the existing approach shown in [76].

CHAPTER 3. MIXED INTEGER PARTICLE SWARM OPTIMIZATION

A mixed integer PSO algorithm is the platform on which all the optimization problems in this research are solved, hence it is described prior to actual formulation of the optimization models.

This chapter is divided into five sections, namely

- The introduction of the fundamentals of the PSO algorithm
- The test of integer PSO approach described in [76]
- The formulation of the binary voting approach
- The justification of the voting approach
- The description of the mixed integer PSO algorithm.

3.1 FUNDAMENTALS OF PSO

The PSO algorithm is based on the analogy of movement and optimization of flocks of bird or schools of fish. The PSO algorithm searches for the global maximum or minimum of a cost function by simulating movement and interaction of particles in a swarm. The position of a particle corresponds to the possible solution of the optimization problem. Each particle represents a complete solution set. Each dimension of a particle represents the solution of one variable in the solution set.

In every iteration a new set of particle position is computed for each particle, using the following equation,

$$P_{a,b}(k+1) = P_{a,b}(k) + V_{a,b}(k+1), \tag{3.1}$$

where

$P_{a,b}(k)$	The value of the b-th dimension of the a-th particle at the k-th iteration.
$V_{a,b}(k)$	The velocity of the b-th dimension of the a-th particle at the k-th iteration, which is given by (3.2).

$$V_{a,b}(k+1) = w_e \cdot V_{a,b}(k) + C_1 \cdot R \cdot (pbest_{a,b} - P_{a,b}(k)) + C_2 \cdot R \cdot (gbest_b - P_{a,b}(k)), \quad (3.2)$$

where

w_e	The inertia coefficient.
C_1, C_2	These are the social rate coefficients, which control the pull to the global best position.
R	This is a function that generates uniformly distributed random numbers in the interval from 0.0 to 1.0.
$pbest_{i,j}$	This is the current best solution for the a-th particle.
$gbest_j$	This is the current global best solution.

Hence, the particle position for the $(k+1)$-th iteration can be written as

$$P_{a,b}(k+1) = P_{a,b}(k) + w_e \cdot V_{a,b}(k) + C_1 \cdot R \cdot (pbest_{a,b} - P_{a,b}(k)) + C_2 \cdot R \cdot (gbest_b - P_{a,b}(k)). \quad (3.3)$$

The particle positions and velocities are initially randomly assigned. The processes of computing the fitness of the particles and derivation of the new particle positions are repeated until the stop criteria are met.

3.2 MIXED INTEGER PSO INVESTIGATION

From Chapter 2, Section 2.7.5, the mixed integer PSO algorithm described in [76] appears to meet the optimization requirements of this research. This algorithm will be referred to as the "mixed integer PSO" from this point onwards.

The mixed integer PSO solves the continuous and integer variable simultaneously. All of the variables are initially solved as continuous ones. The mixed integer PSO uses an additional penalty function to penalize the variables which are supposed to be integer but are not. This additional penalty function forces the selected variables to move toward their nearest integer value. The degree of penalization is based on the amount of deviation of the variable from its nearest integer value. This additional penalty function is modified for binary variable applications and is shown in (3.4).

For the rest of this section, binary variables will be the only type of variable involved.

$$\phi(P_a) = \sum_{b=1}^{B_{bi}} \frac{1}{2}\{sin[2\pi(P_{a,b} - 0.25)] + 1\}, \tag{3.4}$$

where

$\phi(P_a)$	The value of the integer penalty function for a-th particle.
B_{bi}	The total number of binary dimensions in the a-th particle.

The fitness of a particle is computed by the augmented objective function shown in (3.5).

$$F(P_a) = f(P_a) + y\phi(P_a) + r_c \sum_{n=1}^{N_{con}} C_n(P_a), \tag{3.5}$$

where

$F(P_a)$	The fitness value of the a-th particle.
$f(P_a)$	The objective function value of the a-th particle.
n	The constraint indicator.
N_{con}	The total number of constraints.
C_n	The n-th constraint equation or value.
r_c	The weight of the constraints.
y	The penalty parameter, which is determined by (3.6)

$$y(k+1) = \begin{cases} y(k)e^{[1+\phi(gbest(k))]} & \text{, if } E_c > \varepsilon, \\ y(1) & \text{, if } E_c \leq \varepsilon, \end{cases} \tag{3.6}$$

where

$gbest(k)$	The particle with the best fitness value in the k-th iteration.
E_c	The convergence indicator, which is computed by (3.7).
ε	The convergence criteria, which should be a small positive number.
$y(1)$	The initial penalty parameter, which is computed by (3.8).

$$E_c = \frac{|F(gbest(k)) - f(gbest(k))|}{|F(gbest(k))|}. \tag{3.7}$$

$$y(1) = 1 + \min\{\phi(P_a) : \ a = 1, 2, ..., A_T\}, \tag{3.8}$$

where

min	A function that finds the minimum value term in an array.
A_T	The total number of particles.

In the end the best result obtained can be rounded off to obtain a true binary solution.

Theoretically this method should be able to compute the result accurately and efficiently. However, actual simulations show that the mixed integer PSO is not as effective as hoped for. It was found that the mixed integer PSO is very difficult to implement and the solution obtained is very often the local extreme and not the desired global extreme.

The reasons for such poor performance are

- additional local extrema introduced by the additional penalty function; and
- uncertainty in the choice of ε value.

3.2.1 Additional local extrema

The values of a simple one variable objective function is plotted against the corresponding variable values in Figure 3.1. It can be seen that this objective function has one local minimum and one global minimum. The particles in the PSO algorithm will search along this curve for the global extrema and in this case should be able to find the global extreme with ease.

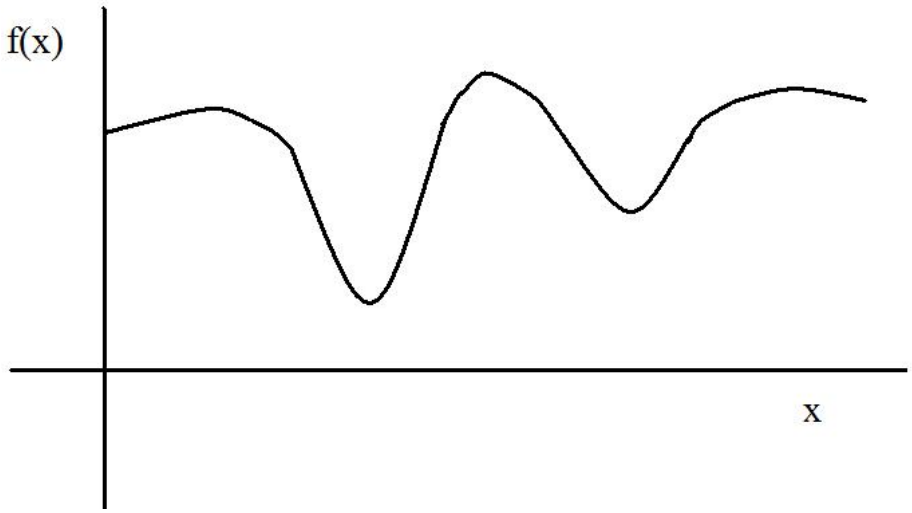

Figure 3.1: A simple one-dimensioned objective function variable relationship.

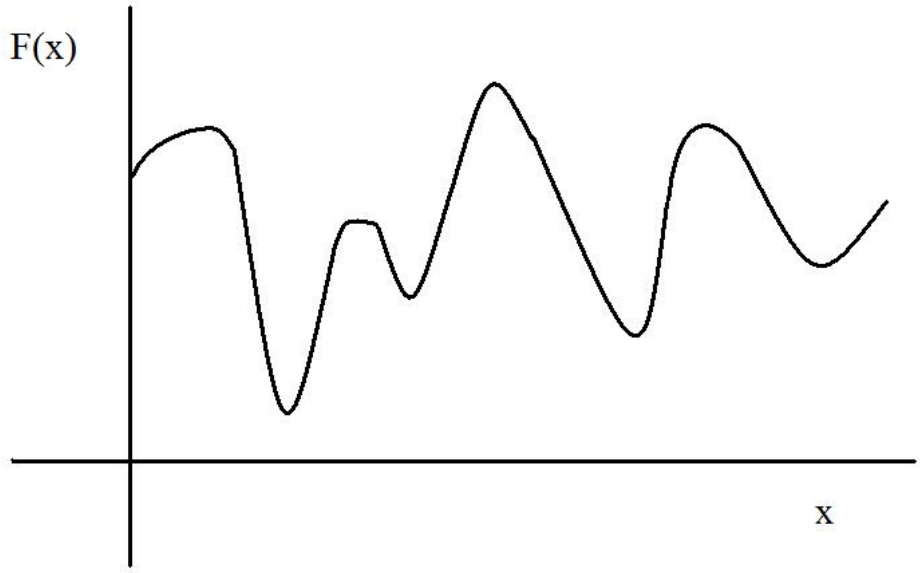

Figure 3.2: An example of an augmented objective function variable relationship.

Sometime particles might land in a local minimum; unless other particles find a better solution, this will be the final, but non-optimal solution.

As the objective function grows more complicated, more local extrema extrema are introduced. For example, in (3.5), the penalty function and constraints might transform a simple objective function curve in Figure 3.1 into something like Figure 3.2.

As the number of variables increases, so do the dimensions of the objective function curve. This will further increase the number of local extrema, but there is always just one global maximum and minimum. To improve the performance and accuracy of the PSO algorithm, the number of local extrema should be as low as possible.

In (3.5), the additional integer penalty $y\phi(P_a)$ consists of two parts, y and $\phi(P_a)$ which are described in (3.6) and (3.4) respectively. Both y and $\phi(P_a)$ are functions of the variables, and they introduce additional local extrema into the objective function and complicate the search for the global extreme. The additional local extrema introduced by the integer penalty function could be one of the reasons for the poor performance of the mixed integer PSO.

3.2.2 ε value

The purpose of penalty parameter y in (3.5) is to add cumulative penalties such that the variables can converge to the integer values more rapidly. The penalty parameter y is computed by (3.6). The choice of the ε value is the crucial factor; however, no proper guidance is provided on the choice of the ε value.

It was found, through repeated simulations, that in the majority of the cases where the ε value is small, typically smaller than 0.1, $y(k)$ derived from (3.6) tends to grow continuously at a very rapid rate without any limitations, causing (3.5) to malfunction and no optimal solution can be found. In most cases of large ε valued, ε is always greater than E_C and $y(k)$ is always equal to $y(0)$ and the rate of convergence is very slow.

3.3 VOTING BINARY PSO APPROACH

From the above studies, the integer penalty function $y\phi(P_{a,b})$ seems to be the cause of the poor performances. By improving or eliminating this function completely, the performance of the algorithm should be improved. This is the motivation for the development of a novel binary PSO strategy, the voting approach.

The greatest advantage of the proposed voting approach is that the variables stay in binary format throughout the optimization procedures, hence eliminating the need for the integer penalty functions such as $y\phi(P_{a,b})$. The voting binary PSO approach is simple to implement and understand, yet effective in solving constrained binary optimization problems.

The voting approach is formulated based on the principles of the continuous PSO variable computation shown in (3.3). From Figure 3.3 it can be seen that the new particle position of a continuous variable is determined by four components. They are the current and previous position of the particle, the particle's best fitness position and the global best fitness position. The new position or state of binary particles must also be decided by these components. These four components will be referred to as the decision

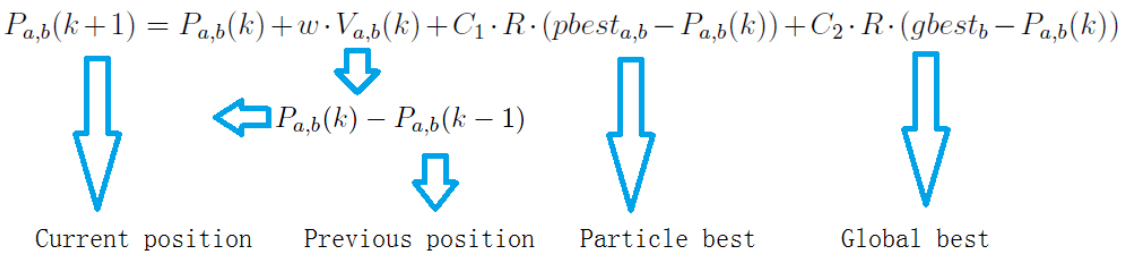

Figure 3.3: The four components that determine the future position of the particle.

components for the rest of the chapter.

In the case of only binary operations, these decision components will all be in binary format. Each of the four decision components can be imagined as members of the parliament and the future particle state is a legislation in which these members must decide by vote. The 1 or 0 of the binary value which each decision component takes on can be interpreted as an agree or disagree decision. Each of the decision components will "vote" according to its own state. The votes for the state of $P_{a,b}(k+1)$ can be computed by summing the state of these four decision components as shown below,

$$vote_{a,b}(k+1) = P_{a,b}(k) + P_{a,b}(k-1) + pbest_{a,b}(k) + gbest_b(k), \tag{3.9}$$

where

$vote_{a,b}(k+1)$	The votes count to determine the state of the b-th dimension of the a-th particle for the $(k+1)$-th iteration.
$P_{a,b}(k)$	The state of the b-th dimension of the a-th particle for the k-th iteration.
$P_{a,b}(k-1)$	The state of the b-th dimension of the a-th particle for the $(k-1)$-th iteration.
$pbest_{a,b}(k)$	The state of the b-th dimension of the best fitness solution achieved by the a-th particle up until the k-th iteration.
$gbest_b(k)$	The state of the b-th dimension of the best fitness solution achieved by any particle up until the k-th iteration.

If this outcome is greater than the expected value of $vote_{a,b}(k+1)$, which is 2, the particle state, $P_{a,b}(k+1)$, for the next iteration will be 1, otherwise it will be 0. This is illustrated by (3.10).

$$P_{a,b}(k+1) = \begin{cases} 1, & \text{if } vote_{a,b}(k+1) > E_{exp}(vote), \\ 0, & \text{if } vote_{a,b}(k+1) < E_{exp}(vote). \end{cases} \tag{3.10}$$

where

$E_{exp}(vote)$ The expected value of $vote$.

There is another important component in PSO, namely the randomness or craziness. It helps to protect the algorithm from being trapped in a local extreme.

Randomness is introduced into the continuous variable PSO by multiplying random numbers to the *pbest* and *gbest* values. This will not work for the proposed binary PSO, since *pbest* and *gbest* components are binary, which means there is a 50% chance that they are 0, and multiplication with a random number will have no effect.

The randomness will be added instead through a uniformly distributed random variable R_v with a range of $\pm r$. (3.9) now becomes

$$vote_{a,b}(k+1) = P_{a,b}(k) + P_{a,b}(k-1) + pbest_{a,b}(k) + gbets_b(k) + R_v. \tag{3.11}$$

If the four components can be considered as members of the parliament, then the random variable R_v can be seen as the president. It has the power to overthrow the voting result completely. It does so based on the value it takes on.

The degree of randomness described in this binary algorithm is referred to as the chance of an upset. An upset is when the outcome is a 0 when all four decision components voted for 1, or the outcome is a 1 when all four decision components voted for 0. The value of R_v must be smaller than -2 when all components vote for 1 and greater than 2 when they all vote for 0 to achieve an upset.

The chance of an upset can be accurately controlled by proper selection of the range r of R_v. Since R_v is a uniformed distributed variable, the required range can be computed using (3.12).

$$r = \frac{E(vote)}{1 - 0.02 \cdot x}, \tag{3.12}$$

where

x The desired chance of an upset in percent.

The advantage of this configuration is that the degree of randomness can be controlled precisely. The addition of R_v also eliminates the chance of a tie in the voting.

3.4 ALGORITHM JUSTIFICATION

To evaluate the performance of the proposed voting approach, it is tested against the mixed integer PSO algorithm and the binary optimization tool "*bintprog*" of MATLAB under scenarios similar to the case study used in this research.

The *bintprog* function is a reliable optimization tool that has been used effectively to solve many binary optimization problems such as in [53]. Because of its known reliability, its solution will be assumed to be the true optimal solution, and it is used as the reference to evaluate the accuracy of the results of the mixed integer PSO and voting approach.

The three algorithms are simulated to solve a pump operation optimal on/off scheduling problem. The optimization problem is described at the beginning of Chapter 5, Section 5.3. The formulation of the objective function and constraints are the same as the one described in Chapter 5, Section 5.4.4.

The simulations are conducted for three different control horizon durations, which are 12, 24 and 48 hours. The control horizon duration corresponds to a number of dimensions in a particle, hence the greater the control horizon duration, the greater the number of variables to be solved simultaneously.

Each of the algorithms is simulated repeatedly for 5 to 10 times for each scenario, depending on the duration of the simulations, and the averaged algorithm performance data are summarized in Table 3.1. Each of three methods is evaluated based on three criteria, namely iteration, time and deviation. Iteration is the number of iterations needed to solve the optimization problem for the mixed integer PSO and the voting approach. The number of iterations is chosen based on a balance between the solution accuracy and time consumption. Time is the amount of time required to complete the number of iterations, or in the *bintprog* case to derive the solution. Deviation is the percentage of the optimal solution of the variables deviating from the optimal solution of the *bintprog* method.

From Table 3.1, it can be seen that the voting approach outperforms the mixed integer PSO in the case study environment. The voting approach is able to find the optimal

Table 3.1: PSO strategy comparison results.

Control horizon	**Criteria**	**Mixed integer**	**Vote**	**Bintprog**
12	Iteration	10000	100	-
	Time (sec)	51.23	0.4663	0.03375
	% deviation (%)	20	0	-
24	Iteration	200000	1000	-
	Time (sec)	148.1	5.8945	1.974
	% deviation (%)	42	0	-
48	Iteration	1000000	20000	-
	Time (sec)	1352	230.0	3521
	% deviation (%)	58	0	-

solution faster and with more accuracy than the mixed integer approach. Hence it is justifiable to use the voting approach in this research.

3.5 MIXED INTEGER PSO ALGORITHM FORMULATION

The following is a description of the mixed integer PSO algorithm formulation used to solve the minimization problems in the later chapters.

Step 0:

Initialization. The continuous dimensions of a particle are initialized with a random value within a set of upper and lower limits according to (3.13). The binary dimensions are initialized according to (3.14).

$$P_{a,b} = L_p + R(U_p - L_p), \text{for } a = 1, ..., A_T, \text{ and } b = 1, ..., B_c, \tag{3.13}$$

where

L_p and U_p	The lower and upper limit of the continuous variable.
B_c	The total number of continuous variable dimensions in the particles.

$$P_{a,b} = \begin{cases} 1 & \text{if } R > 0.5, \\ 0 & \text{if } R \leq 0.5, \end{cases} \quad \text{for } a = 1, ..., A_T, \text{ and } b = B_c + 1, ..., B_T. \tag{3.14}$$

where

B_T The total number of dimensions in the particles, which is equal to the sum of the number of binary and continuous dimensions.

Particle velocity $V_{a,b}$ for the continuous dimensions are initialized in accordance with (3.13) with a range of between L_v and U_v. The previous state of the binary dimensions, $P_{a,b}(-1)$, also has to be initialized with a random binary value and they are initialized in accordance with (3.14).

Variables $pbest_a$ and $gbest$ are initialized with a large value.

Step 1:

Determine whether the stop criteria have been met. If so, go to Step 6, else go to Step 2.

Step 2:

Compute fitness, F_a, of each particle. F_a is the sum of two components, namely the objective function fitness, f_a, and the constraint fitness, c_a.

The objective function fitness, f_a, can be calculated by substituting the a-th particle into the objective function.

The constraint fitness c_a is calculated based on the degree of constraints violation. The constraint fitness is computed by (3.15).

$$c_a = \sum_{n=1}^{N_{con}} \sum_{b=1}^{B_T} (X + Y E_{c,a,b}), \tag{3.15}$$

where

X and Y	They are both constants.
$E_{c,a,b}$	The amount of violation of the c-th constraint caused by the particular dimensions.

Step 3:

Determine $pbest_a$ and $gbest$. The aim is to find the particle that results in the minimum fitness value.

The fitness of each particle, F_a, is compared to the best fitness value of that particle, $pbest_a$. If F_a is smaller than $pbest_a$, $pbest_a$ will be replaced by F_a and the $pbestp_a$, which stores the particle position of $pbest_a$, is replaced by P_a.

The fitness of each particle, F_a, is compared to the global best value $gbest$. If F_a is smaller than $gbest$, $gbest$ will be replaced by F_a and the $gbestp$, which stores the particle position of $gbest$, is replaced by P_a.

Step 4:

Determine the new particle position for the next iteration. The continuous and binary dimensions of a particle are treated separately. For the continuous dimensions, the particle position for the next iteration is computed according to (3.3). For the binary dimensions, the (3.9) and (3.10) are used.

Step 5:

Increment the iteration number by 1 and go back to Step 1.

Step 6:

Output $gbest$ as the lowest calculated operating cost and $gbestp$ as the optimal control strategy.

CHAPTER 4. PHYSICAL COORDINATION

An important part of the operation category focuses on the matching of equipment. In this chapter, an optimal pump capacity selection model is defined and tested. This optimization algorithm computes the optimal pumping capacities at different levels of a multi-level pumping system, based on the optimal operation strategy under different tariff structures, water demands and reservoir sizes.

The optimal pump capacity selection in this chapter focuses only on the fixed speed pumps, since ideally, an optimally selected pump should not require additional investments on flow rate adjustment devices such as valves and VSDs.

This chapter is divided into three sections, namely

- The formulation of the optimal pump capacity selection model
- The simulation test results
- The optimal design limitations.

4.1 OPTIMIZATION ALGORITHM

The aim of the optimal pump capacity selection algorithm is to select the optimal capacity of the pump, which will yield a minimum operation energy cost. The greater the pump capacity, the more operations can be shifted out of the peak period, and hence the greater the energy cost savings. However, greater capacity results in poor EE and higher energy consumption. The optimal pump capacity selection model selects the optimal pump capacity by considering the effects of the capacity of both EE and LS.

The objective function of the optimal pump capacity selection model is given below,

$$\min_{u_{r,i},q_r} \sum_{r=1}^{R_c} \sum_{i=1}^{I_c} c_i f_r(q_r) u_{r,i} Z + M_{md} C_{md}, \tag{4.1}$$

where

r	The level indicator and r=1,...,R_c.
R_c	The total number of levels.
I_c	The the number of control intervals in which all of the operation parameters can be assumed to be repeating.
Z	The number of repeating cycles of duration I_c within the control horizon and the product of I_c and Z represents the total number of control intervals in the control horizon.
i	The i-th discrete control interval and i=1,...,I_c.
$u_{r,i}$	The on/off status of the pump at the r-th level and i-th control interval.
q_r	The capacity of the pump at the r-th level in m^3/hour.
$f_r(q_r)$	The capacity-power function that finds the pump input power corresponding to the pump capacity.
c_i	The TOU energy cost for the i-th control interval.
C_{md}	The MD charge factor in R/kW.
M_{md}	The function that finds the MD.

The optimal value of $u_{r,i}$ and q_r need to be solved by the optimization algorithm over the control horizon. Note that q_r is the total capacity at the r-th level and it is up to the designer to decide whether this capacity will be achieved using a single pump or a combination of pumps.

This optimization model is formulated based on the tariff described in [19]. The MD charge described in [19] is a monthly charge based on the recorded MD for that month. Hence the duration of the control horizon, which is represented by the product of I_c and Z should be equivalent in time to one month. For example, in a month of 30 days in which operation is assumed to repeat every 24 hours, the choice of I_c and Z will be 24 and 30 respectively.

The MD is measured as the highest averaged demand in kVA during any complete half hour integrating period. The average power over a half hour interval (T, T+0.5) can be computed as,

$$2\int_{T}^{T+0.5} w(t)dt, \tag{4.2}$$

where

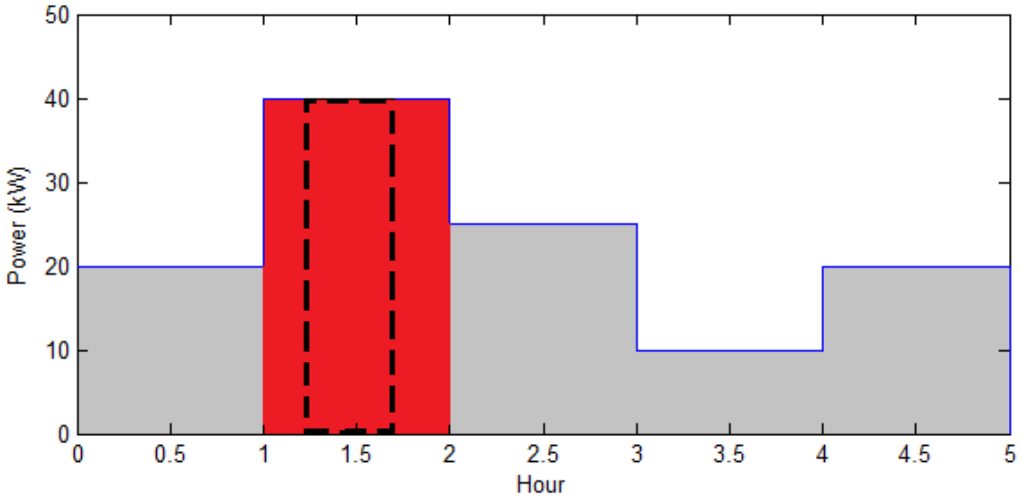

Figure 4.1: Graphical illustration of the MD property.

t	The time indicator.
$w(t)$	The instantaneous power consumption in kW as a function of t.
T	The starting point of a half-hour period.

It is assumed that the operation of the pump and therefore the pump power consumption, $w(t)$, will be taken as a constant unit within a control interval. Therefore, by choosing a control interval duration that is greater than or equal to half an hour, the half-hour MD period will fall completely within the control interval with the highest power consumption. The MD value will be approximately proportional to the power consumption of the control interval with the highest power consumption. This property is illustrated graphically in Figure 4.1.

In Figure 4.1, 5 hours of $w(t)$ is represented by the blue line and it varies on an hourly basis. The red colored block represents the control interval with the highest power consumption. The half-hour MD period is represented by the area encircled by the dash line.

Therefore, in conditions of control interval duration greater than or equal to the MD integrating period and where $w(t)$ remains constant within a control interval

$$MD = \max\{w(t)\}, \tag{4.3}$$

where

max	A function that finds the maximum value within an array of data.

The duration of the control interval is chosen to be one hour throughout this dissertation. Other reasons for this choice are that the TOU tariff varies on an hourly basis and a longer duration reduces the wear and tear from regular operational adjustments.

Based on (4.3), the MD value, M_{md}, in (4.1) can be computed as:

$$M_{md} = \max\{\sum_{r=1}^{R_c} f_r(p_r)u_{r,i} \ : i = 1, ..., I_c\}, \tag{4.4}$$

As shown in the literature review, the input power of a fixed speed pump can be computed using the hydraulic equation shown below,

$$p = \frac{9.81hq}{3.6\eta}, \tag{4.5}$$

where:

p	The input power to the pump in kW.
q	The capacity of the pumps.
h	The pressure head generated by the pump in m.
η	The efficiency of the pump.

The pump pressure head and the capacity can be related to each other using the system curve shown in Figure 4.2.

A system curve represents the required pressure from the pump to achieve a particular flow rate. This pressure is required to lift the water to the destination and overcome the friction of the pipes between the pump and its destination. This relationship is fixed regardless of the choice of pump.

In a multi-level pumping system, the piping arrangement at each level is different. Hence for every level of pumps, there is a unique system curve. A system curve can be estimated by the second order quadratic equation shown below,

$$h = Aq^2 + Bq + C, \tag{4.6}$$

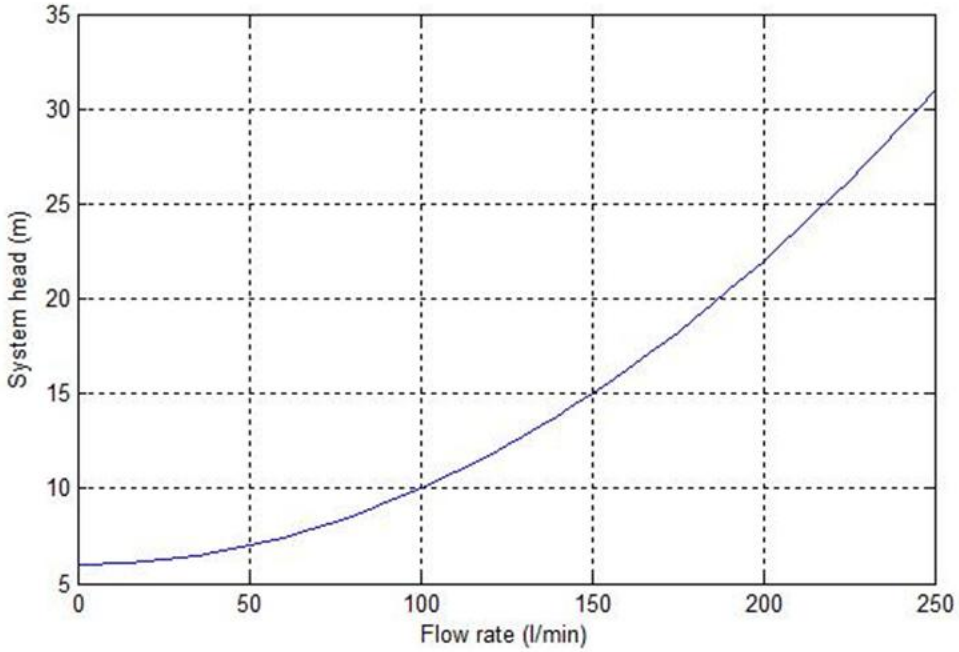

Figure 4.2: An example of a system curve.

where

A, B, C They are constants and are unique for a given system curve.

The operational efficiency η is assumed to be a constant. The power factor is assumed to be one. Substituting (4.6) into (4.5) yields the required capacity-power function.

It is important to note that this capacity-power function is a third order polynomial equation, hence the pump power consumption relates to the pump capacity cubically. This means that a small increase in capacity will be amplified into a much greater power consumption increase.

The water levels of the reservoirs must not exceed their upper and lower limits at any time during the operation. Hence the optimization algorithm is bounded by the following constraint,

$$LL_j \leq l_{j,i} \leq UL_j, \tag{4.7}$$

where

j	The reservoir indicator and j=1,...,J_c, where J_c is the total number of reservoir.
$l_{j,i}$	The level of the j-th reservoir at the i-th control interval.
LL_j and UL_j	The lower and upper level limits of the j-th reservoir.

The water level in the reservoir at the beginning of the $(i+1)$-th operational interval can be defined as:

$$l_{j,i+1} = l_{j,i} + \sum_{r}^{R_c} a_{r,i} u_{r,i} - d_{j,i}, \tag{4.8}$$

where

$a_{r,i}$	The flow rate of the r-th pump at the j-th reservoir at the i-th control interval.
$d_{j,i}$	The net amount of water inflow or outflow of the j-th reservoir from sources other than the pumps in m^3/hour.

4.2 SIMULATION RESULTS

A case study of one pump and one reservoir is considered such that the capacity selection ability of the algorithm can be focused on. Three simulations are performed under different scenarios, namely

- Design under high demand TOU tariff with sufficient reservoir storage volume
- Design under low demand TOU tariff with sufficient reservoir storage volume
- Design under high demand TOU tariff with insufficient reservoir storage volume.

The MD charge is ignored for the purpose of a more clear demonstration of a balanced EE and LS pump capacity selection.

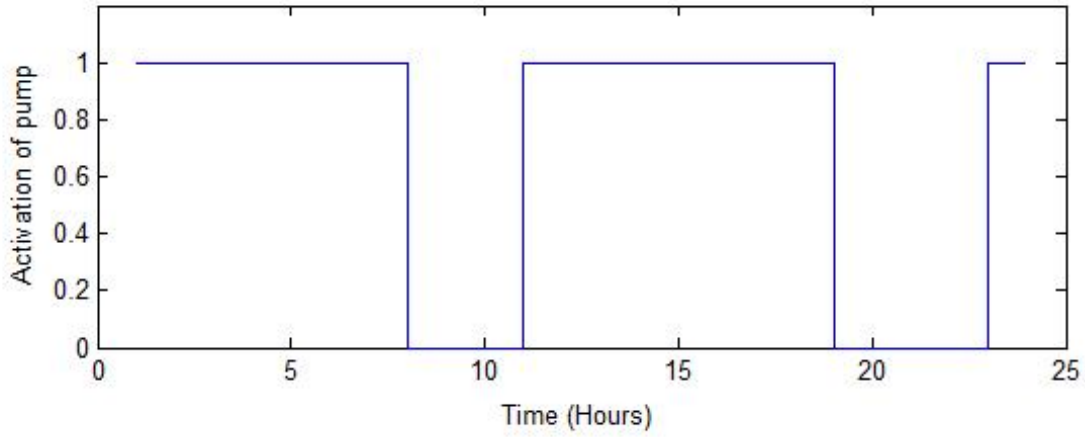

Figure 4.3: The optimal schedule of the pump.

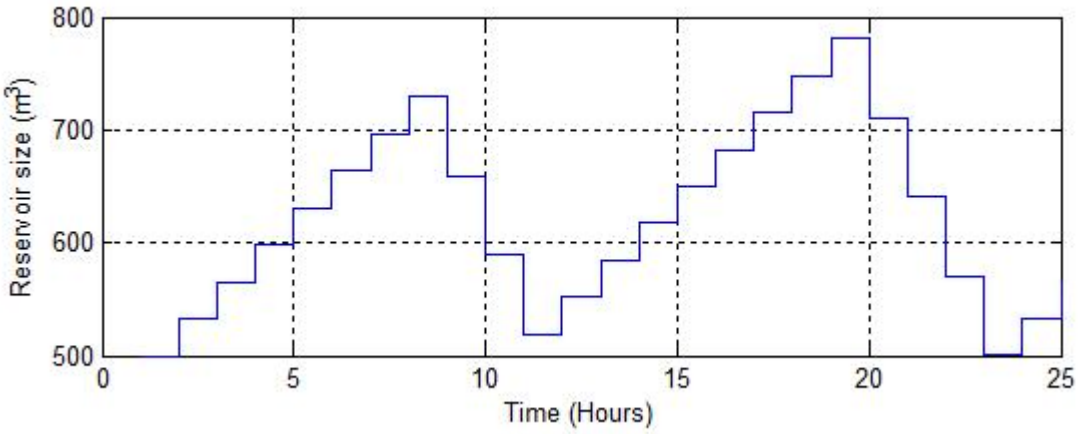

Figure 4.4: Change in reservoir level.

4.2.1 High demand TOU

An optimal design simulation is conducted under the high demand season TOU tariff. The lower limit on the reservoir is set to be 500 m^3, the upper limit of the reservoir is set at 1000 m^3. I_c is 24 hours. The demand is set to be constant at 70 m^3/hour such that,

$$d_i = 70, \ \forall i. \tag{4.9}$$

The optimal pump capacity is computed as 103.023 m^3/hour, and the corresponding optimal operation schedule and the change in reservoir volume are shown in Figures 4.3 and 4.4 respectively.

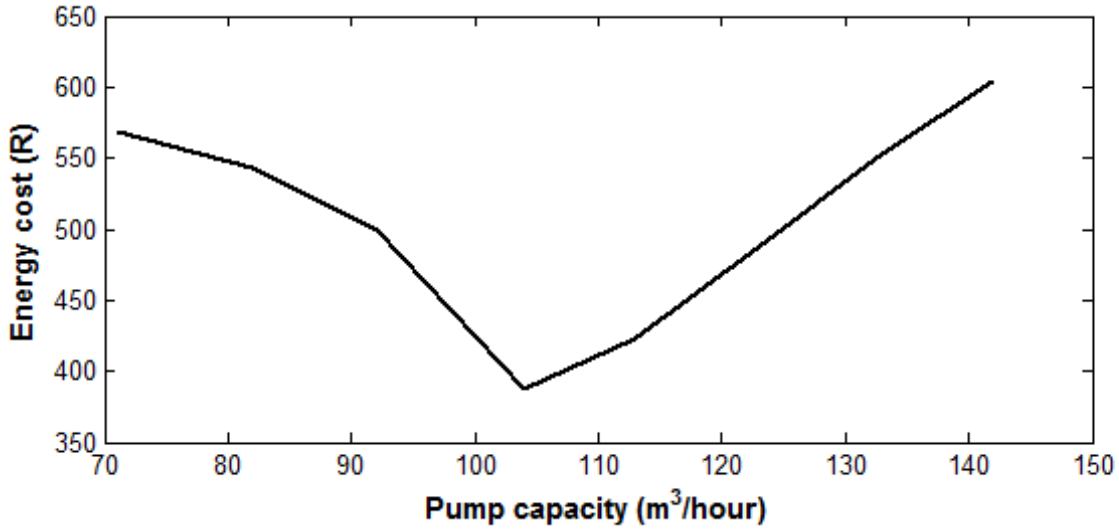

Figure 4.5: Relationship of operational energy cost and pump capacity.

Figure 4.3 demonstrates that the pump has enough capacity to shift the entire load out of the peak period. In Figure 4.4 it can be seen that during the 23-rd hour, which is the end of the peak period, the reservoir volume is at the minimum level. These two figures demonstrate that the pump capacity is just enough to shift the load completely out of the peak period.

Because the peak energy price is about six times more expensive than the off-peak one, the LS component is expected to be the dominating saving contributor, and the algorithm to maximize the level of LS. The EE component only prevents the pump capacity from being greater than what is required from LS.

To prove that this solution is optimal, a series of simulations are conducted to investigate the changes in the energy cost associated with pump capacity selection. These simulations compute the operational energy costs for different pump capacities ranging from 70 m^3/hour to 140 m^3/hour. The operational parameters are the same as the previous optimal selection simulation. The simulated energy costs of the optimal operations of the different pump capacities are plotted in Figure 4.5.

The typical pump capacity choice of an EE only optimal design algorithm is most likely to be just above 70 m^3/hour, and as seen from Fig. 4.5 the corresponding energy cost is very high. As pump capacity increases, more loads can be shifted out of the peak hours and the energy cost is reduced. The optimal pump capacity is shown to be 103 m^3/hour. At this point the pump manages to shift all of the loads out of the peak period. Additional increase in pump capacity offers no additional LS savings. As mentioned earlier, the flow rate input power relation is a cubic one, and a small increase in the capacity results in a much greater input power and energy consumption increase.

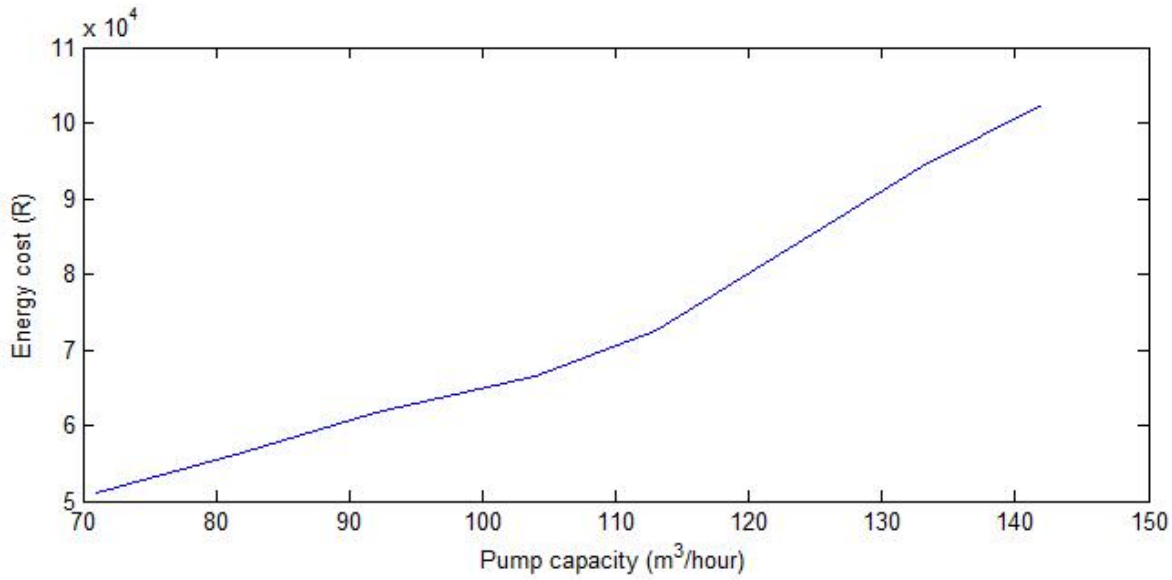

Figure 4.6: The relationship of operation energy cost and pump capacity.

Therefore, beyond the optimal point further capacity increase only results in an increase in the energy cost.

It can be seen that LS and EE are two contradictory terms; the improvement of the one is at the cost of sacrificing the other. The optimal capacity selection model maximizes the combined saving contributions from LS and EE and minimize the operational energy cost.

4.2.2 Low demand TOU

Another simulation is conducted under the low demand TOU tariff. The rest of the simulation parameters are the same as the previous high demand TOU simulation. The optimal pump capacity is computed as 70.0132 m^3/hour. This is the same as the demand, which means that no LS is permitted despite the higher peak hour electricity price. This appears to be unreasonable, but the following investigation shows that the simulation result is correct.

A series of simulations are conducted to investigate the changes in the energy cost associated with pump capacity change. The procedures are the same as the previous high demand TOU tariff case, except that the tariff is changed to low demand TOU. The results of the simulations are plotted in Figure 4.6. It can be seen that the pump capacity with minimum operational energy cost is 70 m^3/hour.

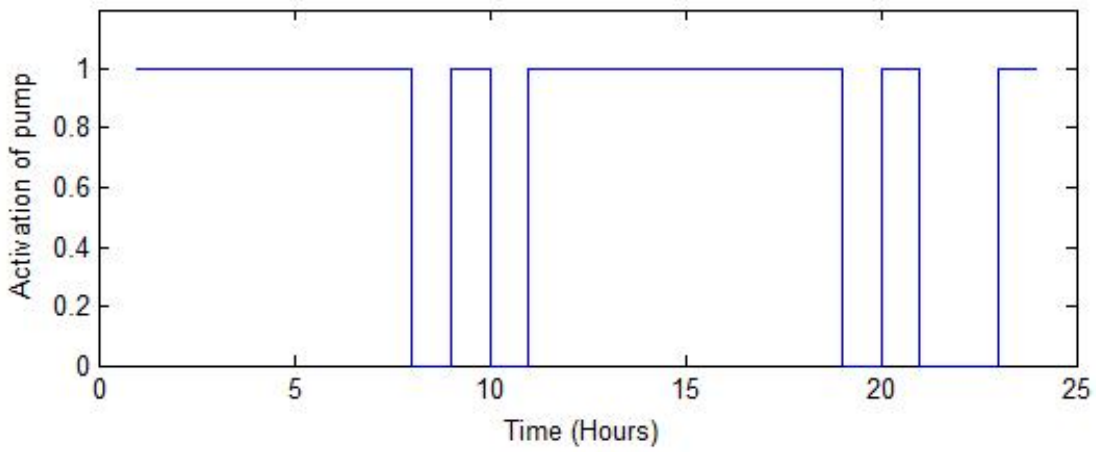

Figure 4.7: The optimal on/off schedule of the pump.

This result shows that increasing the capacity of the pump to allow LS is not always the solution of choice in the case of water pump operation when TOU tariff is involved. The additional capacity needed to shift the load out of the peak hours can cause a significant increase in the input power of the pump, which might be greater than the savings from LS.

4.2.3 Reservoir limitation

Additional simulation is conducted under the high demand TOU tariff with a reservoir size that is insufficient to support a high level of LS.

The upper limit of the reservoir is set to be 700 m^3, while the lower limit remains the same. The computed optimal pump capacity is 90.588 m^3/hour. This is significantly lower than that of the computed capacity in Section 4.2.1. Since the level of LS is restricted by the reservoir size, there is no need for such a high capacity pump. Hence the algorithm chooses the smallest pump capacity that is capable of achieving the limited level of LS.

The optimal operation and the reservoir level changes are plotted in Figures 4.7 and 4.8. It can be seen that the level of LS is significantly restricted by the reservoir size, and the pump capacity is sufficient to allow the full utilization of the available reservoir storage capacity.

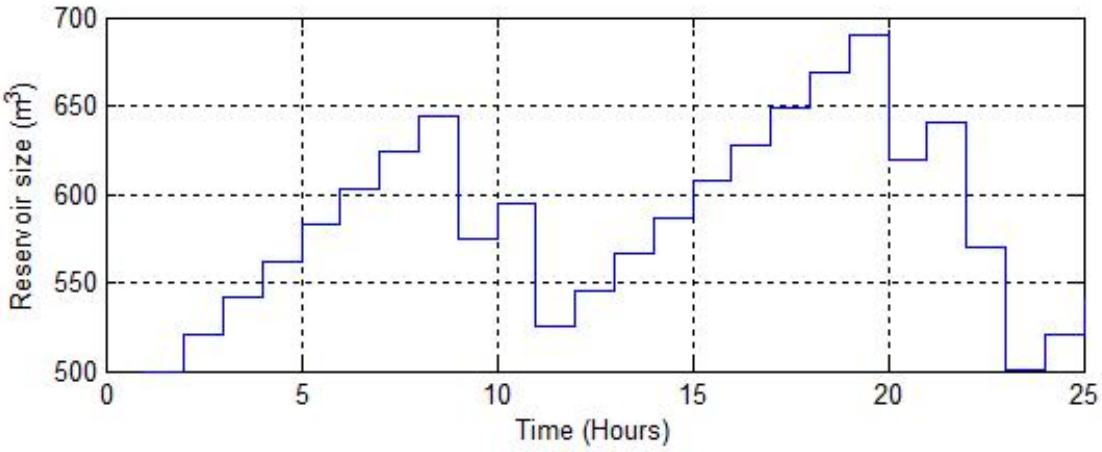

Figure 4.8: The reservoir level variation.

4.2.4 Purchase cost of the pump

The purchasing cost differences associated with different pump capacities is small in comparison to the pump life cycle energy cost, hence the purchase price of a pump is not included in the algorithm.

4.3 DESIGN ALGORITHM LIMITATIONS AND SOLUTION

Rigidness is an issue of optimal design. The optimal design tends to lose its optimality when the operational parameters change, for example change in tariff and demand. Designers often have to compensate for the risks of parameter variation by designing for the worst case scenario, which will significantly reduce operational efficiency.

Ideally, a flexible pump control mechanism can be used to compensate for this design rigidness. This flexible controller should be easily adjusted to adapt to the system changes without additional hardware modifications, ensuring that the operational energy cost remains minimal.

CHAPTER 5. TIME COORDINATION PART I: OPEN-LOOP CONTROL

The second part of the operation category focuses on the optimal operation of the equipment. This chapter proposes and analyzes an open-loop optimal pump control strategy with the objective of minimizing the operational energy cost. This optimal control system is flexible enough to adapt to different operational parameter variations and hence compensates for the inflexibility of the design model.

The proposed control system is called a VSD on/off controller. As the name implies, this system consists of both a VSD and an on/off controller. The VSD controller allows the pump to operate at the lowest flow rate possible to maximize the EE. The on/off controller allows LS to take place. Hence this system employs a combination of both EE and LS techniques to minimize the operational energy cost.

The VSD on/off control is best suited to single pump operations, in other words, one pump at each level. The purpose of the VSD is to allow flow rate adjustments. For multiple interconnected pumps at the same level, the adjustment in the net flow rate can be achieved by switching on a different number of pumps. This type of multi-pump control is an effective energy cost reduction strategy, as shown in [54]. Using VSD on/off control in multiple interconnected pumps operational control will offer more precise control and further improved EE; however, these improvements might not be significant enough to justify the initial cost, since VSD on/off control requires a VSD for each pump. Therefore, for multiple interconnected pumps' operation, the method illustrated in [54] is recommended. For the rest of the text, it is assumed that there is only one pump at each level of the multi-level pumping system.

This chapter is divided into four sections, namely

- The formulation of the open-loop optimal control objective function
- The formulation of the operational flow-power model
- The simulation results

- The energy costs comparison.

5.1 OBJECTIVE FUNCTION

The objective is to minimize the operational energy cost of a multi-level pumping system over a control horizon. The energy cost consists of both TOU and/or MD charges. The objective function is defined as,

$$\min_{q_{r,i},u_{r,i}} \sum_{r=1}^{R_c} \sum_{i=1}^{I_c} v_r(q_{r,i}) u_{r,i} c_i Z + C_{md} M_{md}, \tag{5.1}$$

where:

$q_{r,i}$	The flow rate setting of the pump at the r-th level at i-th control interval.
$v_r(q_{r,i})$	A function that finds the pump input power corresponding to a flow rate setting based on the flow-power function defined in Section 5.2.

$$M_{md} = \max\{\sum_{r=1}^{R_c} v_r(p_{r,i}) u_{r,i} \ : i = 1, ..., I_c\}, \tag{5.2}$$

The optimal values of $q_{r,i}$ and $u_{r,i}$ need to be solved by the optimization algorithm over the control horizon.

The water level constraints shown in (4.7) and the reservoir level equation in (4.8) also apply to the open-loop optimal control model.

5.2 FLOW-POWER RELATION FORMULATION

This section illustrates the formulation of the flow-power function.

Two approaches are described in this section, namely

- The analytical approach
- The measurement approach.

The analytical approach is to formulate the flow-power function using the manufac-

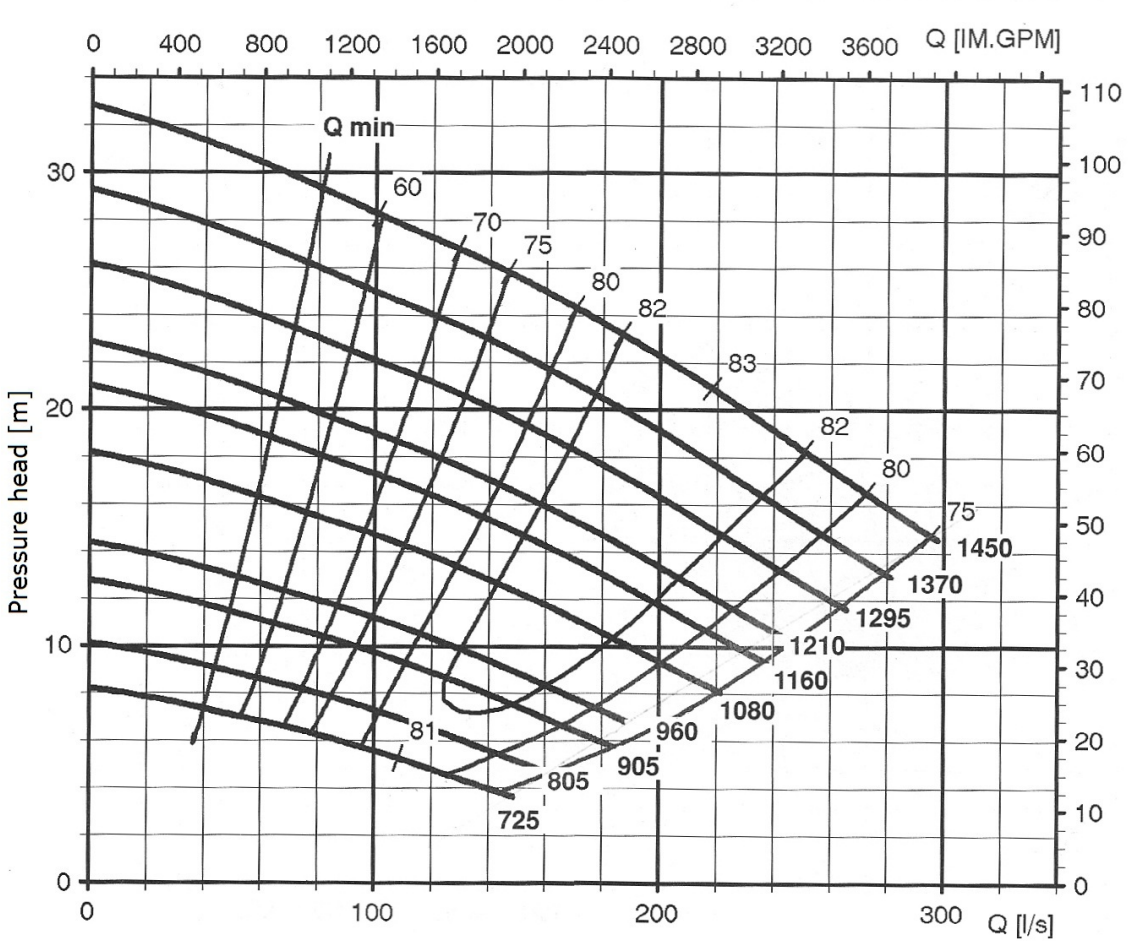

Figure 5.1: Example of a pump characteristic curve [77].

turer's pump data booklet and other available system information without any physical measurements. The measurement approach is to conduct measurements physically and formulate the flow-power function by interpolating the collected data.

5.2.1 Analytical approach

The analytical approach derives an approximation of the pump system flow-power relationship from available pump characteristic information, the system information and the affinity laws.

The information regarding the hydraulic performance and power consumption of a pump is locked within the pump characteristic curves, which include the pump performance curves shown in Figure 5.1 and the pump power curves shown in Figure 5.2.

Each of the parallel curves in Figure 5.1 represents the relationship between the flow rate, q, and the pump generated head, h, for a particular motor rotation speed, n. Each of

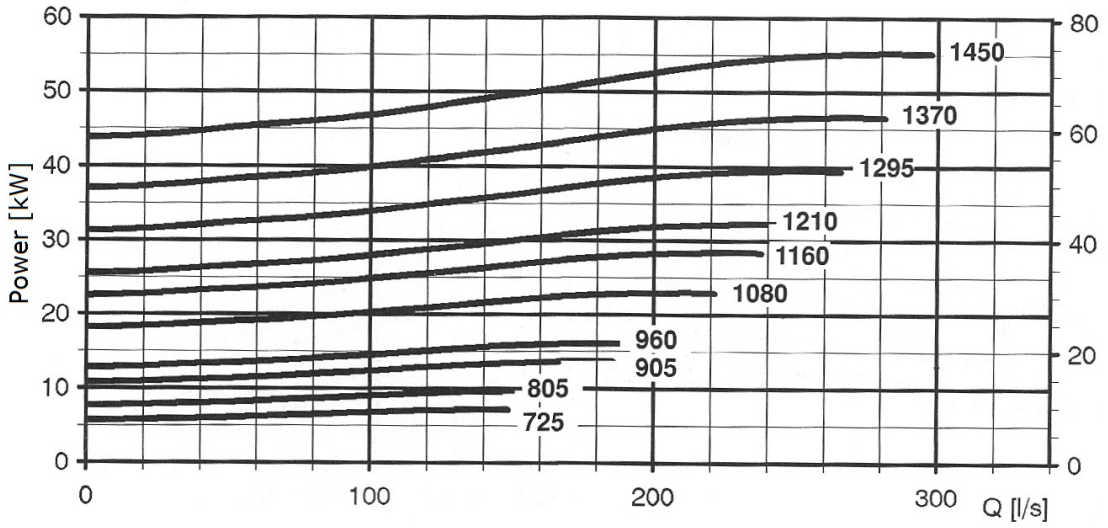

Figure 5.2: Example of a pump power curve [77].

the curves can be mathematically estimated by a second order quadratic equation. The top curve of amongst the many parallel performance curves represents the relationship at the full motor rotation speed, n_{full}, between the flow rate, q_{full}, and the generated head, h_{full}. The corresponding mathematical estimation of this full rotation speed performance curve is shown in (5.3),

$$h_{full} = Dq_{full}^2 + Eq_{full} + F, \tag{5.3}$$

where

D, E, F They are constants and they are derived from the full motor rotational speed performance curve.

The power curves in Figure 5.2 illustrate the pump power consumption, p, for different flow rates at different speeds. From the capacity-power function of Chapter 4, Section 4.1, it can be seen that the relationship between the flow rate and the power consumption is a third order relationship. In addition, most of the power curves, such as the one in Figure 5.2, have shown the third order quadratic equation characteristic "s"-shape. Therefore a third order quadratic equation is used to approximate the power curves. The quadratic equation for the full motor rotation speed power curve is shown in (5.4),

$$p_{full} = Gq_{full}^3 + Hq_{full}^2 + Iq_{full} + J, \tag{5.4}$$

where

p_{full}	The power consumption of the pump at full motor rotation speed.
G, H, I, J	They are constants and are derived from the full motor rotation speed power curve.

Note that the pump performance curves represent the possible operating points of the pump. Pumps with rotation speed adjustment devices, such as VSDs, can operate at any point in the area between the top and bottom curves. The exact point of operation is determined by the influence of system characteristics and the motor rotation speed.

The characteristics of the system in which the pump operates is represented by the system curve. The system curve is described in detail in Chapter 4, Section 4.1 and is shown in Figure 4.2.

The affinity laws [48] provide a generalized method to predict the changes in the pump flow rate, generated head and power consumption with respect to the change in the motor rotation speed of a free-running pump, in other words, a pump without influence from the system. The affinity laws can be rewritten in the following formats,

$$q_{full} = \frac{n_{full}}{n} q, \tag{5.5}$$

$$h_{full} = (\frac{n_{full} h}{n})^2 h, \tag{5.6}$$

$$p_{full} = (\frac{n_{full}}{n})^3 p. \tag{5.7}$$

Let $s = \frac{n}{n_{full}}$ and substitute (5.5) (5.6), and (5.7) into (5.3) and (5.4), yield,

$$h = Aq^2 + Bsq + Cs^2, \tag{5.8}$$

$$p = Gq^3 + Hq^2 s + Iqs^2 + Js^3. \tag{5.9}$$

The performance and power consumption function of (5.3) and (5.4) are transformed into functions of both motor rotational ratio and flow rate demonstrated in (5.8) and (5.9).

A speed-flow relationship is a function that defines the relationship between the motor rotational speed and the flow rate of a pump system. The speed-flow relationship can be formulated by equating the h of (4.6) and (5.8). This rotational speed flow rate

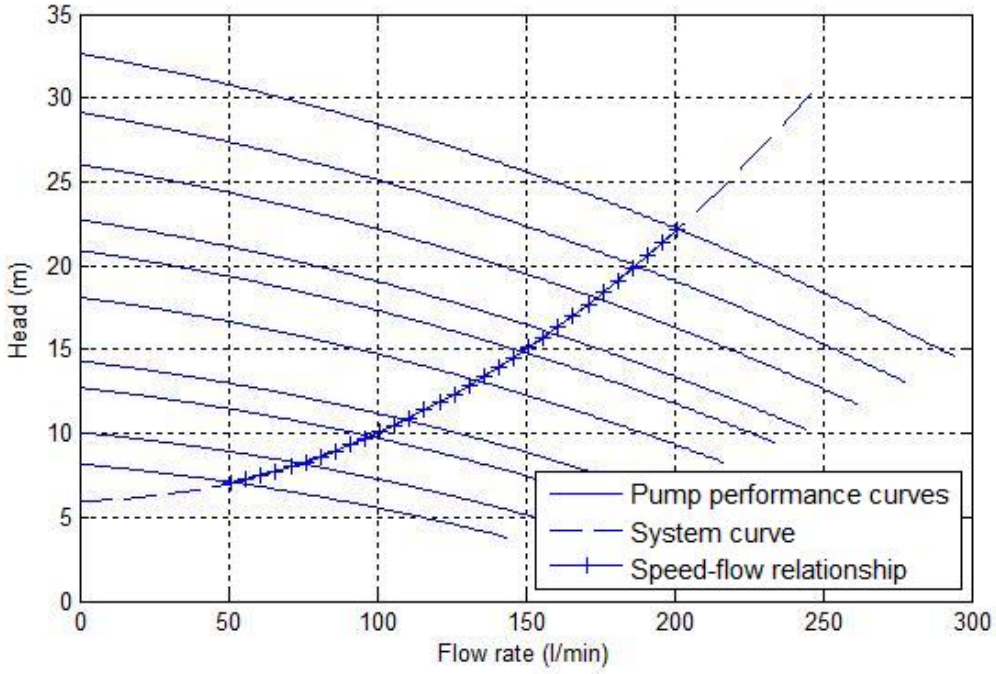

Figure 5.3: The pump power curve redrawn from the interpolated equation.

relationship can be estimated using (5.10),

$$s = Kq + L \tag{5.10}$$

where K, L are constants.

The speed-flow relationship described in (5.10) can be illustrated graphically in Figure 5.3. The operating flow rate of a pump is determined by the intersection of the system curve and the pump characteristic curves, which is indicated by the curve marked by "+" in Figure 5.3. The pump system can operate at any point on the curve marked by "+" with different motor rotational speed settings, and the relationship between the motor rotational speed and the operating point, or the flow rate, is represented by (5.10).

Equation (5.10) can be used to compute the VSD speed control settings based on the required flow rates.

The flow-power function can be derived from (5.10) and (5.9). The result function can be estimated using the third order polynomial equation shown in (5.11),

$$p = Mq^3 + Nq^2 + Oq + Q, \tag{5.11}$$

where

M, N, O, Q They are constants.

The analytical approach can be summarized into the steps shown below, and the MATLAB codes that are used to derive the flow-power function are shown in Appendix B.

1. Interpolate the full motor rotational speed pump performance curve into (5.3) and obtain the values of constants D, E and F.
2. Interpolate the full motor rotational speed pump power curve into (5.4) and obtain the values of constants G, H, I and J.
3. Interpolate the system curve into (4.6) and obtain the values of constants A, B and C.
4. Derive (5.10) based on (4.6) and (5.8).
5. Derive (5.11) based on (5.10) and (5.9).

For the pumps at each level, a separate flow-power relation must be derived. The flow-power relations are not interchangeable between two pumps unless both the pumps and systems are the same.

5.2.2 The measurement approach

The measurement approach is the preferred approach, since the derived flow-power function is a more accurate and up-to-date representation of the pumping system than the analytical approach. Also, by conducting physical measurements in operational conditions, the system characteristics are automatically included.

To derive the flow-power function, a set of different pump flow rates and power consumption values are recorded and interpolated into the flow-power function shown in (5.11). There are four constants in (5.11), therefore at least four measurements are required. Because of the poor accuracy of the flow rate measuring devices, this number should be at least doubled to eight. These data should cover the entire flow rate range of the pump.

The following steps describe a suggested measuring procedure,

1. Make sure that the pump is in its normal operating conditions, such as being properly installed and pumping the correct fluids.
2. Set the motor to operate at its maximum rotation speed.
3. Record the motor rotation speed, the flow rate and the power consumption.
4. Reduce the motor rotation speed and repeat the measurements.
5. Repeat step 4 until the manufacturer-specified minimum rotation speed is reached.

The collected flow rate and power consumption data are used to formulate the operation flow-power function utilizing interpolation tools. The recorded motor rotation speed and the corresponding flow rates are used to formulate the speed-flow relationship.

5.3 SIMULATION RESULTS

In this section, a series of simulations are performed to evaluate the VSD on/off control system.

The VSD on/off optimal control model is simulated based on a one pump one reservoir case study in order to focus on the saving ability of the VSD on/off controller. In this case study the pump is pumping fresh water into a reservoir, while the demand is draining water from the reservoir. The water demand is summarized in (5.12).

$$d_i = \left\{ \begin{array}{ll} 55, & \mathrm{i} \in [0, 8] \\ 90, & \mathrm{i} \in [8, 16] \\ 75, & \mathrm{i} \in [16, 24]. \end{array} \right\} \tag{5.12}$$

The speed-flow rate function for this case study is computed to be

$$s = 0.0071q + 0.2791. \tag{5.13}$$

The maximum and minimum motor rotation speeds are 1450 and 960 rpm. The corresponding maximum and minimum flow rates are 102 m^3/hour and 54 m^3/hour respectively. The upper and lower limits of the reservoir are 1000 m^3 and 500 m^3 .

The flow-power function for the pump is formulated as,

$$p = (3.8969e-6)q^3 + (2.1851e-5)q^2 + 0.01117q + 0.13102. \tag{5.14}$$

The simulations are conducted under different tariff structures to illustrate the adaptivity of the proposed system; these tariff structures include:

- High demand TOU
- High demand TOU with MD tariff
- Low demand TOU
- Low demand TOU with MD tariff
- MD charge and flat tariff.

The simulation results are summarized in the flowing sub-sections.

5.3.1 High demand TOU

Figure 5.4 illustrates the 24-hour variation in the TOU tariff, computed pump flow rate and reservoir level variations. Since the electricity price during peak hours is significantly higher, the algorithm shifts the loads as much as possible to the off-peak and standard periods. This is clearly illustrated during the morning peak hours (8:00 to 11:00) where the on/off controller switches off the pump completely. During the evening peak hours (19:00-23:00) the pump has to be switched on twice to prevent the reservoir level dropping below the lower limit. When the pump is switched on during the peak hours, it is operating at the minimum operational flow rate to keep the cost down.

It can be observed from the reservoir level sub-plot that the reservoir level constraint is satisfied. It can also be observed that water is being accumulated in the reservoir prior to the peak period when the electricity cost and the water demand are low.

5.3.2 High demand TOU with MD

Figure 5.5 shows the variation in the pump flow rates under high demand TOU with MD charge. The result appears to be similar to Figure 5.4. However, in Figure 5.5 the output flow rates of the pump are more even and leveled in the periods other than the peak hours. This is due to the effect of the additional MD charges. As mentioned

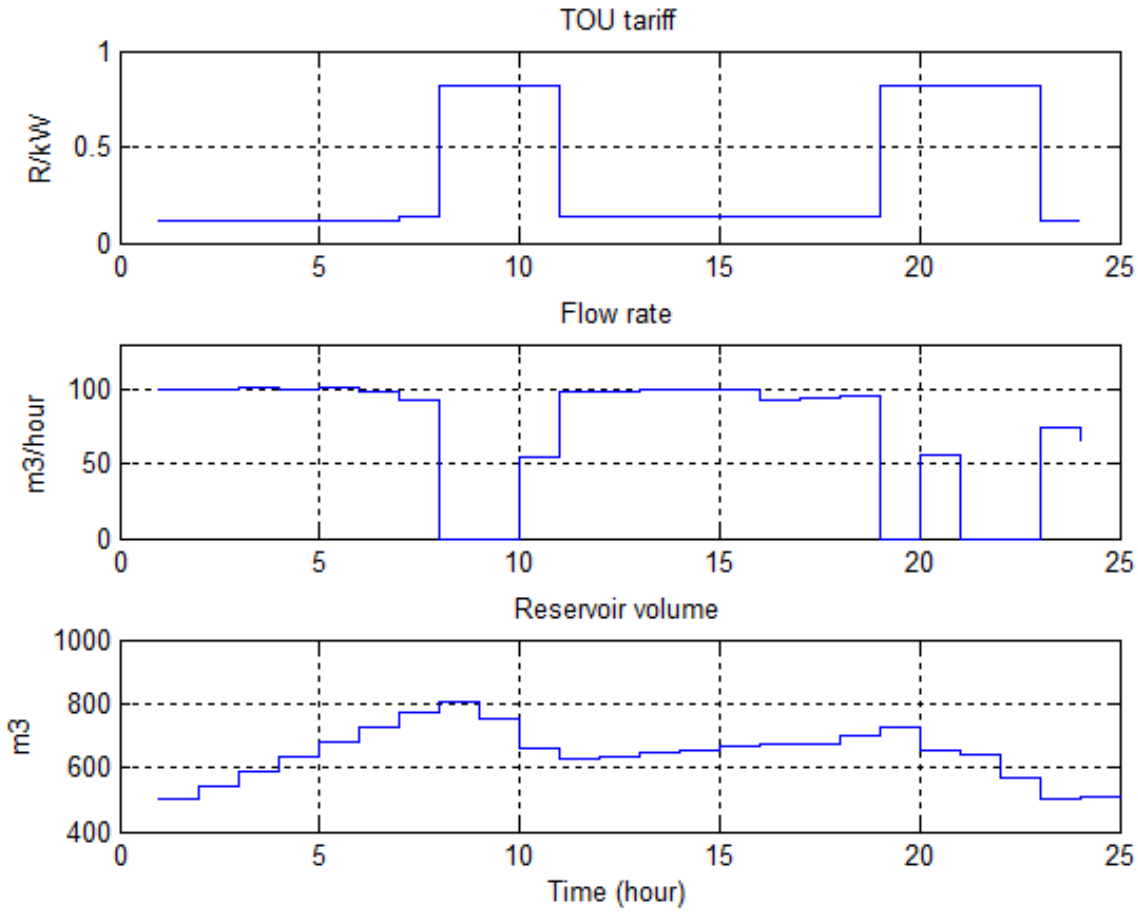

Figure 5.4: Illustration of the 24-hour changes to the tariff, flow rate and reservoir level under high demand TOU tariff.

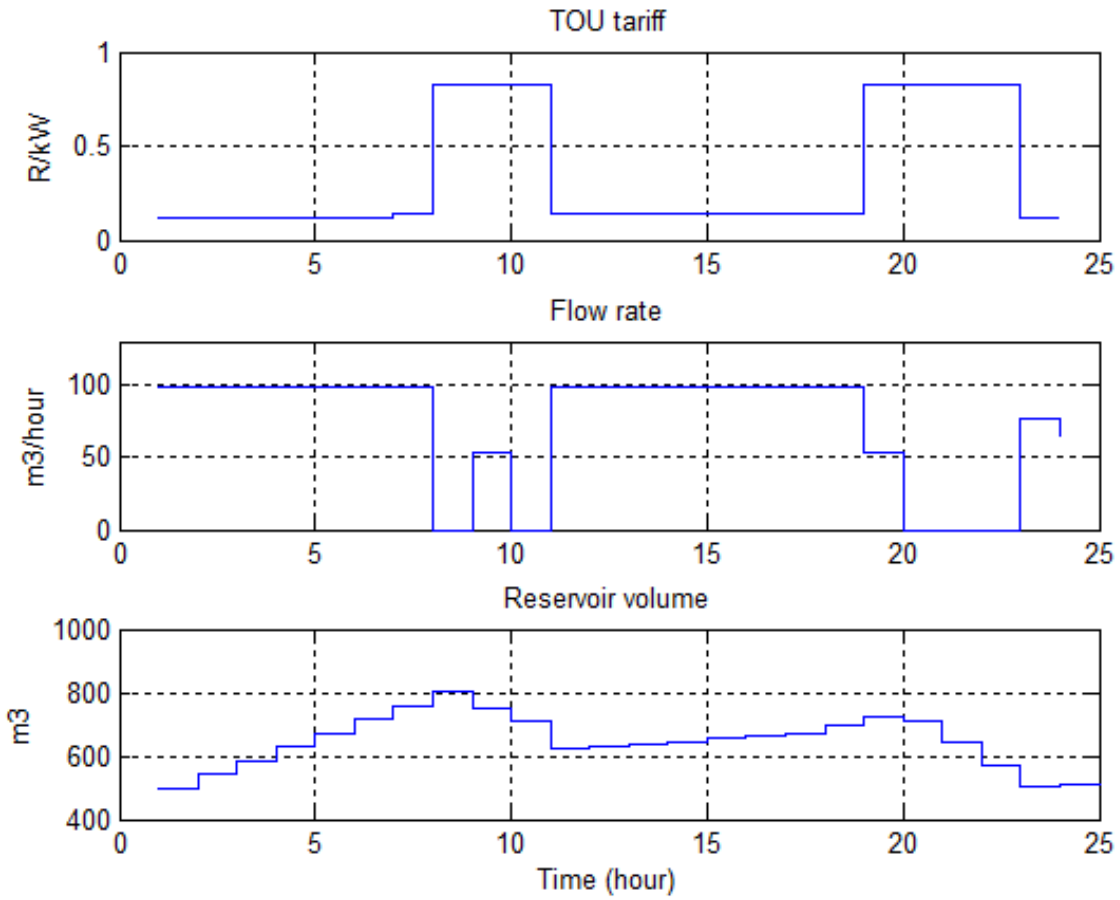

Figure 5.5: Illustration of the 24-hour changes to the tariff, flow rate and reservoir level under high demand TOU tariff and MD charge.

earlier, the MD charge is a charge based on the maximum power demanding period. In order to minimize this cost, the algorithm spreads the loads out as evenly as possible and therefore limits the pump to operate at a slightly lower and constant rate.

Figure 5.6 illustrates the differences in the power consumption of the pump flow rate settings presented in Figures 5.4 and 5.5. Since the flow-power function is cubic, this maximum flow rate reduction of 2.8% in 5.5 is amplified to a 6.62% reduction in the maximum demand.

5.3.3 Low demand TOU

Figure 5.7 shows the pump flow rates under low demand TOU tariff. The flow rate sub-plot differs significantly from the one in Figure 5.4. The most significant difference is that the pump is no longer switched off during peak hours but rather operating at a lower rate. Since the peak-hour electricity price of the low demand TOU tariff is much lower than the high demand one, it becomes more profitable to sacrifice some of the LS

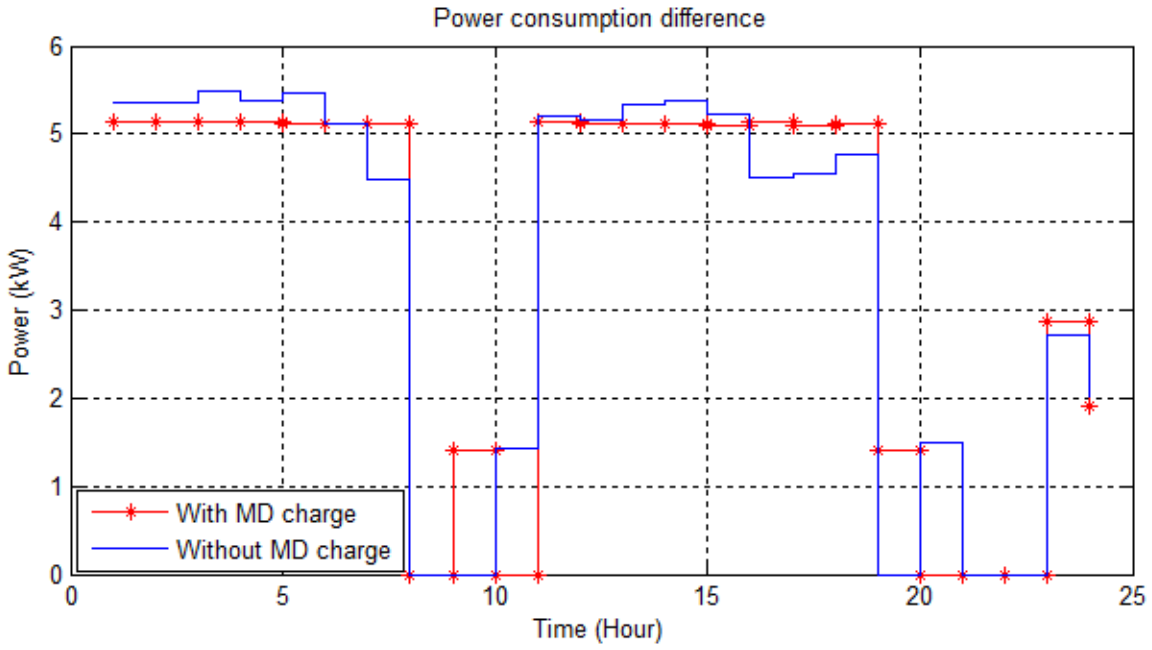

Figure 5.6: The demand reduction when charged with additional MD tariff.

for EE. As mentioned earlier, a slight reduction in the flow rate results in a significant reduction in power consumption. Therefore, by operating the pump during peak hours, the overall pump flow rate in other periods can be reduced. The overall EE is improved and energy consumption cost is reduced.

5.3.4 Low demand TOU with MD

The pump flow rates under summer TOU and MD tariff are shown in Figure 5.8. As expected, the flow rates are leveled at a very constant rate. The peak-hour operation is further increased to allow a further reduction in the maximum flow rate and MD cost.

Figure 5.9 illustrates the differences in power consumption of the flow rate settings presented in Figure 5.7 and 5.8. The MD is reduced by 34.12% in this case. The reason for such a high level of reduction in MD in comparison with the high demand TOU case is that the average energy cost of the low demand TOU tariff is much lower than the average energy of the high demand TOU tariff and the additional MD charge has a much greater weight in the total operational cost in the low demand case. Hence greater effort is spent to reduce the MD cost.

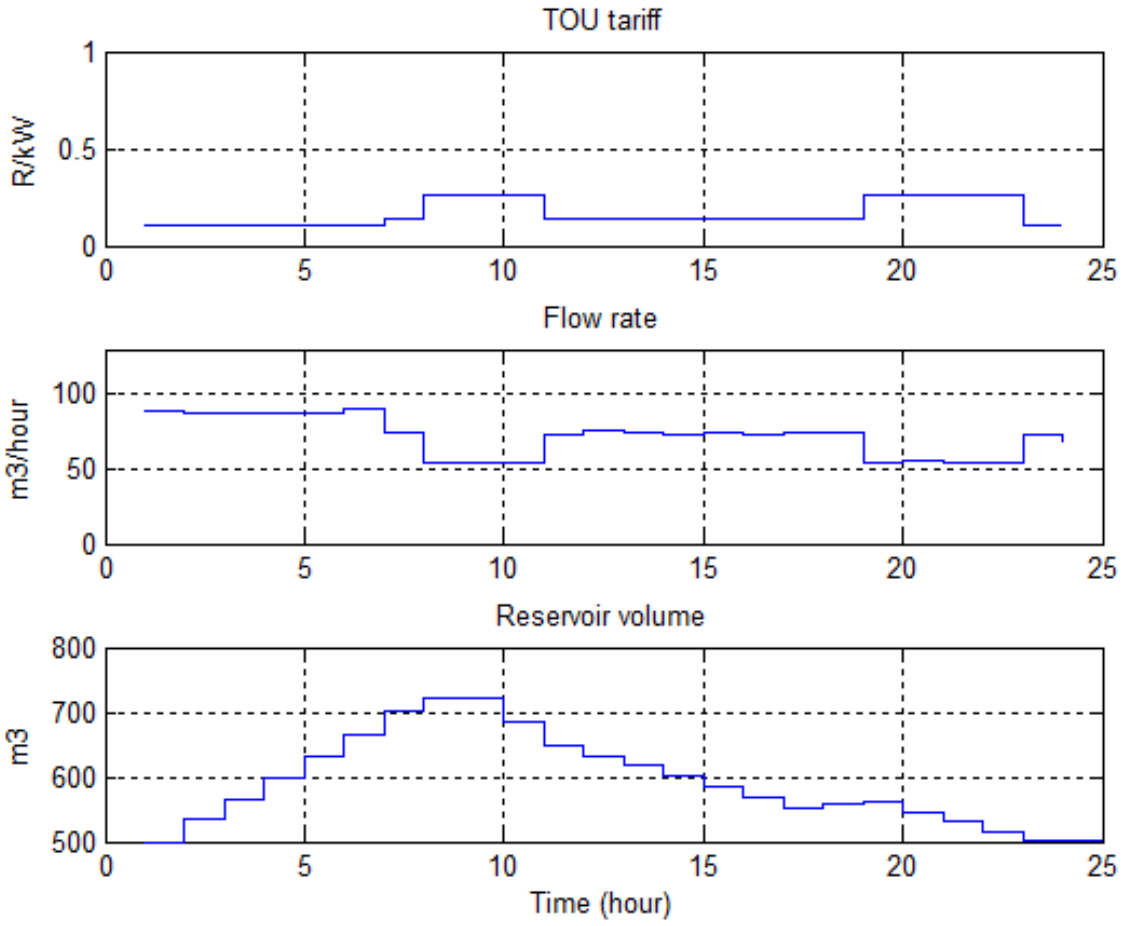

Figure 5.7: Illustration of the 24-hour changes to the tariff, flow rate and reservoir level under low demand TOU tariff.

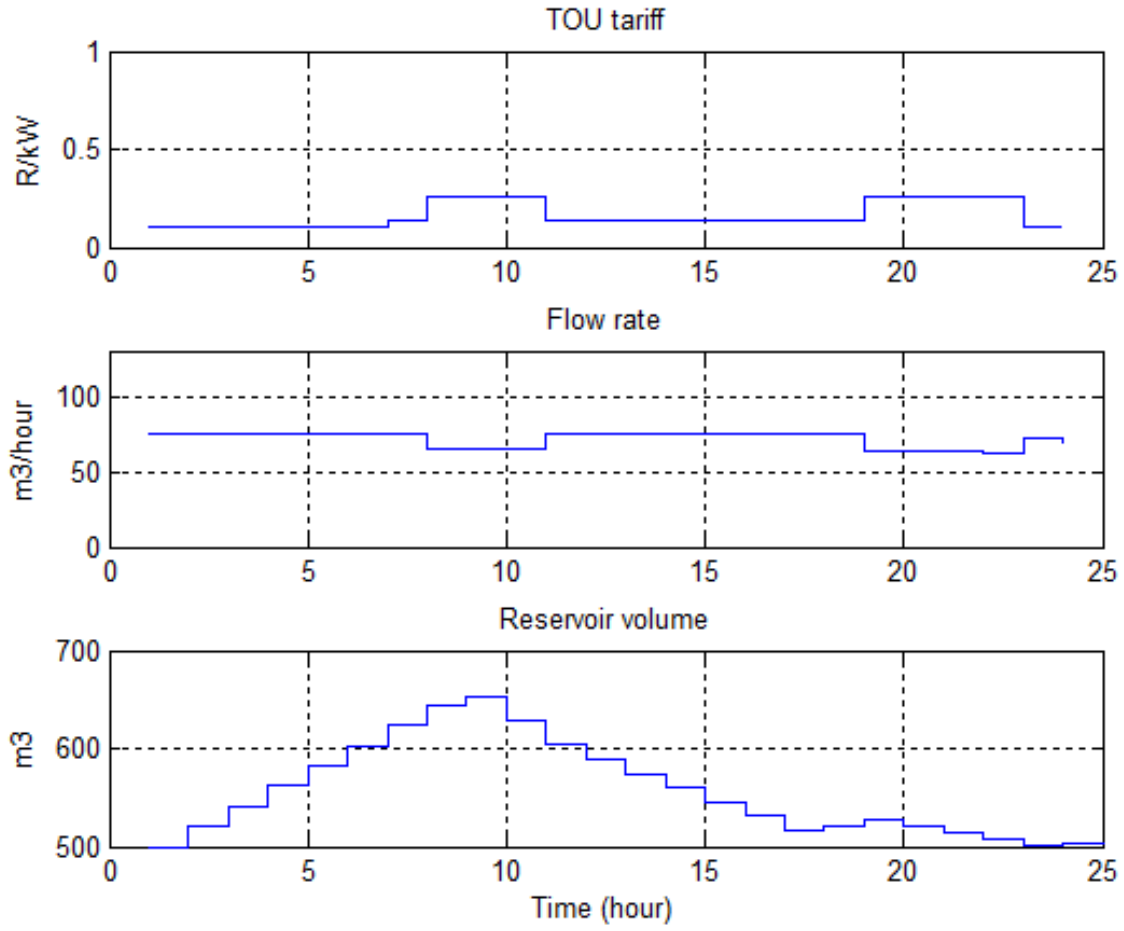

Figure 5.8: Illustration of the 24-hour changes to the tariff, flow rate and reservoir level under low demand TOU tariff and MD charge.

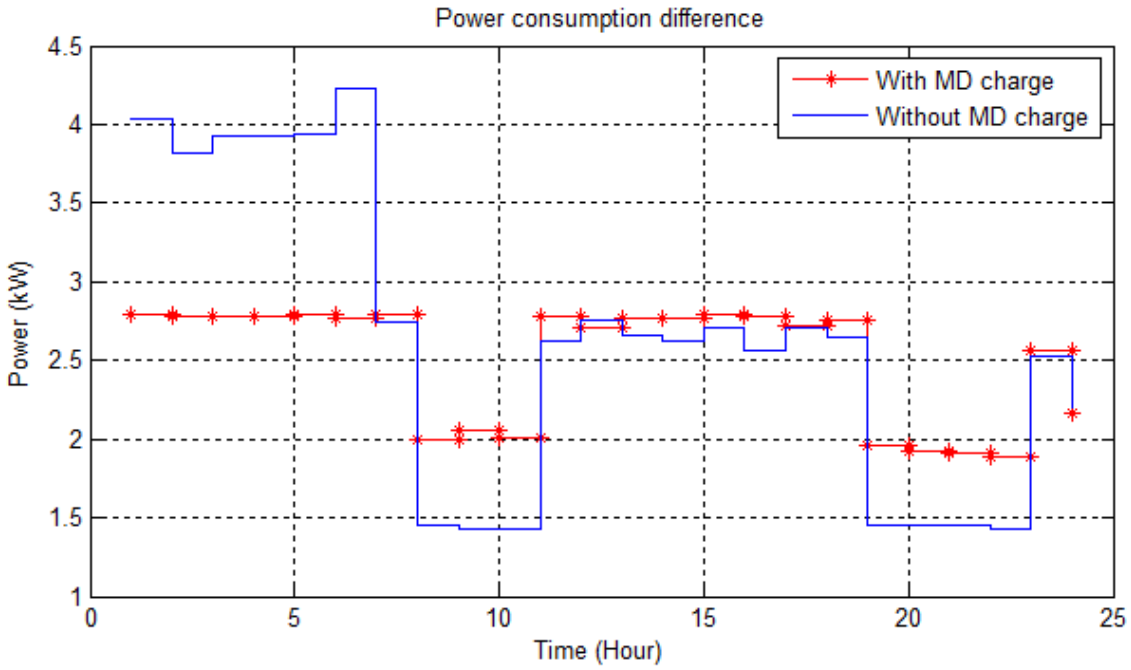

Figure 5.9: The demand reduction when charged with additional MD tariff.

5.3.5 MD charge and flat tariff

Figure 5.10 illustrates the computed optimal strategy under a flat tariff without MD charges for a 24-hour period. Since there is no TOU tariff, EE is the only cost reduction contributor. The control model reduces the flow rates to a minimum level to maximize the EE improvements. The simulation result under a flat tariff with MD charge is the same as in Figure 5.10. Since the flow rates in Figure 5.10 are all at a constant level, the maximum flow rate and the MD are all at their minimum levels.

5.3.6 Section conclusion

Subsection 5.3.1 demonstrates the LS capability of the VSD on/off control; subsection 5.3.5 illustrates the EE capability; subsection 5.3.3 illustrates the ability of the VSD on/off control to adjust the the contributions from EE and LS freely to minimize the energy cost; subsections 5.3.2 and 5.3.4 demonstrate that the VSD on/off control is also capable of minimizing the MD and the associated charges.

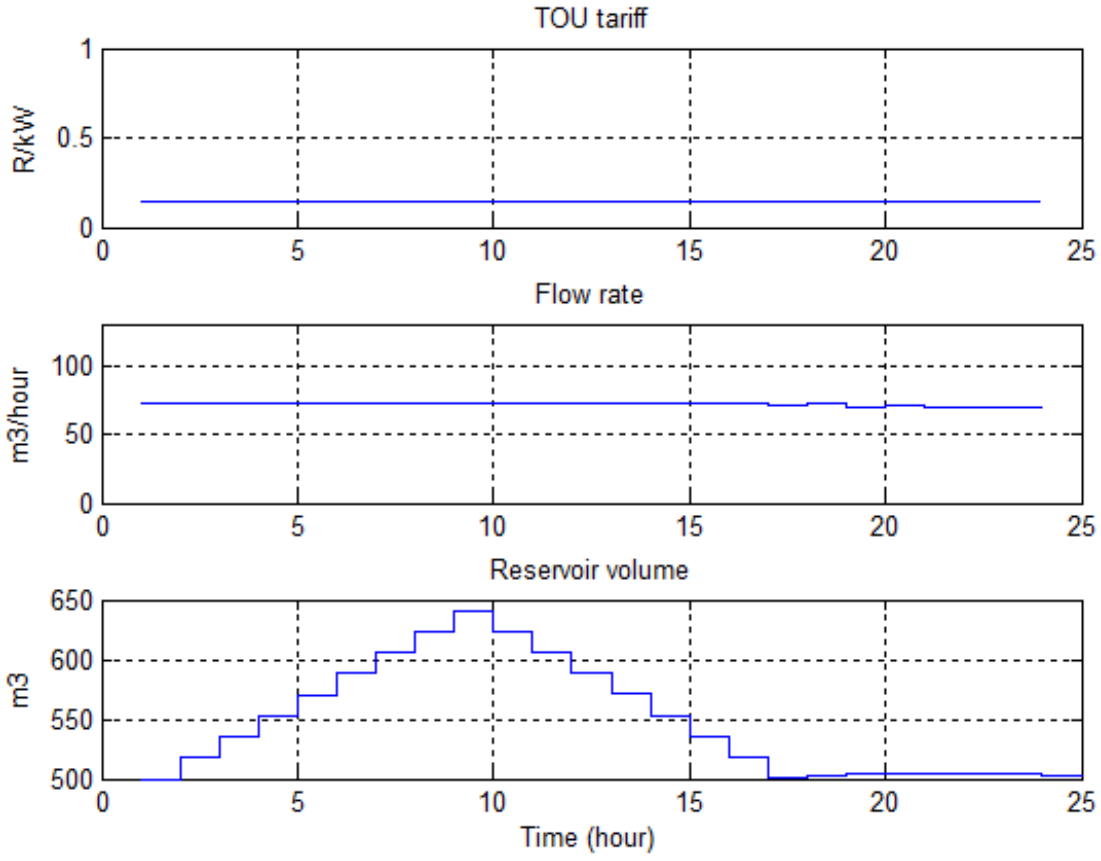

Figure 5.10: Illustration of the 24-hours change to the tariff, flow rate and reservoir level under flat tariff with/without MD charge.

5.4 ENERGY COST COMPARISON

In order to evaluate the financial benefit of the VSD on/off control system, a host of other existing control methods are simulated under the same operating conditions as the VSD on/off control system, and their operational energy costs are compared with the VSD on/off control. Six tariff structures are considered, namely high demand TOU without/with MD charge, low demand tariff without/with MD charge, and flat tariff without/with MD charge.

Four of the most common pump control methods are selected, and they are, valve control, VSD control, level based on/off control, and optimal on/off LS control.

5.4.1 Valve control

With valve control, the pump is operating constantly at full power (p_{full}), regardless of the output flow rate requirements. The energy consumption can easily be simulated by multiplying the full power of the pump with the duration of the operation. The operational energy cost under valve control, Y_{valve}, can be computed by the following equation,

$$Y_{valve} = \sum_{i=1}^{I} p_{full} c_i Z + C_{md} p_{full}. \tag{5.15}$$

5.4.2 VSD control

VSD control is an EE-only initiative, which matches the pump flow rate with the water demand requirements and reduces unnecessary power wastage. This means that q_i=d_i. Therefore the power consumption at control interval i can be computed, using the flow-power model, as $v_r(d_i)$. The operation energy cost under VSD control, Y_{VSD}, can be computed as

$$Y_{VSD} = \sum_{i=1}^{I_c} v_r(d_i) c_i Z + C_{md} V_{md}. \tag{5.16}$$

where V_{MD} The function that find the maximum power consumption within the control horizon and is given by (5.17).

$$V_{MD} = \max\{v_r(d_i) \ : i = 1, ..., I_c\}. \tag{5.17}$$

5.4.3 Level based on/off control

The level based on/off control controls the water level in the reservoir by sampling the reservoir volume at the beginning of each control interval, and if the water level drops below the critical level, the pump is switched on for the entire control interval, otherwise the pump is off. Once the pump is on, it operates at its full flow rate and power. The critical level is chosen to be 800 m^3. The water level and the on/off schedule of the pump, u_i, are computed by (5.18) and (5.19) respectively.

$$l_{i+1} = l_i + u_i q_{full} - d_i, \tag{5.18}$$

$$u_i = \begin{cases} 1 & \text{if } l_i \leq 500, \\ 0 & \text{if } l_i > 500. \end{cases} \tag{5.19}$$

The operational energy cost of the level based on/off control, $Y_{on/off}$, can be computed as

$$Y_{on/off} = \sum_{i=1}^{I_c} u_i c_i Z + C_{md} p_{full}. \tag{5.20}$$

5.4.4 Optimal on/off control

The optimal on/off control strategy is simulated using a binary optimal control model. The objective is to minimize the electricity cost. The objective function is shown in (5.21).

$$\min_{u_i} \sum_{i=1}^{I_c} u_t p_{full} c_t Z, \tag{5.21}$$

The objective function is subject to the following water level constraint,

$$LL \leq l_i \leq UL \tag{5.22}$$

The reservoir level, l_i, is computed by (5.18).

The MD charge is excluded from the objective function, since the only way for on/off based pump control to reduce MD is to operate the pump in a control interval shorter than the half hour MD integrating period [53]. The control interval for this research is fixed at one hour, hence the MD cost cannot be altered by the control model. The operational energy cost of the optimal on/off control can be computed with (5.20).

5.4.5 Comparison results

The operation energy cost of different pump control strategies under different tariff structures are summarized in Figure 5.11. The blue columns represent the monthly energy costs, the red columns represent the MD cost and the green columns represent the savings in comparison to the valve control.

As shown in Fig. 5.11, the valve control has the highest energy cost and level based on/off control has the second highest. The energy cost of the VSD control and optimal LS control varies significantly with different tariff structures. These two controls alternate the third and fourth highest energy cost positions for different tariff structures. The VSD on/off control achieves the lowest energy cost under all scenarios considered. These results illustrate that the VSD on/off control is capable of adapting to different tariffs and effectively reducing the operational energy cost.

The percentages of energy savings of different control strategies in comparison to valve control are summarized in Table 5.1.

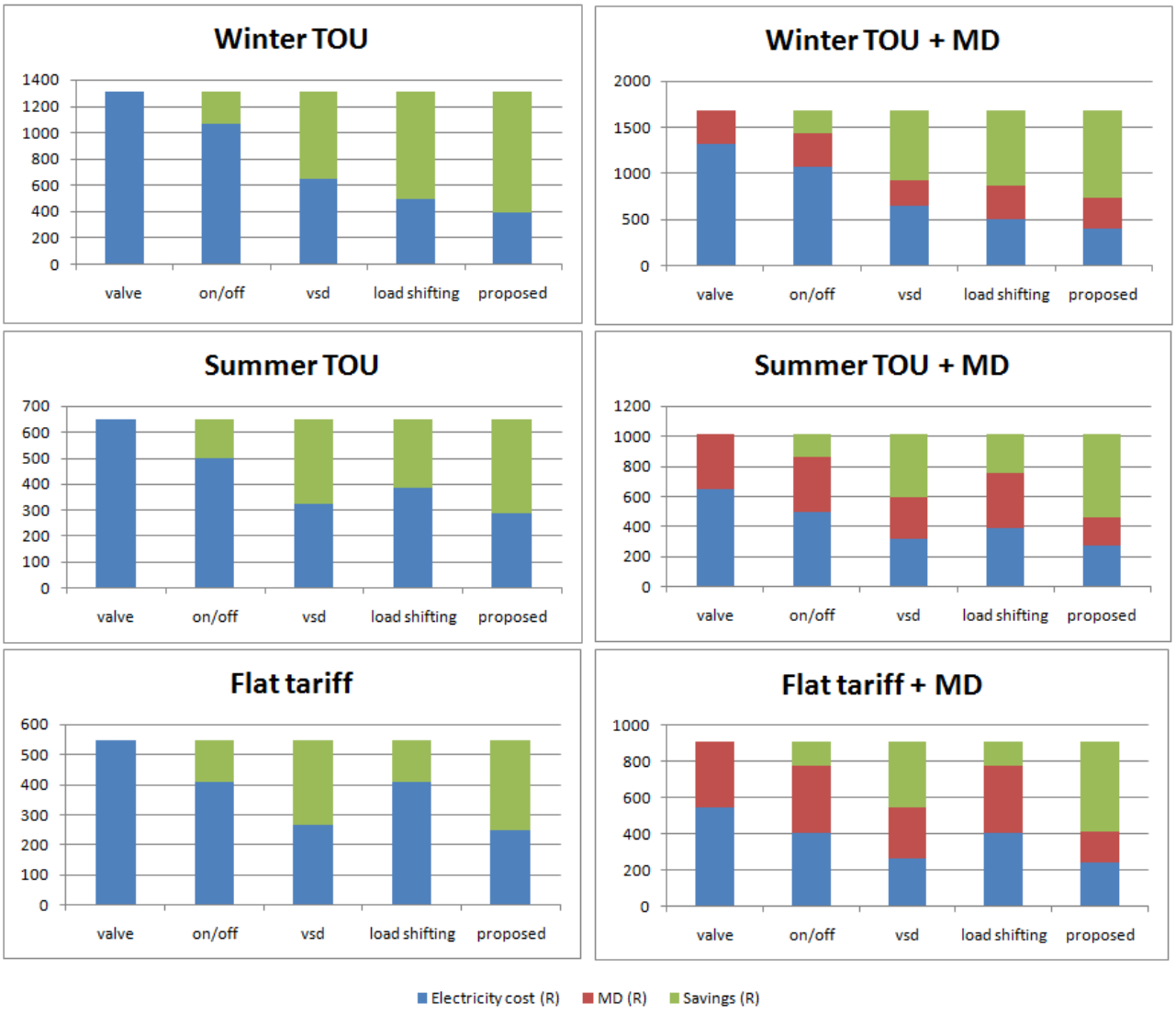

Figure 5.11: The operational energy costs comparison of different control strategies under different tariff structures.

Table 5.1: The summary of the percentage savings

High demand TOU		**High demand TOU with MD**	
Control strategy	**Savings**	**Control strategy**	**Savings**
On/off	18.6%	On/off	14.5%
VSD	50.3%	VSD	44.1%
LS	61.8%	LS	48.4%
Proposed	70.5%	Proposed	55.9%
Low demand TOU		**Low demand TOU with MD**	
Control strategy	**Savings**	**Control strategy**	**Savings**
On/off	22.6%	On/off	14.5%
VSD	50.1%	VSD	40.8%
LS	40.2%	LS	25.7%
Proposed	55.3%	Proposed	62.2%
Flat tariff		**Flat tariff with MD**	
Control strategy	**Savings**	**Control strategy**	**Savings**
On/off	25.0%	On/off	22.5%
VSD	50.7%	VSD	39.8%
LS	25.0%	LS	22.5%
Proposed	54.8%	Proposed	54.3%

CHAPTER 6. TIME COORDINATION PART II: CLOSED-LOOP CONTROL

This chapter documents the formulation and simulations of the closed-loop MPC model. It is divided into two parts, namely

- The formulation of the closed-loop MPC model
- Simulation test results.

6.1 MPC MODEL FORMULATION

The open-loop objective function, (5.1), is modified into the closed-loop objective function and is defined as below:

$$\min_{q_{r,i},u_{r,i}} \sum_{r=1}^{R_c} \sum_{i=1+m}^{I_c+m} v_r(q_{r,i}) u_{r,i} c_i Z + C_{md} M_{md}, \tag{6.1}$$

where $m = 1,...,M_{mpc}$, and M_{mpc} represents the last switching interval. M_{mpc} can be considered as infinite if the controller is running none-stop. The control horizon of (6.1) is over $(m, m + I_c)$.

In (6.1) the open-loop optimal control problem is solved repeatedly over a finite control horizon at each control interval i, and only the first control step is implemented after each iteration. At the next control interval $(i + 1)$ the reservoir level is sampled again and the process of optimization is repeated over the new control horizon $[m, I + m]$.

The reservoir level constraint of the open-loop model also applies to the closed-loop model. The only difference is that this constraint needs to be updated after each control interval is implemented.

The MPC control strategy can be explained further using Figure 6.1, which is simulated based on the case study parameters with one pump and one reservoir. The prediction

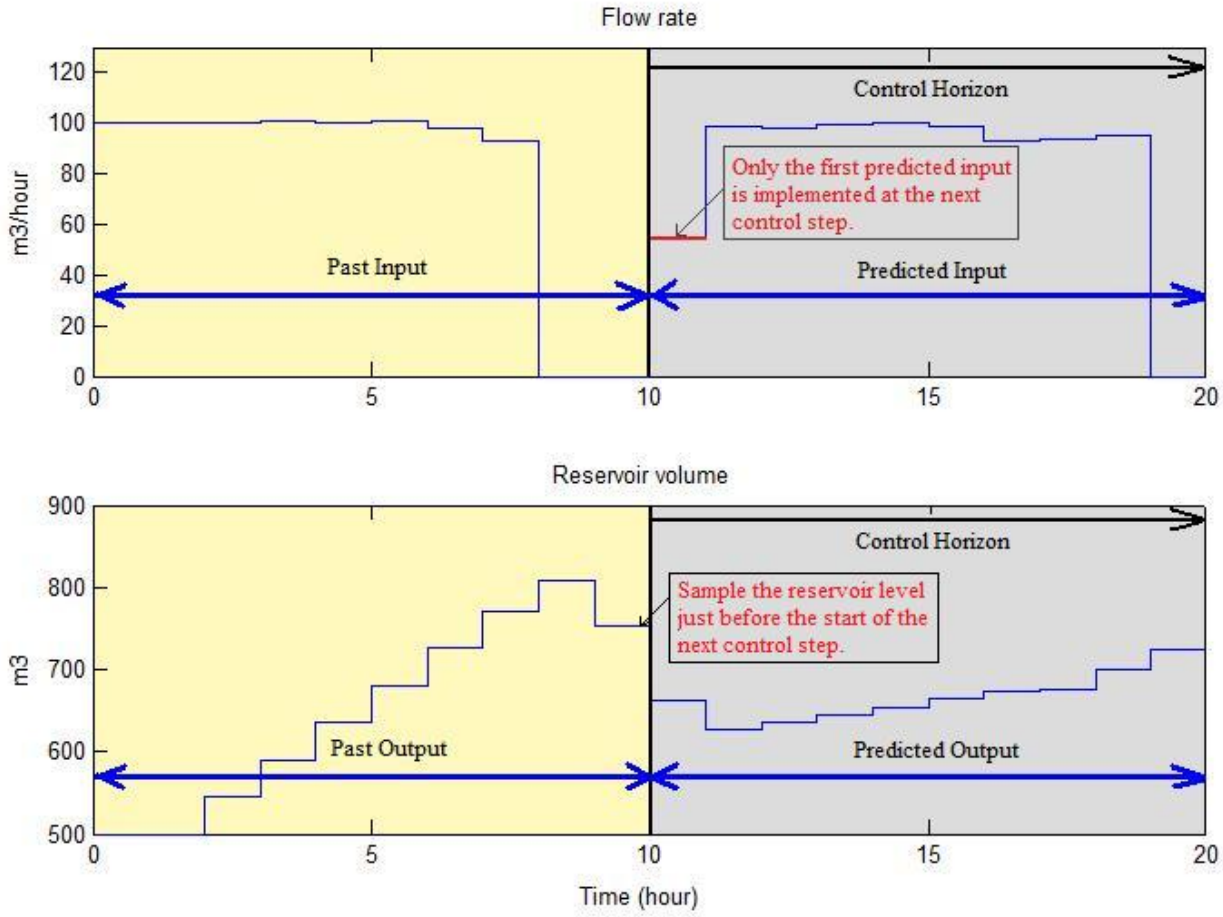

Figure 6.1: Graphical illustration of the MPC operation.

horizon is chosen to be 10 hours. The computed optimal flow rate settings, $q_i u_i$, and reservoir level, l_i, are plotted in the corresponding plots in Figure 6.1.

Figure 6.1 shows that the current time is 10:00, which means that the inputs and outputs prior to 10:00 are historical and the inputs and outputs after 10:00 are the future predicted values.

The process of the MPC controller in Figure 6.1 can be described as follows: at the current time (10:00) the controller, using the measured current reservoir level, applies all the constraints, predicts the future pump flow rates and optimizes the energy cost over the next ten hours. The calculated pump flow rates are referred to as the predicted inputs. Figure 6.1 shows that the pump should operate at a flow rate of 54 $m^3/hour$ for the next hour (10:00 to 11:00) along with the operational settings for the other nine hours. The predicted reservoir levels are plotted in the reservoir subplot.

Once the predicted inputs have been calculated, only the input for the first hour is implemented and the rest of the inputs are discarded. After the first predicted input

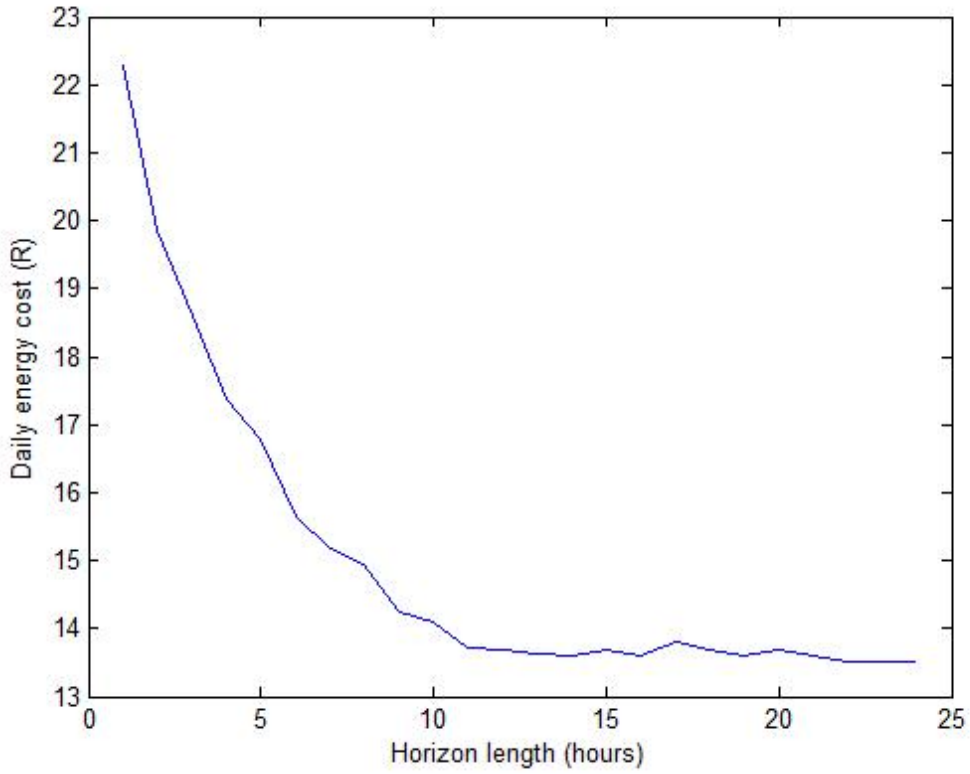

Figure 6.2: Changes in daily energy cost with respect to the length of the control horizon.

has been implemented, the entire optimization process is repeated.

6.1.1 Prediction horizon

The control horizon is a trade-off between computational time and quality of the control strategy. In this research, the quality of the control strategy is the level of energy cost savings. The effects of different control horizon durations are investigated with simulations based on the case study. The result is shown in Figure 6.2.

Owing to the randomness and the limited number of iterations of the PSO algorithm, the curve of Figure 6.2 is not very straight, but a clear relationship can be observed. It can be seen that if the operational energy cost is minimized the duration of the control horizon should be at least 12 hours. However, because of the randomness of the PSO algorithm and for the purpose of accurate system testing, a 24-hour control horizon is used for the closed-loop simulations.

This result is important, because it allows the selection of shorter control horizons, which will reduce the computation time per iteration without affecting the level of savings.

The optimality of the optimal MD level is independent on the length of the control

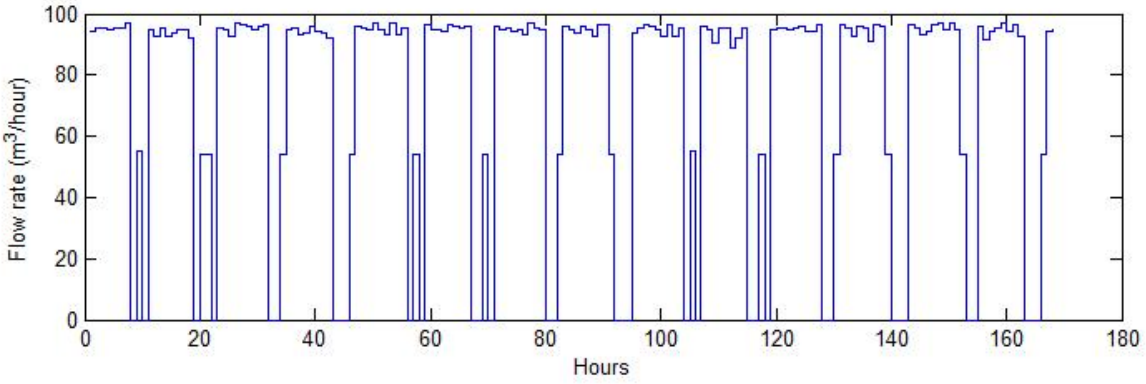

Figure 6.3: Computed flow rate for one week.

horizon. With sufficient a number of iterations, the algorithm will always be able to find an optimal MD level in which the total energy cost (MD and TOU) is minimized.

6.2 SIMULATION RESULTS

The MPC control model described in (6.1) is simulated with the same operational parameters and constraints as in the open-loop case, which is described in Chapter 5, Section 5.3. The high demand TOU tariff is used in combination with the MD charges. Different tests are performed to evaluate the operational performance and robustness of the MPC control model, and the results are summarized in the following sections.

6.2.1 MPC simulation over seven days

Figure 6.3 shows seven days' worth of hourly pump flow rate. It can be seen that the outputs are fairly consistent. The level of LS is comparable with that of the open-loop case and the maximum flow rate, hence the MD is kept at a fairly constant level.

The level of fluctuation of the flow rate in Figure 6.3 is much higher than the open-loop case in Figure 5.4. This is because in the open-loop case all of the flow rates are computed in one single calculation with the same optimal MD and maximum flow rate limitations. Hence the flow rates are uniformly limited at a particular level. In the case of closed-loop MPC, each individual flow rate is computed by a separate calculation. Each of the calculations has a different starting reservoir level and different net required water volume to be pumped. These translate to different MD limitations and hence flow rate fluctuations.

Figure 6.4 shows the seven days' worth of predicted reservoir level changes. It can be

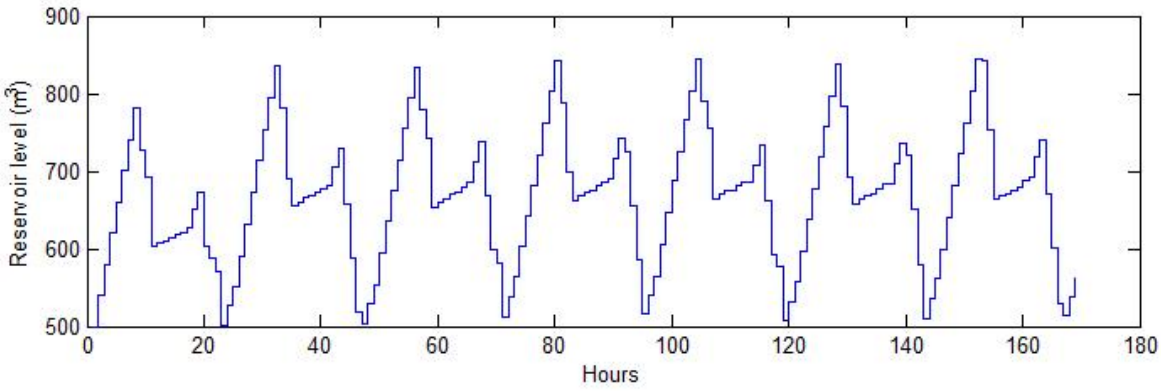

Figure 6.4: Volume changes in the reservoir for one week.

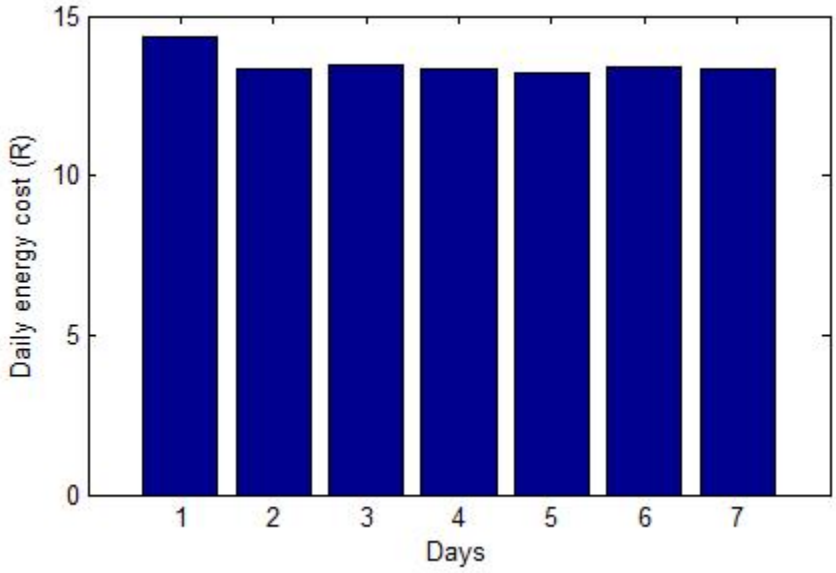

Figure 6.5: Daily energy cost.

seen that at no time is the reservoir level exceeded beyond the allowed range of between 1000 m^3 and 500 m^3. The shapes of the curves are also very consistent with the rise and fall of the water levels corresponding to the daily accumulation and LS processes.

Figure 6.5 shows the energy cost for each of the seven days. The energy cost of the first day is noticeably higher than that of the other six days. This is because the reservoir level at the start of the optimization is at the minimum value of 500 m^3 and in the first day a greater volume of water is pumped to push the water level to a higher level to ease the operation on the following days. It can be observed in Figure 6.4 that the water levels of the first 24 hours are lower in comparison to the other six days, hence the energy cost is slightly higher. After the first day the control system is stabilized, and the reservoir level flow rate and energy cost are confined within a small range of deviations.

The monthly energy cost, which is computed by multiplying the average of the daily cost by 30, is R 404.65. The maximum demand cost is R330.41. The total energy cost is R735.06 which is comparable with the open-loop monthly cost of R 740.23.

6.2.2 Control system robustness

The greatest motivation for the implementation of the closed-loop MPC approach is the improvement it brings about in the system's robustness. The following simulation illustrates how the MPC control model detects and compensates for the errors in the system.

The control model is simulated for 48 hours. The operational parameters are the same as in Chapter 5, Section 5.3 for the first 24 hours. At the beginning of the 25-th hour an additional constant 20 m^3/hour water demand is introduced such that,

$$d_{i+24} = d_i + 20, \ : \ \text{i=1,2,...,24.} \tag{6.2}$$

This increase in demand could be due to a leakage or additional demand of water. The 48-hour water demand profile, flow rates and the reservoir levels are plotted in the demand, flow rate and reservoir level sub-plots of Figure 6.6.

Note that the only communication between the MPC control model and the actual plant is through the reservoir level feedback. The MPC model is unaware of the water demand increase and continues to use the normal or forecast water demand to compute the flow rate.

The process of detecting and correcting the error can be divided into two stages, which are indicated by the different color shades in Figure 6.6.

The first stage, indicated by the yellow-shaded area, is when the error is not significant enough to be noticed by the control model, and there is no significant difference in the flow rates compared to the corresponding time slot of the previous 24 hours.

The reason for this is that most of the control intervals in the first stage occur during the off-peak hours, which means the pump is operating at a very high flow rate. Although the reservoir level is lower than what it should have been because of the accumulation of the additional water demand, it is still significantly above the lower limit and does not cause much of a problem to the control model. It can be seen that the reservoir level is still sufficient to allow LS to take place in the 32-th hour.

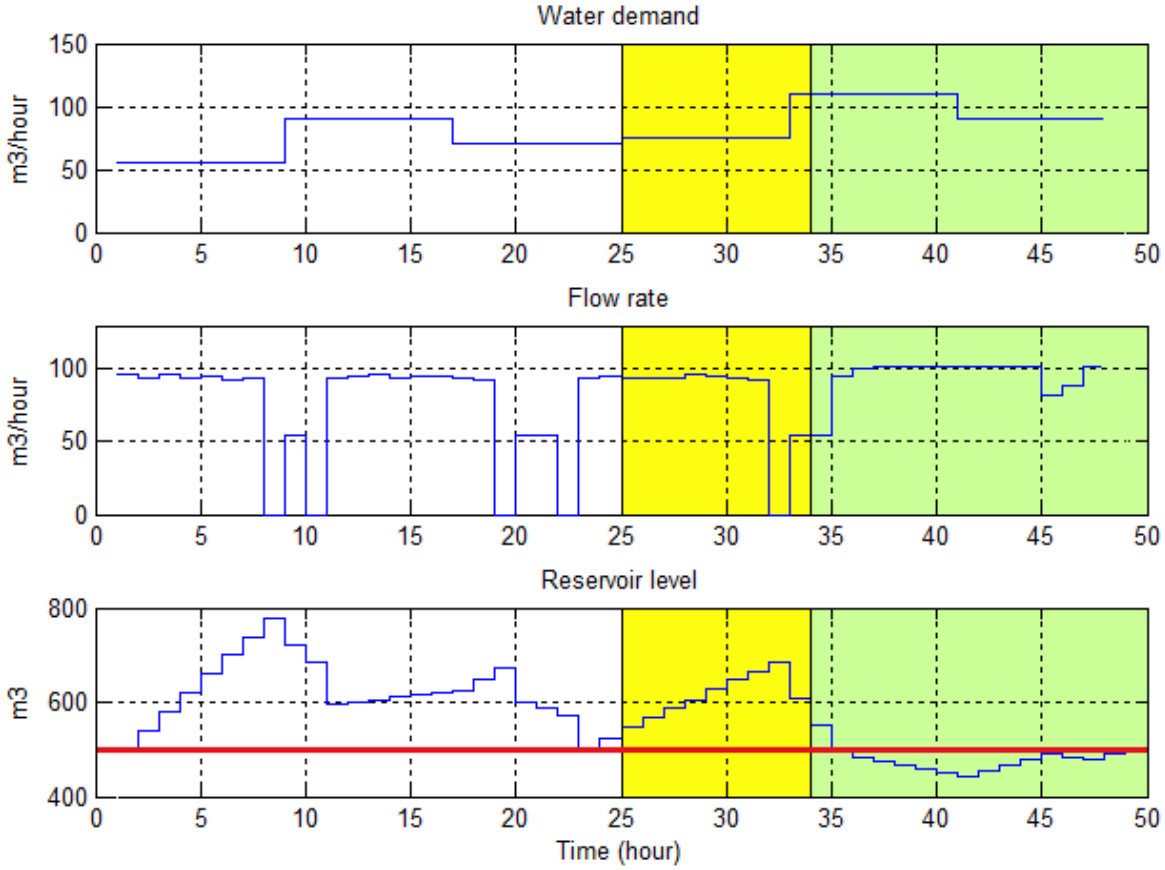

Figure 6.6: Illustration of the MPC control model error correction.

Since the control horizon is 24 hours, the flow rate for a control interval is derived by computing a whole 24 hours' worth of flow rates and only the first one is used. The total 24 hours' forecast water demand is much lower than the 24 hours' full pumping capacity. The control model is unaware of the extra water demand and "assumes" it can easily recover the amount of water level deficit through the 24-hour operation. The control model tends to spread this minor water level adjustments evenly across the 24-hour operation to minimize the MD, and therefore little change in the flow rate is observed at this stage.

By the 34-th hour, the pump has to be switched on to keep the water level above the limit. It means that the errors in the system have accumulated to such an extent that drastic measures have to be taken. This marks the start of the second stage, the active correction stage indicated by the blue shaded area.

Since the peak time electricity price is very high under high demand TOU, it is mandatory to operate the pump at the minimum flow rate. The flow rates during the peak hours should only be sufficient to keep the water level just above the limit. Unfortunately this minimal flow rate is computed by the control model based on the forecast demand of water, and in this case the forecast demand is much lower than the actual one. This results in a much lower flow rate than what is actually required, which leads to the reservoir level dropping below the allowed limit during the 35-th hour.

At the beginning of the 36-th hour, a violation of the water level constraint is detected, and the highest priority of the control model is to increase the water level to above the minimum level as soon as possible. However, the water demand, from the 33-rd to the 41-st hour, are higher than the full capacity of the pump. Despite the efforts of the pump operating at full power and sacrificing the MD savings, the water level continues to drop until the high water demand period ends.

Hours 42 to 46 are evening peak hours. It can be seen that very little LS took place, and savings from LS are further sacrificed in an attempt by the control model to correct the water level. Very limited LS occurred only during the 45-th and 46-th hour.

Because of the efforts of the MPC control model, the water level is stabilized and is almost at the acceptable level by the end of the 48-th hour. Figure 6.7 shows the same simulation but with the open-loop control model.

In the case of the open-loop control model, there is no feedback; the model is isolated from the actual plant and unaware of any changes in the system. The error will continue to accumulate without any correction and eventually lead to a possible system failure. This is illustrated in Figure 6.7, where the reservoir level has dropped to almost 0.

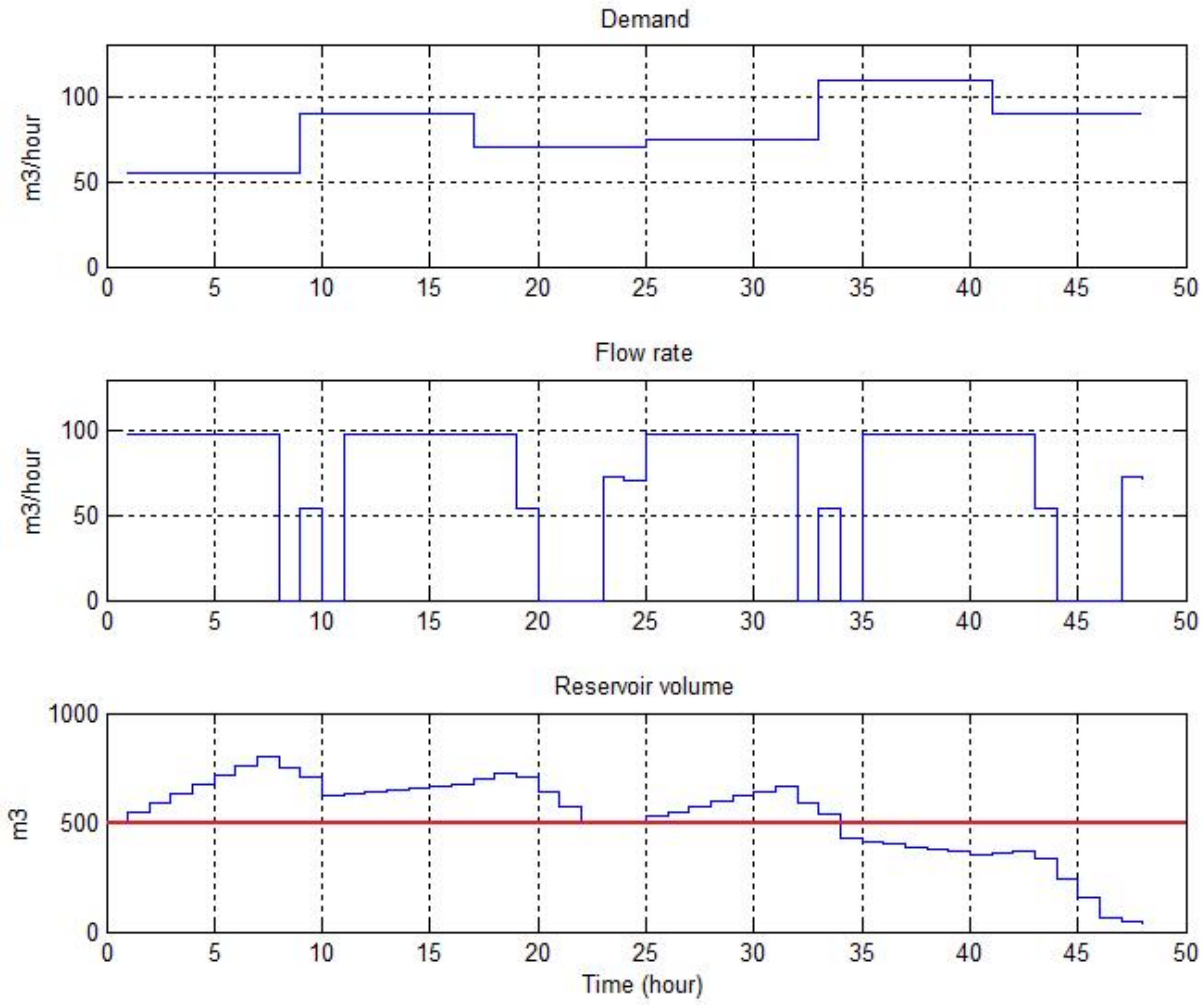

Figure 6.7: Illustration of the open-loop control model operation with demand variation.

The 24-hour water demand from the 25-th to 48-th hour is increased to 2200 m^3 from the 1720 m^3 level of the previous 24 hours. The MPC control model pumped a total of 2151.73 m^3 of water from the 25-th to the 48-th hour while the open-loop model only pumped 1723.13 m^3. The volume of water pumped in the MPC case is very close to the actual demand, and significantly higher than that in the open-loop case. This further illustrates the benefit of the robustness of the MPC control model.

MPCs are also suitable for automatically resolving a host of other system errors, such as design mistakes and poor modeling accuracy. The mechanisms of error correction are the same as in the above simulation.

CHAPTER 7. CONCLUSION

This dissertation defined a pump operation EE improvement strategy based on the physical and time coordinations of the operation category of the POET framework.

For the physical coordination section, an optimal pump capacity selection model is proposed and verified. In this model, additional capacity requirements for sufficient LS are also considered along with the traditional EE requirements. It has been shown that if a facility is charged under a TOU tariff, it is financially more beneficial to include LS in the selection of the optimal pumping capacity.

It is also shown that by increasing the capacity of the pump, more load can be shifted out of the high electricity price periods and the cost of electricity is reduced. However, by increasing the capacity of the pump, the pump efficiency deteriorates significantly and as a result the energy consumption is increased. The aim of the optimal capacity selection model is to find a balance between these two opposing factors and minimize the operational energy cost. The simulations under the South African high demand TOU tariff illustrated that the operational energy cost for the pump capacity selected by the proposed model is 37% less than the traditional EE based capacity choice. The flexibility of this optimal capacity selection model is shown through a simulation where the reservoir size is limited to a low value.

The time coordination is divided into two parts. The first part is the formulation of an open-loop pump optimal operation control strategy, the VSD on/off control. The objective of this control strategy is to balance the EE and LS contributions during the operation and minimize the operational electricity cost. In addition, this control model is very flexible and can be adjusted to adapt to different operational conditions. This flexibility compensates for the rigidness of the system design.

A flow rate input power relationship is formulated such that the power consumption for variable speed pump operation can be accurately predicted. Two methods of formulation are described; one is through measurements and the other is using theoretical analysis. This flow-power function is simplified into a third order quadratic equation. This enables it to merge into the optimal control model with relative ease.

The optimal control model is simulated in a case study under a variety of electricity tariffs, which include flat tariff, high demand TOU with/without MD charge and low demand TOU with/without MD charge. The flexibility of the proposed control model is demonstrated through these simulations. The origin of this flexibility is the balancing of the EE and LS contributions. For example, when the peak electricity of the TOU tariff is very high, LS dominates and the focus is on shifting the loads out of the peak periods; and when the peak price is low with MD charge, more savings are allocated to EE.

Four existing pump control strategies are also simulated under the same operating conditions to evaluate the effectiveness of the proposed optimal control strategy. The existing control strategies considered are valve control, level based on/off control, VSD control and optimal LS control. The proposed control strategy achieved the lowest operational energy cost in all of the simulations in comparison to the four existing control strategies.

The control system's robustness under system and operational uncertainties is improved using the MPC approach. The open-loop optimal control model is converted into a closed-loop MPC approach.

Simulating the MPC model is very time consuming and hence the optimal number of iterations and duration of the control horizon are investigated such that the computation time can be minimized without effecting the quality of the result.

The closed-loop control strategy is simulated for a seven-day period. The result shows that the performance of the closed-loop control model is comparable with the open-loop one in terms of operational energy cost reduction.

The effect of disturbances and an inaccurate system model are simulated for the open- and closed-loop control models. The results show that an open-loop control model does not compensate for the disturbances or an inaccurate system model, while the closed-loop control model does.

A binary PSO algorithm, the voting approach, is formulated. This algorithm is designed to run together with the continuous variable PSO algorithm. The voting approach is tested and shows excellent performance over other similar algorithms in the case study.

The contributions of this research in the context of the existing works were also discussed. In summary, the contributions are: affirms the practical applicability of the POET framework; demonstrates the financial benefits to include LS considerations in the optimal selection of pump capacity; derives a combined EE and LS optimal pump operation control strategy, and illustrates its financial benefits in comparison to existing strategies; demonstrates the robustness of the MPC controller; and lastly formulates a

binary PSO algorithm.

The practicality of the proposed strategy is described below. The results from the capacity selection model can serve as recommendations for the designer; however, the designer must still apply safety margins and analyze the available pumps before the final decision is made. The optimal control strategy is not recommended to be implemented without any form of feedback, since the control model is formulated based on significant amounts of assumptions and simplifications, such that a feedback mechanism is essential.

It is recommended that further research be conducted to improve the capacity selection and optimal control models by considering additional costs, such as the cost of maintenance. It is also recommended that further research be carried out to apply this pump efficiency improvement strategy to a case study with much greater complexity. Lastly, further research on pump efficiency improvements can be attempted to follow other categories of the POET framework.

Bibliography

[1] DME, "National respponse to South Africa's electricity shortage," 2008, Available:http://www.dme.gove.za/pdf/energy/naional-resp-plan.pdf. Last accessed on 20 April 2009.

[2] Eskom, "Annual report 2008," 2008, Available: http://www.eskom.co.za. Last accessed on 22 April 2009.

[3] T. Nortje, "South Africa's DSM Programme: A savings opportunity," in *International Pump User Conference*, Johannesburg, 8-9 June 2005.

[4] D. Loughran, J. Kulick, "Demand-side management and energy efficiency in the United States," *The Energy Journal*, vol. 25, no. 1, pp. 19-43, 2004.

[5] C. Gellings, "The concept of demand-side management for electricity utilities," Proceedings of the IEEE, vol. 73, no. 10, pp. 1468-1470, October 1985.

[6] X. Xia, J Zhang, "Energy audit - from a POET perspective," in *International Conference on Applied Energy*, Singapore, 21-23 April 2010, pp. 1200-1209.

[7] X. Xia, J. Zhang, "Energy efficiency and control systems - from a POET perspective," in *IFAC Conference on Control Methodologies and Technology for Energy Efficiency*, Vilamoura, Portugal, 29-31 March 2010.

[8] J. Boivin, "Demand side management - the role of the power utility," *Pattern Recognition*, vol. 28, pp. 1493 - 1497, October 1995.

[9] Eskom, Energy efficiency and demand side management programme overview, 2008, Available: http://www.eskomdsm.co.za. Last accessed 2 June 2009.

[10] D. Loughran, J. Kulick, "Demand-side management and energy efficiency in the United States," *The Energy Journal*, vol. 25, no. 1, pp. 19-43, 2004.

[11] D. Hammerstorm, "Pacific Northwest GridWise test bed demonstration project Part I: Olympic peninsula project," Pacific Northwest Laboratory, PNNL 17167, pp. 5.1 - 5.6, Oct. 2007.

[12] E. Martinot, N. Borg, "Energy-efficient lighting programs: Experience and lessons from eight countries," *Energy Policy*, vol. 26, no. 14, pp. 1071-1081, December 1998.

[13] J.A. Rooks, A.K. Wallace, "Energy efficiency of VSDs," *IEEE Industry Applications Magazine*, vol. 10, no. 3, pp. 57-61, May 2004.

[14] B. Batidzirai, E.H. Lysen, S. van Egmond, W.G.J.H.M. van Sark "Potential for solar water heating in Zimbabwe," *Renewable and Sustainable Energy Reviews*, vol. 13, no. 3, pp. 567-582, April 2009.

[15] P. Pillay, K.A. Fendley, "The contribution of energy efficient motors to demand and energy savings in the petrochemical industry," *IEEE Transactions on Power Systems*, vol. 10, no. 2, pp. 1085-1093, May 1995.

[16] N. Beute, G.J. Delport, "An historic overview of controlling domestic water heating," in *Proceedings of the 4th Domestic Use of Energy Conference*, Cape Town, 18-19 April 2006, pp. 41-46.

[17] G. Barbose, C. Goldman, B.Neenan, "A survey of utility experience with real time pricing," Environmental Energy Technologies Division, Ernest Orlando Lawrence Berkeley National Laboratory, Rep. LBNL-54238, December 2004.

[18] J.N. Sheen, C.S. Chen, J.K. Yang, "Time-of-use pricing for load management programs in Taiwan PowerCompany," *IEEE Transactions on Power Systems*, vol. 9, no. 1, pp. 388-396, Febuary 1994.

[19] Tshwane, "Electricity tariffs for Tshwane metropolitan municipality," Available: http://www.tshwane.gov.za. Last accessed 4 May 2009.

[20] Eskom, "Eskom tariffs and charges booklet for 2007/2008," Available: http://www.eskom.co.za/tariffs. Last accessed 2 May 2009.

[21] S. Lu, J. Wu, "Optimal selection among different domestic energy consumption patterns based on energy and energy analysis," *Energy Conservation and Management*, vol. 51, pp. 1398-1406, 2010.

[22] E. Gabbrielli, "Optimal selection of major equipment in dual purpose plants," *Desalination*, vol. 36, pp. 1-23, 1981.

[23] H. Sogaard, C. Sorensen, "A model for optimal selection of machinery sizes within the farm machinery system," *Biosystems Engineering*, vol. 89, pp. 13-28, 2004.

[24] M. Geylling, "Computer aided selection tool aids German municipality in pump search," *World Pumps*, pp. 30-32, April 2005.

[25] J. Tolvanen, "Life cycle energy cost savings through careful system design and pump selection," *World Pumps*, pp.34-37, July 2007.

[26] E. Larralde, "Centrifugal pump selection process," *World Pumps*, pp. 24-28, Febuary 2010.

[27] D. Kaya, E. Yagmur,"Energy efficiency in pumps," *Energy Conversion and Management*, vol. 49, pp. 1662-1673, 2008.

[28] M. Moreno, P. Carrion, "Measurement and improvement of the energy efficiency at pumping stations," *Biosystem Engineering*, vol.98, pp. 479 - 486, 2007.

[29] E. Larralde, R. Ocampo, "Pump selection: a real example," *World Pumps*, pp. 28-33, March 2010.

[30] G, Addie, A, Sellgen, "Design, selection, sizing, and control considerations for cyclone feed slurry pumps," *Powder Technology*, vol. 104, pp. 233-239, 1999.

[31] W. van der Westhuizen, T. Cattaert, "Power station pump selection Part 1," *World Pumps*, pp. 16-19, December 2009.

[32] D. Brockway, "Intelligent pump selection in the 21th Century," *World Pumps*, pp. 22-25, November 2001.

[33] R. Hardy, "Pump selection software," *World Pumps*, pp. 54-55, May 2001.

[34] C. Pulido-Calvo, J.Gutierrez-Estrada, "Optimal design of pumping stations of inland intensive fishfarms," *Aquacultural Engineering*, vol. 35, pp. 283-291, 2006.

[35] M. Moreno, P. Planells, J.I. Corcoles, J.M. Tarjuelo, P.A. Carrion, "Development of a new methodology to obtain the characteristic pump curves that minimize the total cost at pumping stations," *Biosystem Engineering*, vol. 102, pp. 95-105, 2009.

[36] H. Mousavi, A. Ramamurthy, "Optimal design of multi-reservoir systems for water supply," *Advance Water Resource*, vol. 23, pp. 613-624, 2000.

[37] Sulzer Brothers LTD, *Sulzer Centrifugal Pump Handbook*, New York: Elsevier Science Publisherd LTD., 1989.

[38] G. Irvine, I. Gibson, "The use of variable frequency drives as a final control element in the petroleum industry," in *Proccedings on Industry Application Conference*, Rome, 8-12 October 2000, pp. 2749-2758.

[39] M. Savar, Hrvoje Kozmar, Igor Sutlovic, "Improving centrifugal pump efficiency by impeller trimming," *Desalination*, vol. 249, pp. 654 - 659, 2009.

[40] K. Yang, J. Zhai, "Particle Swarm Optimization algorithms for optimal scheduling of water supply systems," in *2nd International Symposium on Computational Intelligence and Design*, Shangsha, 12-14 December 2009, pp.509-512.

[41] S. Wei, H. Leung, "An improved genetic algorithm for pump scheduling in water injection systems for oilfield," in *IEEE Conference on Evolutionary Computation*, Hong Kong, 1-6 June, 2008, pp. 1027 - 1032.

[42] M. Yin, J. Andrews, "Optimum simulation and control of fixed-speed pumping stations," *Environment Engineering* vol. 122, pp. 205-211, 1996.

[43] K. Lansey, K. Awumah, "Optimal pump operations considering pump switches," *Journal of Water Resources Planning and Management*, vol. 120, pp. 17-35, 1994.

[44] R. Errath, "Integrated variable speed drive - the energy saver," in *IEEE Cement Industry Technical Conference*, Mexico City, 21-23 May 1991, pp. 135 - 149.

[45] M. Lonnberg, "Variable speed drive for savings in hospitals," *World Pumps*, pp. 20-24, November 2007.

[46] E. Turner, C. LeMone, "Adjustable-speed drive applications in the oil and gas pipeline industry," *IEEE Transactions on Industry Application*, vol. 25, pp. 30-35, 1989.

[47] R. Carlson, "The correct method of calculating energy savings to justify adjustable-frequency drive on pumps," *IEEE Transaction on Industry Application*, vol. 36, no. 6, Nov. 2000.

[48] X. Meng, H. Wang, "Application of hybrid genetic algorithm in frequency speed control pumping station," in *4th International Conference on Natural Computation*, Shan Dong, China, 12-14 June 2008, pp. 337 - 341.

[49] D. Guo, Y, Qi, "Operation parameters optimization of centrifugal pumps in multi-sources water injection system," in *International Technology and Innovation Conference*, 6-7 November 2006, pp. 2216-2222.

[50] F. Vieira, H. Ramos, "Hybrid solution and pump-storage optimization in water supply system," *Energy Policy*, vol.36, pp. 4142-4148, 2008.

[51] Bachus, A. Custodio, "The affinity laws," *Know and Understand Centrifugal Pumps*, pp. 39-43, 2003.

[52] D. Hewitt, "Advances in ultrasonic controllers - new energy-saving solutions for pump control," *World Pumps*, pp. 44-46, May 2006.

[53] A. van Staden, J. Zhang, X. Xia, "A model predictive control strategy for load shifting in a Water pumping scheme with maximum demand charge," in *IEEE Bucharest Power Tech Conference*, Bucharest, Romania, 28 June - 2 July, 2009, pp. 1-7.

[54] W. Jowitt, G. Germanopoulos, "Optimal pump scheduling in water-supply networks," *Journal of Water Resources Planning and Management*, vol. 118, vol. 4, pp. 406-422, July 1992.

[55] C. Biscos, M Mulholland, MV Le Lann, CA Buckley, "Optimal operation of water distribution network by predictive control using MILP," *Water SA*, vol. 3, pp. 393-404, October 2003.

[56] G. McCormick, R. Powell, "Optimal pump scheduling in water supply systems with maximum demand charges," *Journal of Water Resources Planning and Management*, vol. 129, vol. 5, pp. 372-379, September 2003.

[57] G. McCormick, R. Powell, "Derivation of near optimal pump schedules for water distribution by simulated annealing," *Journal of the Operational Research Society*, vol. 55, pp. 728-736, July 2004.

[58] J. Wang, J. Chen, "An enhanced genetic algorithm for bi-objective pump scheduling in water supply," *Expert Systems with Applications*, vol. 36, pp. 10249-10258, 2009.

[59] M. Lopez-Ibanez, "Multi-objective optimization of the pump scheduling problem using SPEA2," *Evolution computation*, vol. 1, pp. 435-442, 2005.

[60] B. Baran, C. von Lucken, "Multi-objective pump scheduling optimization using evolutionary strategies," *Advances in Engineering Software*, vol.36, pp. 39-47, 2005.

[61] E. Kamdem, "Measurement and verification on combined load management and energy efficiency project," Available: http://www.eskom.co.za/content/CombinedLM-EE.pdf. Last accessed 7 May 2009.

[62] F. Vieira, H. Ramos, "Hybrid solution and pump-storage optimization in water supply system," *Energy Policy*, vol.36, pp. 4142-4148, 2008.

[63] S. Zhang, X. Xia, "Optimal control of operation of belt conveyor system," *Applied Energy*, vol.87, pp. 1929-1937, 2010.

[64] J. Rawlings, *Model Predictive Control: Theory and Design*, Madison, Wis., Nob Hill Publication, 2009.

[65] C. Pan, K. Tsai, J. S. Lin, "Coordinate control of multi-adjustable speed drives for a variable water volume subsystem," in *TENCON IEEE Region 10*, 21-24 November 2004, vol. 4, pp. 159 - 162.

[66] U. Gogolyuk, V. Lysiak, I. Grinberg, "Mathematical modeling of a synchronous motor and centrifugal pump combination in steady state," in *IEEE Power Systems Conference*, 10-13 October 2004, pp. 1444-1448.

[67] M. Izquierdo, J. Jimenez, "Matlab software to determine the saving in parallel pumps optimal operation systems, by using variable speed," in *IEEE Energy 2030 Conference*, Atlanta, GA, 17-18 November 2008, pp. 1-8.

[68] J. Kennedy, R. Eberhart, "Particle swarm optimization," in *IEEE International Conference on Neural Networks*, Perth, WA, 27 November - 1 December 1995, pp. 1942-1948.

[69] Y. Shen, Y. Bu, M.Yuan, "A novel chaos particle swarm optimization (PSO) and its application in pavement maintanence decision," in *4th IEEE Conference on Industrial Electronics and Applications*, 25-27 May 2009 , Xi An, China, pp. 3521-3526.

[70] Z. Lian, X. Gu, B. Jiao, "A similar particle swarm optimization algorithm for permutation flowshop scheduling to minimize makespan," *Applied Mathematics and Computation*, vol. 175, pp. 773-785, 2006.

[71] M. Khanesar, M. Teshnehlab, M. Shoorehdeli, "A novel binary particle swarm optimization," in *Mediterranean Conference on Control and Automation*, 27-29 July 2007, Athens, Greece, pp. 1-6.

[72] E. Chen, Z. Pan, Y. Sun, X. Liu, "A binary particle swarm optimization based on proportion probability," in *Third International Conference on Business Intelligence and Financial Engineering*, 13-15 August 2010, Hong Kong, pp. 14-19.

[73] J. Kennedy, R. Eberhart, "A discrete binary version of the particle swarm algorithm," in *IEEE International Conference of Systems*, Man, and Cybernetics, 12-15 October 1997, Orlando, pp. 4104-4108.

[74] X. Jun, H. Chang, "The discrete binary version of the improved particle swarm optimization algorithm," in *International Conference on Management and Service Science*, 20-22 September 2009, Wuhan, China, pp. 1-4.

[75] E. Laskari, K. Parsopoulos, M. Vrahatis,"Particle swarm optimization for integer programming," in *Conference on Evolutionary Computation*, 12-17 May 2002, Honolulu, pp. 1582-1587.

[76] S. Kitayama, K. Yasuda, "A Method for Mixed Integer Programming Problems by Particle Swarm Optimization," *Electrical Engineering in Japan*, Vol. 157, No. 2, pp. 813-820, 2006.

[77] KSB, *Volute Casing Pump Offer Curves*, KSB industry, 2007.

APPENDIX A. MATLAB Programs (Binary voting strategy)

```
%Binary PSO to find the optimal on/off schedule of pump operation using
% the voting approach

iteration=1000; particles = 50; dimension = 24; c1 = 2; c2 = 2;
g_best=10000; best_val=10000;
tariff=[0.1187;0.1187;0.1187;0.1187;0.1187;0.1187;0.1411;0.8205;
0.8205;0.8205;0.1411;0.1411;0.1411;0.1411;0.1411;0.1411;0.1411;
0.1411;0.8205;0.8205;0.8205;0.8205;0.1187;0.1187];
%demand (m^3)/hour
D=[60;60;60;60;60;60;60;60;100;100;100;100;100;100;100;100;75
;75;75;75;75;75;75;75];

P=[3.8969e-6; 2.1851e-5; 0.01117; 0.13102]; power= P(1)*(101)^3 +
P(2)*(101)^2 + P(3)*(101)+P(4);


%reservor data
UL=1000; LL=500; LVo=800;

for i=1:particles
    for j = 1:dimension

        if rand>=0.5
            particle_position(i,j) = 1;
        else
            particle_position(i,j) = 0;
        end
         if rand>=0.5
            prev_position(i,j) = 1;
        else
            prev_position(i,j) = 0;
        end

        pbest(i,j) = particle_position(i,j);
        cost(i,j)=0;
    end
end
```

```
for i=1:particles
    p_best_fitness(i)=100000;

end

for k=1:iteration

    for i=1:particles
    fitness(i)=0;
    end
 %compute solution and fitness with constraints
    for i = 1:particles
        % flag indicating violation of volume constraint
        vol_flag=0;
        j=1;
        %vol is the volume of the reservoir starting value is the initial
        %volume
        vol=LVo;

        while (vol_flag~=1)&&(j<=dimension)

            %compute the cost of one set of 24 hour flow manangement or one
            %particle
            cost(i,j)=power*tariff(j)*particle_position(i,j);
            fitness(i)=fitness(i)+cost(i,j);

            %compute the reservoir volume and determing whether constaint
            %is violated or not
            vol=vol+101*particle_position(i,j)-D(j);
            if (vol<LL)||(vol>UL)
                vol_flag=1;
                fitness(i)=10000;
            end
            j=j+1;
        end

    end

   %p best
   for i = 1:particles
       if fitness (i) <= p_best_fitness(i)
           p_best_fitness(i) = fitness(i);
           for j = 1:dimension
                p_best(i,j)= particle_position(i,j);
           end
       end

   end
```

```
   %gbest
   [g_best_val,g_best_index] = min(fitness);

    for j = 1:dimension
        g_best(j) = particle_position(g_best_index,j);
    end
     if g_best_val<best_val
            best_val = g_best_val;
            for j = 1:dimension
            best_position (j) = particle_position(g_best_index,j);
        end
     end


 % Determine the new paritcle position and velocity
    for i = 1:particles

       for j = 1:dimension
           current_position(j) = particle_position(i,j);
           storage_position(j) = particle_position(i,j);
           position_indication = current_position(j)+prev_position(i,j)
           +g_best(j)+p_best(i,j)-2.3+rand*(2*2.3);
           if position_indication>=2
               particle_position (i,j)=1;
           else
               particle_position (i,j)=0;
           end
       end

       for j = 1:dimension
           prev_position(i,j) = storage_position(j);

       end
   end

end
```

APPENDIX B. MATLAB Programs (Flow-power function formulation)

```
% This is the MATLAB code for the derivation of the pump flow rate and input
% power static model

% The values read off from the pump characteristic and power curves

Q=[20
    60
    100
    140
    180
    220
    260
    ];

H=[32.1
    30.5
    28.2
    26.2
    23.8
    20.8
    17.5
];

P=[44.5
    45.3
    47
    49
    51.5
    54
    55
];

%system curve, this is estimated value, normally it should be
% solved just like the HQ and PQ curve
s= [0.0004 0 6];

% estimate pump curve using quadratic equation
```

```
h = polyfit(Q,H,2);
% estimate the power curve using quadratic equation
p = polyfit(Q,P,3);

%First step is to combine pump characteristic quadratic equation with the
%system quadratic equation, this cancels out H. Solve for N result in a
%function of N in term of Q.
E = solve('a*Q^2 + b*N*Q+c*N^2 = g*Q^2+k','N');

% Substitute the function of N in term of Q into the power quadratic
% equation and derive the function of P in terms of Q.
E2 = subs('l*Q^3+d*N*Q^2+e*N^2*Q+f*N^3', 'N', E(1));

%Replace the constants a to h with actual values
P1=subs(E2, 'a', h(1)); P2=subs(P1, 'b', h(2)); P3=subs(P2, 'c',
h(3)); P4=subs(P3, 'd', p(2)); P5=subs(P4, 'e', p(3)); P6=subs(P5,
'f', p(4)); P7=subs(P6, 'g', s(1)); P8=subs(P7, 'k', s(3));
P9=subs(P8, 'l', p(1));

%simplify the equation
P10=simplify(P9);

%Declare a function to substituting values in place of Q
Pt=@(Q) subs(P10, 'Q', Q);

%Compute t number of values using the above function
t=0:5:250; PW2=Pt(t);

%Estimate the third order quadratic equation.
%The output pw is the desired model.
pw=polyfit(t, PW2,3)
```

APPENDIX C. MATLAB Programs (Optimal capacity selection)

```
%This is the MATLAB code for the optimal pump capacity selection model

%Algorithm initialization parameters
iteration=30000; particles = 50; dimension = 24; c1 = 2; c2 = 2;
g_best=10000000; best_val=10000000;
%tariff=[0.1187;0.1187;0.1187;0.1187;0.1187;0.1187;0.1411;0.8205;
0.8205;0.8205;0.1411;0.1411];

%High demand TOU tariff
tariff=[0.118700000000000;0.118700000000000;0.118700000000000;
0.118700000000000;0.118700000000000;0.118700000000000;0.141100000000000;
0.820500000000000;0.820500000000000;0.820500000000000;0.141100000000000;
0.141100000000000;0.141100000000000;0.141100000000000;0.141100000000000;
0.141100000000000;0.141100000000000;0.141100000000000;0.820500000000000;
0.820500000000000;0.820500000000000;0.820500000000000;0.118700000000000;
0.118700000000000;];
%Low demand TOU tariff
%tariff=[0.104900000000000,0.104900000000000,0.104900000000000,
0.104900000000000,0.104900000000000,0.104900000000000,0.138300000000000,
0.262800000000000,0.262800000000000,0.262800000000000,0.138300000000000,
0.138300000000000,0.138300000000000,0.138300000000000,0.138300000000000,
0.138300000000000,0.138300000000000,0.138300000000000,0.262800000000000,
0.262800000000000,0.262800000000000,0.262800000000000,0.104900000000000,
0.104900000000000;];

%minmum and maximum pump selection range
AVD=70; MAXD=120;

%Minimum and maximum reservoir level
AVR=500; MAXR=1000; LL=500; UL=1000;

%Initial reservoir volume
LVo=500;

%demand (m^3)/hour
%D=[60;60;60;60;100;100;100;100;60;60;60;60];
D=[70;70;70;70;70;70;70;70;70;70;70;70;70;70;70;70;70;70;70;70;70;70;
```

```
70;70;70;];

%maximum demand cost
dc=0;

%system equation used to compute the input power of the pump
system=[0.00112946428571429,0.00228214285714281,3.99785714285715];

%efficiency
eff=0.8;

g_best=10000000; best_val=10000000;

% Inialization of the variables and velocity
    for i=1:particles
        for j = 1:dimension

            %initialization of the binary variables the on/off schedule
            if rand>=0.5
                particle_position(i,j) = 1;
            else
                particle_position(i,j) = 0;
            end
            if rand>=0.5
                prev_position(i,j) = 1;
            else
                prev_position(i,j) = 0;
             end

            p_best(i,j) = particle_position(i,j);
            cost(i,j)=0;
            pbest(i,(j)) = particle_position(i,(j));
            exceed(i,j)=0;

        end
         %initialization of the continous variables the pump capacity
        particle_position(i,dimension+1) = AVD+rand*(MAXD-AVD);
        particle_velocity(i,dimension+1) = AVD-rand*(2*AVD);
        prev_position(i,dimension+1) = AVD+rand*(MAXD-AVD)/1.5;

    end

    for i=1:particles
        p_best_fitness(i)=10000000;
        fitness(i)=0;
    end

    for k=1:iteration

        for i=1:particles
```

```
        fitness(i)=0;
        end
        %compute solution and fitness with constraints
        for i = 1:particles

            vol(i,1)=LVo;
            for j=1:dimension
               exceed(i,j)=0;
            end

            %Compute the power consumptio for a particular pump capacity
            %using the hydraulic equation
                        head(i)=system(1)*(particle_position(i,(dimension+1)))^2
                        + system(2)*(particle_position(i,(dimension+1)))+system(3);
            power(i)=head(i)*(particle_position(i,(dimension+1)))/3600*9.81/eff;

            for j = 1:dimension

                %compute the cost of one set of 24 hour flow manangement
%for one particle
                cost(i,j)=power(i)*tariff(j)*particle_position(i,j);
                fitness(i)=fitness(i)+cost(i,j);

                %compute the reservoir volume and determing whether constaint
                %is violated or not
                %%%%%%%%%%%%%%%%%%%%%%%%%%%%%%%%%%%%%%%%%%%%%%%%%%%%%%%%%%%

                vol(i,(j+1))=vol(i,j)+particle_position(i,(dimension+1))*
                particle_position(i,(j))-D(j);
                if vol(i,(j+1))<LL
                    exceed(i,j)=0;
                    exceed(i,j)=LL-vol(i,(j+1));
                    fitness(i)=fitness(i)+1+0.05*exceed(i,j);
                end
                if vol(i,(j+1))>UL
                    exceed(i,j)=0;
                    exceed(i,j)=vol(i,(j+1))-UL;
                    fitness(i)=fitness(i)+0.8+0.05*exceed(i,j);
                end
                %%%%%%%%%%%%%%%%%%%%%%%%%%%%%%%%%%%%%%%%%%%%%%%%%%%%%%%%%%%

            end
            MD=power(i)*dc;
            fitness(i)=fitness(i)*30+MD;

            fitness(i)=fitness(i)/30*365*15;

        end

       %determine p best
```

```
for i = 1:particles
    if fitness (i) <= p_best_fitness(i)
        p_best_fitness(i) = fitness(i);
        for j = 1:(dimension+1)
             p_best(i,j)= particle_position(i,j);
        end
    end

end

%determine gbest
[g_best_val,g_best_index] = min(fitness);

 for j = 1:(dimension+1)
     g_best(j) = particle_position(g_best_index,j);

 end
 if g_best_val<best_val
         best_val = g_best_val;
         for j = 1:(dimension+1)
             best_position (j) = particle_position(g_best_index,j);

         end
         for j = 1:(dimension)
             best_exceed(j) = exceed(g_best_index,j);
         end
  end


% Determine the new paritcle position and velocity
   for i = 1:particles
      for j = 1:dimension
          current_position(j) = particle_position(i,j);
          storage_position(j) = particle_position(i,j);
          position_indication = current_position(j)+prev_position(i,j)
          +g_best(j)+p_best(i,j)-2.444+rand*(2*2.444);
          if position_indication>=2
              particle_position (i,j)=1;
          else
              particle_position (i,j)=0;
          end

      end

      for j = 1:dimension
          prev_position(i,j) = storage_position(j);

      end
      current_position((dimension+1)) =
      particle_position(i,(dimension+1));
```

```
        particle_velocity(i,(dimension+1)) =
        ((particle_velocity(i,(dimension+1))*(1-k/iteration)) +
        c1*rand*(p_best(i,(dimension+1))-
        current_position((dimension+1))) +
        c2*rand*(g_best((dimension+1))-
        current_position((dimension+1))))/1.8;

        %particle_velocity(i,(dimension+1)) =
        ((particle_velocity(i,(dimension+1)))
         + c1*rand*(p_best(i,(dimension+1))-
         current_position((dimension+1)))
         + c2*rand*(g_best((dimension+1))-
         current_position((dimension+1))))/1.1;

        if particle_velocity(i,(dimension+1))>(AVD/5)
                particle_velocity(i,(dimension+1))=(AVD/5);
            end
            if particle_velocity(i,(dimension+1))<-(AVD/5)
                particle_velocity(i,(dimension+1))=-(AVD/5);
            end
            particle_position (i,(dimension+1)) =
            current_position((dimension+1))
            + particle_velocity(i,(dimension+1));

    end
end
```

APPENDIX D. MATLAB Programs (Optimal control model)

```
%The code for optimal operation control under high demand TOU and MD tariff
%structure.

%Initial parameters
iteration=20000; particles = 50; dimension = 24; c1 = 2; c2 = 2;

    %dc=demand_charge(1);
    dc=60.5;
    best_val=10000;
    tariff=[0.1187;0.1187;0.1187;0.1187;0.1187;0.1187;0.1411;0.8205
    ;0.8205;0.8205;0.1411;0.1411;0.1411;0.1411;0.1411;0.1411;0.1411;
    0.1411;0.8205;0.8205;0.8205;0.8205;0.1187;0.1187;0.1187;0.1187;
    0.1187;0.1187;0.1187;0.1187;0.1411;0.8205;0.8205;0.8205;0.1411;
    0.1411;0.1411;0.1411;0.1411;0.1411;0.1411;0.1411;0.8205;0.8205;
    0.8205;0.8205;0.1187;0.1187];
    g_best=10000;

    %demand (m^3)/hour
    D=[60;60;60;60;60;60;60;60;100;100;100;100;100;100;100;100;
    75;75;75;75;75;75;75;75];

    %model of the pump power vs flow relation.
    P=[3.8969e-6; 2.1851e-5; 0.01117; 0.13102];

    %reservor data
    UL=1000;
    LL=500;
    LVo=800;

    for i=1:particles
        for j = 1:dimension

            %random continuous position of a particle's dimension 1-24
            particle_position(i,j) = 54+rand*(101-54);
            particle_velocity(i,j) = (-25)+rand*50;
            prev_position(i,j) = 54+rand*(101-54);
            %random binary position of a particle's dimension 25-48
            if rand>=0.5
```

```
            particle_position(i,(j+dimension)) = 1;
        else
            particle_position(i,(j+dimension)) = 0;
        end
         if rand>=0.5
            prev_position(i,(j+dimension)) = 1;
        else
            prev_position(i,(j+dimension)) = 0;
        end

        pbest(i,j) = particle_position(i,j);
        cost(i,j)=0;
        pbest(i,(j+dimension)) = particle_position(i,(j+dimension));
        exceed(i,j)=0;

    end
end


for i=1:particles
    p_best_fitness(i)=10000;
    fitness(i)=0;
end

for k=1:iteration

    for i=1:particles
    fitness(i)=0;
    end
 %compute solution and fitness with constraints
    for i = 1:particles

        vol(i,1)=LVo;
        for j=1:dimension
           exceed(i,j)=0;
        end
        for j = 1:dimension

            %Comupte the power for given flow rate
            power(j)=(P(1)*(particle_position(i,j))^3 + P(2)*
            (particle_position(i,j))^2 + P(3)*(particle_position(i,j))
            +P(4))*particle_position(i,(j+dimension));

            %compute the cost of one set of 12 hour flow manangement or one
            %particle
            cost(i,j)=power(j)*tariff(j)*30;
            fitness(i)=fitness(i)+cost(i,j);

            %compute the reservoir volume and determing whether constaint
            %is violated or not
```

```
            vol(i,(j+1))=vol(i,j)+particle_position(i,j)*
            particle_position(i,(j+dimension))-D(j);
            if vol(i,(j+1))<LL
                exceed(i,j)=0;
                exceed(i,j)=LL-vol(i,(j+1));
                fitness(i)=fitness(i)+10+1*exceed(i,j);
            end
            if vol(i,(j+1))>UL
                exceed(i,j)=0;
                exceed(i,j)=vol(i,(j+1))-UL;
                fitness(i)=fitness(i)+10+1*exceed(i,j);
            end
        end
        MD=(max(power))*dc;
        fitness(i)=fitness(i)+MD;
    end

    %p best
    for i = 1:particles
        if fitness (i) <= p_best_fitness(i)
            p_best_fitness(i) = fitness(i);
            for j = 1:(dimension*2)
                p_best(i,j)= particle_position(i,j);
            end
        end

    end

    %gbest
    [g_best_val,g_best_index] = min(fitness);

     for j = 1:(dimension*2)
         g_best(j) = particle_position(g_best_index,j);
     end
     if g_best_val<best_val
            best_val = g_best_val;
            for j = 1:(dimension*2)
                best_position (j) = particle_position(g_best_index,j);
            end
            for j = 1:(dimension)
                best_exceed(j) = exceed(g_best_index,j);
            end
      end


% Determine the new paritcle position and velocity
   for i = 1:particles
      for j = 1:dimension
          current_position(j) = particle_position(i,j);
          particle_velocity(i,j) = ((particle_velocity(i,j)*
```

```
            (1-k/iteration)) + c1*rand*(p_best(i,j)-current_position(j))
             + c2*rand*(g_best(j)-current_position(j)))/1.5;
            if particle_velocity(i,j)>25
                particle_velocity(i,j)=25;
            end
            if particle_velocity(i,j)<-25
                particle_velocity(i,j)=-25;
            end
            particle_position (i,j) =  current_position(j) +
            particle_velocity(i,j);

            if particle_position(i,j)>101
                particle_position (i,j)=101;
            end
            if particle_position (i,j)<54
                particle_position (i,j)=54;
            end

        end

        for j = (dimension+1):dimension*2
            current_position(j) = particle_position(i,j);
            storage_position(j) = particle_position(i,j);
            position_indication = current_position(j)+prev_position(i,j)
            +g_best(j)+p_best(i,j)-2.444+rand*(2*2.444);
            if position_indication>=2
                particle_position (i,j)=1;
            else
                particle_position (i,j)=0;
            end
        end

        for j = (dimension+1):dimension*2
            prev_position(i,j) = storage_position(j);

        end
    end

end
```

APPENDIX E. MATLAB Programs (MPC model)

```
%The algorithm for the MPC simulation. The control horizon is 24 hours.

%control horizon
Horizon = 24;
TOU=[0.1187;0.1187;0.1187;0.1187;0.1187;0.1187;0.1411;0.8205;0.8205;
0.8205;0.1411;0.1411;0.1411;0.1411;0.1411;0.1411;0.1411;0.1411;0.8205;
0.8205;0.8205;0.8205;0.1187;0.1187;0.1187;0.1187;0.1187;0.1187;0.1187;
0.1187;0.1411;0.8205;0.8205;0.8205;0.1411;0.1411;0.1411;0.1411;0.1411;
0.1411;0.1411;0.1411;0.8205;0.8205;0.8205;0.8205;0.1187;0.1187];
%demand (m^3)/hour
Demand=[55;55;55;55;55;55;55;55;90;90;90;90;90;90;90;90;70;70;70;
70;70;70;70;70;55;55;55;55;55;55;55;55;90;90;90;90;90;90;90;90;70;
70;70;70;70;70;70;70];

%reservoir parameters
UL=900; LL=500; LVo=500; iteration=50000; particles = 50;

%maximum demand cost
dc=100; tic

%update the current reservoir volume
for day=1:7
    dddd=day
    if day==1
        reservoir(day,1)=LVo;
    else
        reservoir(day,1)=reservoir((day-1),25);

    end
    for period=1:24
        pppp=period

        % sample the current reservoir volume
        for i = 1:particles
            vol(i,1)=reservoir(day,period);
        end
```

```
%for k=1:24
     %best_val(k)=10000;
%end

dimension = Horizon;
c1 = 2.2;
c2 = 2.2;

% adjust the order of the tariff and demand in accordance to the
% control horizon
tariff=TOU(period:(period+Horizon));
D=Demand(period:(period+Horizon));

best_val=10000;
g_best=10000;

%model of the pump power vs flow relation.
P=[3.8969e-6; 2.1851e-5; 0.01117; 0.13102];

%model initialization
for i=1:particles
    for j = 1:dimension

        particle_position(i,j) = 54+rand*(101-54);
        particle_velocity(i,j) = (-25)+rand*50;
        prev_position(i,j) = 54+rand*(101-54);
        %random binary position of a particle's dimension 13-24
        if rand>=0.5
            particle_position(i,(j+dimension)) = 1;
        else
            particle_position(i,(j+dimension)) = 0;
        end
         if rand>=0.5
            prev_position(i,(j+dimension)) = 1;
        else
            prev_position(i,(j+dimension)) = 0;
        end

        pbest(i,j) = particle_position(i,j);
        cost(i,j)=0;
        pbest(i,(j+dimension)) = particle_position(i,(j+dimension));
        exceed(i,j)=0;

    end
end


for i=1:particles
    p_best_fitness(i)=10000;
    fitness(i)=0;
```

```
end

for k=1:iteration

    for i=1:particles
    fitness(i)=0;
    end

     %compute fitness and constraints satisfaction
    for i = 1:particles
        for j=1:dimension
           exceed(i,j)=0;
        end
        for j = 1:dimension

        %Comupte the power for given flow rate
        power(j)=(P(1)*(particle_position(i,j))^3 + P(2)*
        (particle_position(i,j))^2 + P(3)*(particle_position(i,j))
        +P(4))*particle_position(i,(j+dimension));

        %compute the cost of one set of 12 hour flow manangement or one
        %particle
        cost(i,j)=power(j)*tariff(j)*30;
        fitness(i)=fitness(i)+cost(i,j);

        %compute the reservoir volume and determing whether constaint
        %is violated or not
        vol(i,(j+1))=vol(i,j)+particle_position(i,j)*
        particle_position(i,(j+dimension))-D(j);
        if vol(i,(j+1))<LL
            exceed(i,j)=0;
            exceed(i,j)=LL-vol(i,(j+1));
            fitness(i)=fitness(i)+10+1*exceed(i,j);
        end
        if vol(i,(j+1))>UL
            exceed(i,j)=0;
            exceed(i,j)=vol(i,(j+1))-UL;
            fitness(i)=fitness(i)+10+1*exceed(i,j);
        end
        end
    %add maximum demand cost
    MD=(max(power))*dc;
    fitness(i)=fitness(i)+MD;
end

   %calculate the p best
   for i = 1:particles
       if fitness (i) <= p_best_fitness(i)
           p_best_fitness(i) = fitness(i);
           for j = 1:(dimension*2)
```

```
                p_best(i,j)= particle_position(i,j);
            end
        end

    end

    %calculate gbest
    [g_best_val,g_best_index] = min(fitness);

     for j = 1:(dimension*2)
         g_best(j) = particle_position(g_best_index,j);
     end
     if g_best_val<best_val
             best_val = g_best_val;
             for j = 1:(dimension*2)
                 best_position (j) = particle_position(g_best_index,j);
             end
             for j = 1:(dimension)
                 best_exceed(j) = exceed(g_best_index,j);
             end
      end


% Determine the new paritcle position and velocity
   for i = 1:particles
      for j = 1:dimension
          current_position(j) = particle_position(i,j);
             particle_velocity(i,j) = ((particle_velocity(i,j)*
             (1-k/iteration)) + c1*rand*(p_best(i,j)-current_position(j))
              + c2*rand*(g_best(j)-current_position(j)))/1.5;
          if particle_velocity(i,j)>25
              particle_velocity(i,j)=25;
          end
          if particle_velocity(i,j)<-25
              particle_velocity(i,j)=-25;
          end
          particle_position (i,j) =  current_position(j) +
          particle_velocity(i,j);

          if particle_position(i,j)>101
              particle_position (i,j)=101;
          end
          if particle_position (i,j)<54
              particle_position (i,j)=54;
          end

      end

      for j = (dimension+1):dimension*2
          current_position(j) = particle_position(i,j);
```

```
                    storage_position(j) = particle_position(i,j);
                    position_indication = current_position(j)+
                    prev_position(i,j)+g_best(j)+p_best(i,j)-2.444+rand*(2*2.444);
                    if position_indication>=2
                        particle_position (i,j)=1;
                    else
                        particle_position (i,j)=0;
                    end
                end

                for j = (dimension+1):dimension*2
                    prev_position(i,j) = storage_position(j);

                end
            end
        end

        toc
        t=toc

    % output the first control sequence of the 24 hour strategy as the
    % actual MPC strategy.
    MPC_ouput(day, period)= best_position (1);
    MPC_ouput(day, period+24)=best_position(dimension+1);
    % update the reservoir volume
    reservoir(day, period+1)=reservoir(day, period)-Demand(period)+
    (MPC_ouput(day, period)*MPC_ouput(day, period+24));
    end
    %output=rot90(MPC_ouput,3);
end
```